DLR-IB 647-2004/03

SART TN-003/2004

Evaluation of Green Propellants for Space Applications

WP 2200: Propulsion Requirements

Holger Burkhardt

Armin Herbertz

Martin Sippel

Alexander Woschnak

Jörg Riccius

Wednesday, August 04, 2004

This report includes:

94 pages

110 figures

18 tables

40 references

Deutsches Zentrum für Luft- und Raumfahrt e.V.

Institut für Raumfahrtantriebe

Univ. Prof. Dr. W. Koschel

Contents

List of Tables

List of Figures

Nomenclature

A	cross section area	m^2
c*	characteristic velocity	m/s
c_p	specific heat at constant pressure	J/(kg K)
F	Thrust	N
g_0	gravitational acceleration	($g_0 \approx 9.8067$ m/s²)
H*	assigned enthalpy	J/mol
I	specific impulse	s
$\dot{m}$	mass flow	kg/s
M	molar mass	g/mol
p	Pressure	Pa
R	mixture ratio	-
T	Temperature	K
$\Delta_f H$	enthalpy of formation	J/mol
$\Delta_{vap} H$	heat of vaporization	J/mol
ε	expansion ratio	-
ρ	Density	kg/m^3

Subscripts, Acronyms

0	standard reference state
boil	boiling point
c	chamber
e	exit
fu	fuel
gas	gaseous
LH2	Liquid Hydrogen
liq	liquid
LOX	Liquid Oxygen
OMS	Orbital Maneuvering System
Ox	oxidizer
RCS	Reaction Control System
RP	Rocket Propellant
T	Throat
Vac	Vacuum

1 Introduction

Green Propellants have been a subject of R and D for several years. The main interest lies in replacing oftentimes toxic and hazardous propellants, while not neglecting effects on cost, complexity and performance.

This study, as an ESA funded activity in response to [Fratacci03], is focused on carbon based fuels for application in bi-propellant engines for

- large liquid propulsion (booster, main stage and large upper stage)
- small liquid propulsion (RCS, OMS, interplanetary missions)

This technical note is a joint report of the technology and the launcher systems analysis division of the DLR Institute of Space Propulsion.

2 Propellant Properties

Key properties for a set of candidate propellants are presented in Table 3 through Table 6.

A consistent color coding has been applied to identify origin of data (type color) and to assess suitability of propellant (cell color).

Type colour	Origin
NIST Data	[NIST04]
Air Liquide	[AirLiquide04a], [AirLiquide04b]
Sigma Aldrich	[SigmaAldrich04]
T. Edwards	[Edwards03]
Burkhardt et al.	[Burkhardt04]
Koelle	[Koelle61]
SNECMA	[Valentian04]
IARC	[IARC04b]
Shell Chemicals	[Shell04]
MIL Standard	[MIL67]
Wacker	[Wacker02]
BP Chemicals	[bp02]
Oxford Chemicals	[Oxford01]
calculated	deduced from data in table

Table 1: Type color coding of data origin

Melting Point (MP)	Boiling Point (BP)	Density	Critical Temperature and pressure	Other fields
no risk of fuel freezing with LOX as oxidizer	storable	high density	regenerative cooling ok	good
risk of fuel freezing with LOX as oxidizer	storable under pressure / mild cryo	medium density		problematic
risk of fuel freezing (general)	(soft) cryo	low density	regenerative cooling problematic	bad

Table 2: Cell color coding of properties assessment

2.1 Classification of Melting Point Data

The melting point of propellants impacts the design choices of stages and may limit in space storage.

A melting point below the boiling point of LOX is most advantageous, as no risk of fuel freezing exists. Propellants of this category are assigned a positive rating.

Propellants with a melting point above the boiling point of LOX, but below 0 ℃ are assigned a problematic rating.

Propellants with a melting point above 0 ℃ are assigned a negative rating as there is a general risk of fuel freezing.

2.2 Classification of Boiling Point Data

The storage mode of the propellants is linked to the boiling point.

Propellants which can be stored in liquid state are assigned a positive rating.

Propellants with a boiling point below ambient temperature, which can be stored in liquid state under pressure, are rated problematic.

Only cryogenic propellants with a boiling point considerably below ambient temperature are rated negative.

2.3 Classification of Density Data

A high propellant density is desirable to build compact and (relative) light weight stages.

Propellants with a density above 0.7 g/cm³ are rated positive.

Propellants with a density between 0.5 and 0.7 g/cm³ are rated problematic.

Propellants with a density below 0.5 g/cm³ are rated negative.

2.4 Classification of Critical Temperature and Pressure

Critical temperature and pressure are important parameters for the assessment of suitability for regenerative engine cooling.

Propellants with critical temperature below 200 ℃ and critical pressure below 60 bars are rated positive.

2.5 Classification of Carcinogenetic Rating

Confirmed carcinogenicity (IARC class 1) leads to a negative rating.

Probable (IARC class 2a) and possible (IARC class 2b) carcinogens as well as unclassifiable agents (IARC class 3) are rated problematic.

A positive rating is only assigned if the propellant is non-carcinogen.

2.6 Classification of Stability and Reactivity

A positive rating was assigned to propellants when no special precautionary measures are necessary.

Sensitivity to heat, air or light as well as incompatibility with some materials lead to a problematic rating.

Risk of polymerization and risk of violent reactions or decomposition lead to a negative rating.

2.7 Classification of Toxicological Information

A positive rating was assigned to all propellants for which no toxicological effects are known.

Propellants with irritating properties were classified as problematic.

All other propellants were assigned a negative rating.

2.8 Classification of Ecological Information

Minor ecological concerns lead to a problematic rating. The global warming potential of methane is considered part of this category as this effect only comes into play with propellant leaks.

A negative rating was assigned when direct ecological threats are linked to the propellants.

2.9 Classification of Risk phrases

Risk phrases related to flammability of the propellants (R10 through R12) have no negative impact in the assessment process due to the inherent correlation to energetic propellants.

Risk phrases related to temporal or minor health risks (R36 through R38, R66, and R67) and to extreme flammability / explosion risks (R17, R19) lead to a problematic rating.

Risk phrases related to major health risks (R20 through R25, R34, R39 through R41, R45, R46, R65) or major ecological risks (R50 through R53) lead to a negative rating.

Name	Formula	Molar Mass	MP	BP	Density	Critical temp.	Critical pressure	Critical density	ΔH_f liquid	ΔH_f gas	ΔH_f gas	Latent heat
		g	℃	℃	g/cm3	℃	bar	g/cm3	kJ / mol	kJ / mol	kJ / kg	kJ /kg
Methane	**CH4**	16.043	-182.47	-161.52	0.4226	-82.62	45.96	0.1628		-74.5	-4643.77	510.20
Ethane	C2H6	30.07	-183	-88.6	0.54	32	49	0.2075	-93.56	-83.8	-2786.86	324.58
Propane	**C3H8**	44.096	-187.68	-42.04	0.582	96.67	42.5	0.2249	-119.8	-104.7	-2374.37	426.01
Butane	C4H10	58.12	-138	-0.5	0.601	152	38	0.2278		-125.6	-2160.92	386.08
Pentane	C5H12	72.15	-130	35	0.626	196.65	33.6	0.2323	-173.5	-146.8	-2034.64	370.75
Octane	C8H18	114.23	-57	125	0.703	295.75	24.9	0.2323	-250.3	-208.4	-1824.37	363.56
RP 1		172	-50	175-275	0.807	683	21.8		-288.1			246.34
Ethylene	C2H4	28.054	-169.15	-103.71	0.5679	9.5	50.76	0.2141		52.4	1867.83	482.86
Propene, propylene	C3H6	42.08	-185.2	-47.6	0.6139	91.6	46.1	0.2281	4	20.41	485.03	437.94
Propadiene	C3H4	40.065	-136.3	-34.4	0.657	120.7	52.49	0.2473		190.5	4754.77	464.73
Cyclopropane	C3H6	42.08	-128	-32.9	0.68	125.1	55.8	0.2588	35.2	53.35	1267.82	476.57
Propyne	C3H4	40.065	-102.7	-23.2	0.671	129.24	56.28	0.2452		184.9	4615.00	
Methanol	CH4O	32.04	-97.5	63.6	0.791	239.85	81.1	0.2727	-238.9	-201	-6272.99	1098.86
Ethanol	**C2H6O**	46.07	-117.3	78.5	0.7893	243.1	63.1	0.2764	-277.6	-234.8	-5096.59	836.99
2 Propanol	C3H80	60.1	-89.5	82.3	0.785	235.85	49	0.2711	-317	-272.8	-4539.10	663.06
Dimethyl-ether	**C2H6O**	46.07	-141.5	-24.8	0,73	126.95	52.69	0.2465	-203.3	-184.1	-3996.09	466.90
Ethyl methyl ether	C3H80	60.1	-139	7.4	0.7251	165	43.61	0.2722		-216.4	-3600.67	
Propyl ether	(CH3(CH2)2)2O	102.18	-122	91	0.736	257.45	30.28		-328.8	-293	-2867.49	350.26
Dibutyl ether	(CH3(CH2)3)2O	130.23	-95.3	142	0.7689	314.95	30.10		-377.9	-332.8	-2555.48	345.54
Diallyl ether	(CH2CHCH2)2O	98.12		94	0.826							
Acetaldehyde	C2H4O	44.05	-123	20.1	0.7834	187.8	54.7	0.2859	-192.2	-170.7	-3875.14	584.79
Ethylene oxide	C2H4O	44.047	-112	10.4	0,89	195.78	71.91	0.3141	-95.7	-52.6	-1194.18	579.84
Trimethyl-aluminium	C3H9Al	72.086	15.28	127.12	0.752				-149.7	-86.5	-1199.96	580.43

Table 3: Thermodynamical Properties (1)

Name	Formula	Cp liquid	Cp gas	Cp gas	Cp gas handbook	Heat of combustion		CAS Number	Availa-bility	Price	Classification
		J /kg℃	J / mol℃	J /kg℃	J /kg℃	kJ/mol	kJ/kg			€/kg	
Methane	**CH4**	3454.11	35.69	2224.65		890.8	55526	74-82-8	High	0.62 €[1]	Paraffin
Ethane	C2H6	2276.05	52.49	1745.61		1560.7	51903	74-84-0	High		Paraffin
Propane	**C3H8**	2470.21	68.74	1558.87	1557.49	2219.2	50327	74-98-6	High	2 - 2.50 €	Paraffin
Butane	C4H10	2278.26	92.3	1588		2877.5	49507	106-97-8	High		Paraffin
Pentane	C5H12	2317.25	112.55	1559.94		3535.4	49001	109-66-0	High		Paraffin
Octane	C8H18	2214.11	175.69	1538.02		5430.0	47535	111-65-9	High		Paraffin
RP 1		2093				7454	43340		High	1 €	(mostly) Paraffin
Ethylene	C2H4	2402.51	42.9	1529.19	1473.75	1411.2	50303	74-85-1	High	< 2.00 €	Olefin
Propene, propylene	C3H6	2423.95	60.47	1437.02		2058	48907	115-07-1	High		Olefin
Propadiene	C3H4		55.67	1389.49				463-49-0	High (?)		Olefin
Cyclopropane	C3H6	1932.98	50.69	1204.61		2091.3	49698	75-19-4	High (?)		Naphten
Propyne	C3H4		57.65	1438.91				74-99-7	High (?)		Alkin
Methanol		2503.58	42.59	1329.19		726	22658	67-56-1	High		Alcohol
Ethanol	**C2H6O**	2431.08	65.6	1423.92		1366.8	29668	67-17-5	High	< 2.50 €[2]	Alcohol
2 Propanol	C3H80	2562.40	83.72	1393.01		2006.9	33393	67-63-0	High (?)	0.65 €	Alcohol
Dimethyl-ether	**C2H6O**	2220.53	65.5	1421.75		1460.4	31700	115-10-6	High (?)		Ether (single C-C bonds)
Ethyl methyl ether	C3H80		93.3	1552.41		2107.4	35065	540-67-0	High (?)		Ether (single C-C bonds)
Propyl ether	(CH3(CH2)2)2O	2167.25	182.95	1790.47		4033.1	39471	111-43-3	High (?)		Ether (single C-C bonds)
Dibutyl ether	(CH3(CH2)3)2O	2135.91				5342.6	41025	142-96-1	High		Ether (single C-C bonds)
Diallyl ether	(CH2CHCH2)2O							557-40-4			Ether (double C-C bonds)
Acetaldehyde	C2H4O	2021.57	55.3	1255.39		1166.9	26490	75-07-0	High		
Ethylene oxide	C2H4O	1972.89	47.0	1067.04		1306.0	29650	75-21-8	High		
Trimethyl-aluminium	C3H9Al	2158.53				3184.4	44175	75-24-1		2 275 €	

Table 4: Thermodynamical Properties (2), Availability and Cost

[1] Price estimate based on end-consumer natural gas price

[2] Upper bound estimation based on end-consumer price for household grade spirit

Name	Formula	IARC Rating	Flash Point	Lower Flammability Limit (STP)	Upper Flammability limit (STP)	Auto ignition temperature	Odor
			°C			°C	
Methane	**CH4**		-221	5 %	15 %	595	None
Ethane	C2H6		-130	3 %	16 %	515	None
Propane	**C3H8**		-105	2.2 %	9.5 %	470	Sweetish
Butane	C4H10		-60	1.4 %	9.3%	365	Sweetish
Pentane	C5H12		-49	1.4 %	8.3 %	260	
Octane	C8H18		13	0.96 %	6.5 %	220	
RP 1		3	>29	1.6 %	6 %	254	Kerosene odor
Ethylene	C2H4	3	-136	2.7 %	36 %	425	Sweet
Propene, propylene	C3H6	3		2 %	11 %	460	sweetish
Propadiene	C3H4		-101	2.5 %	17 %		Sweetish
Cyclopropane	C3H6			2.4 %	10.4 %	495	Ethereal
Propyne	C3H4			2.3 %	16.8 %		Garlic like
Methanol	CH4O		10	6.1 %	44 %	455	Characteristic
Ethanol	**C2H6O**	1 (oral)[3]	14	3.3 %	19 %	365	Alcohol-like
2 Propanol	C3H80	3	12	2.5 %	12 %	399	
Dimethyl-ether	**C2H6O**		-41	3 %	18.6 %	235	Ethereal
Ethyl methyl ether	C3H80			2 %	10.1 %	190	Ethereal
Propyl ether	(CH3(CH2)2)2O		-28				Pleasant odor, slight odor resembling that of mixt. of ethanol % acetone
Dibutyl ether	(CH3(CH2)3)2O		28	0.9%	8.5 %	180	Pleasant
Diallyl ether	(CH2CHCH2)2O		-7				
Acetaldehyde	C2H4O	2b	-27	4 %	57 %	175	Penetrating, fruity, pungent
Ethylene oxide	C2H4O	1	-20	3 %	100%	440	Ethereal
Trimethyl-aluminium	C3H9Al		-17				

Table 5: Thermal and other data

[3] IARC classification for oral consumption of alcoholic beverages

Name	Stability and Reactivity	Toxicological Information	Ecological Information	Risk Phrases
Methane, g		no known effects	Global warming factor: 21	R12
Ethane		no known effects	no known effects	R12
Propane, g		no known effects	no known effects	R12
Butane		no known effects	no known effects	R12
Pentane	Stable / polymerization will not occur	Harmful by inhalation	dangerous for the environment toxic to aquatic organisms may cause long-term adverse effects in the aquatic environment	R12 R51/53 R65 R66 R67
Octane	Stable / polymerization will not occur	Harmful by inhalation	dangerous for the environment; very toxic to aquatic organisms may cause long-term adverse effects in the aquatic environment	R11 R38 R50/53 R65 R67
RP 1		Harmful by inhalation Irritating to skin	will not biodegrade in anaerobic conditions contains components which have a high potential to bioaccumulate expected to be slightly toxic to fish toxic to aquatic organisms may cause long-term adverse effects in the aquatic environment	R10 R38 R 51/53 R 65
Ethylene		no known effects	no known effects	R12
Propene, propylene, g		no known effects	no known effects	R12
Propadiene	May decompose violently at high temperature and /or pressure or in the presence of a catalyst may react with bases, copper, silver, mercury, magnesium, zinc and their alloys; do not use alloys containing more than 70% copper	no known effects	no known effects	R12
Cyclopropane, g		no known effects	no known effects	R12
Propyne	Forms explosive acetylides with copper, silver and mercury may decompose violently at high temperature and/or pressure or in the presence of a catalyst do not use alloys containing more than 70% copper; may polymerize	Harmful by inhalation Irritating to respiratory system and skin risk of serious damage to eyes	no known effects	R12 R20 R37/38 R41

Methanol	Thermal decomposition is highly dependent on conditions	toxic	Low toxicity	R11 R23/24/25 R39
Ethanol, l	polymerization will not occur	not classified as dangerous practically non-toxic to aquatic organisms	not classified as dangerous readily biodegradable	R11
2 Propanol, l	Materials to avoid: Oxidizing agents, Acids, Acid anhydrides, Halogens, Aluminum polymerization will not occur	not thoroughly investigated Irritating to eyes and skin may be harmful if absorbed through the skin may be harmful if inhaled material may be irritating to mucous membranes and upper respiratory tract may be harmful if swallowed	Ecotoxicity: Guppies LC50: 7.0606 ppm/7 days. Fathead minnow LC50: 11.830 mg/L/1 hr. BOD = 133%/5 days	R11 R36 R67
Dimethyl-ether, g		no known effects	no known effects	R12
Ethyl methyl ether		no known effects	no known effects	R12
Propyl ether		May be harmful by inhalation, ingestion or skin absorption may cause irritation	no data available	R11 R19 R66 R67
Dibutyl ether	Heat sensitive Light sensitive Air sensitive	Irritates eyes, respiratory organs and skin	Likelihood of damaging effect on water organisms not easily biodegradable Bioaccumulation not ruled out	R10 R36/37/38
Diallyl ether	Light sensitive Air sensitive	not thoroughly investigated harmful if swallowed, inhaled or absorbed through skin	no data available	R11 R20/21/22 R36/37/38
Acetaldehyde, liquid	Polymerizes easily with evolution of heat	Irritating to eyes and respiratory system Possible risk of irreversible effects	Marine pollutant	R12 R36/37 R40
Ethylene oxide	may polymerize	Toxic by inhalation Irritating to eyes, respiratory system and skin; may cause cancer by inhalation; may cause heritable genetic damage Damage to red blood cells (haemolytic poison)	no known effects may cause pH changes in aqueous ecological systems	R12 R23 R36/37/38 R45 R46

Trimethylaluminium	Reacts violently with water spontaneously flammable in air handle and store under nitrogen causes burns upon contact polymerization will not occur stable indefinitely in an inert atmosphere at room temperature decomposes slowly above 100 ℃	Material is extremely destructive to tissue of the mucous membranes and upper respiratory tract, eyes and skin. Inhalation may result in spasm, inflammation and edema of the larynx and bronchi, chemical pneumonia and pulmonary edema. may be harmful if swallowed or absorbed through the skin	no data available	R14 R17 R34

Table 6: Stability, Toxicity and Risks

3 Theoretical Combustion Performance

All theoretical combustion performance calculations are made with the one dimensional equilibrium (ODE) code CEA86 (Chemical Equilibrium with Applications) [McBride96], at a chamber pressure of 1.034214 MPa (150 psi) and an expansion ratio of 40.

The program needs the following input for each species to correctly calculate the fluid properties of the combustion:

- Chemical composition
- Fluid temperature
- Assigned enthalpy

The chemical composition is given as listed in Table 7 below in all considered cases.

The considered temperature is the standard temperature (T_0 = 298.15 K) for species with boiling temperatures above the standard temperature. In those cases the standard heat of formation is used as assigned enthalpy:

$$H^* = \Delta_f H^o_{liq} \qquad \text{(if } T_{boil} \geq T_0\text{)}$$

In all other cases the considered temperature is the boiling temperature at standard pressure (p_0 = 100 kPa). The assigned enthalpy is calculated by using the following equation:

$$H^* = \Delta_f H^o_{gas} - \Delta_{vap} H(T_{boil}) - \int_{T_{boil}}^{T_0} c_{p\,gas}(T)\, dT \qquad \text{(if } T_{boil} < T_0\text{)}$$

The heat of formation is taken as assigned enthalpy at standard temperature. Usually the liquid phase of the species is considered for evaluation of theoretical performance. In cases of insufficient data the considered state of aggregation is gaseous (cf. Table 7 below).

The analyzed parameters for each considered propellant combination are:

- specific vacuum impulse: $I_{vac} = \frac{F_{vac}}{\dot{m}\, g_0}$
- characteristic velocity: $c^* = \frac{p_c\, A_t}{\dot{m}}$
- mean propellant density (in tanks) times specific impulse: $\frac{\rho_{fu}\, \rho_{ox}\, (1+R)}{\rho_{ox} + R\, \rho_{fu}}\, I_{vac}$

Fuel	***Phase***	***Composition***	***M_{fuel}*** *[g/mol]*	***T_{fuel}*** *[K]*
Trimethylaluminium	liquid	AlC_3H_9	72.09	298.15
Kerosene (RP-1)	liquid	*	13.97	298.15
Methane (l)	liquid	CH_4	16.04	111.66
Methyl alcohol	liquid	CH_4O	32.04	298.15
Ethylene (l)	liquid	C_2H_4	28.05	169.44
Acetaldehyde	liquid	C_2H_4O	44.05	293.9
Ethylene oxide (l)	liquid	C_2H_4O	44.05	283.72
Ethane (l)	liquid	C_2H_6	30.07	184.52
Dimethyl ether (l)	liquid	C_2H_6O	46.07	249
Ethyl alcohol	liquid	C_2H_6O	46.07	298.15
Propyne	gas	C_3H_4	40.06	298.15
Cyclopropane (l)	liquid	C_3H_6	42.08	240
Propylene (l)	liquid	C_3H_6	42.08	225.6
Propane (l)	liquid	C_3H_8	44.1	231.08
Ethyl methyl ether	gas	C_3H_8O	60.1	283
Isopropyl alcohol	liquid	C_3H_8O	60.1	298.15
Butane (l)	liquid	C_4H_{10}	58.12	272.65
Propyl ether	liquid	$C_6H_{14}O$	102.18	298.15
Octane	liquid	C_8H_{18}	114,23	298,15
Dibutyl ether	liquid	$C_8H_{18}O$	130.23	298.15

Table 7: Considered species for theoretical performance evaluation

*: For RP-1 a composition equivalent to C H1.9423 is used [McBride96].

3.1 Comparison of specific impulse for propellant-combinations using LOX as oxidizer

Table 8 and Figure 1 give an overview over the results of the theoretical Isp-performance analysis of propellant-combinations utilizing liquid oxygen (LOX) as oxidizer. Figure 2 to Figure 20 show the respective specific vacuum impulses of each propellant-combination.

The mixture ratio is varied in steps of 0.01 to find the mixture ratio leading to the maximum values of I_{vac} (labeled "R_{opt}" in Table 8).

Fuel	R_{stoich} *[-]*	R_{opt} *[-]*	I_{vac} *[s]*	T_c *[K]*
Trimethylaluminium	2.663	1.55	362	3514
Kerosene (RP-1)	3.403	2.62	353.9	3411
Methane (l)	3.989	3.28	365	3297
Methyl alcohol	1.498	1.39	336.4	3093
Ethylene (l)	3.422	2.44	366.4	3482
Acetaldehyde	1.816	1.52	335.5	3271
Ethylen oxide (l)	1.816	1.36	351.1	3386
Ethane (l)	3.725	2.96	361.7	3348
Dimethy ether (l)	2.084	1.72	350.2	3273
Ethyl alcohol	2.084	1.81	342.4	3217
Propyne	3.195	2.05	370.6	3622
Cyclopropane (l)	3.422	2.47	364.3	3469
Propylene (l)	3.422	2.53	361.1	3450
Propane (l)	3.628	2.86	359.7	3366
Ethyl methyl ether	2.396	1.92	352.8	3322
Isopropyl alcohol	2.396	2.03	344.7	3266
Butane (l)	3.578	2.81	358.5	3376
Propyl ether	2.819	2.25	351.8	3351
Octane	3.502	2.73	356.5	3390
Dibutyl ether	2.949	2.33	352.4	3363

Table 8: Performance of propellant-combinations using LOX as oxidizer

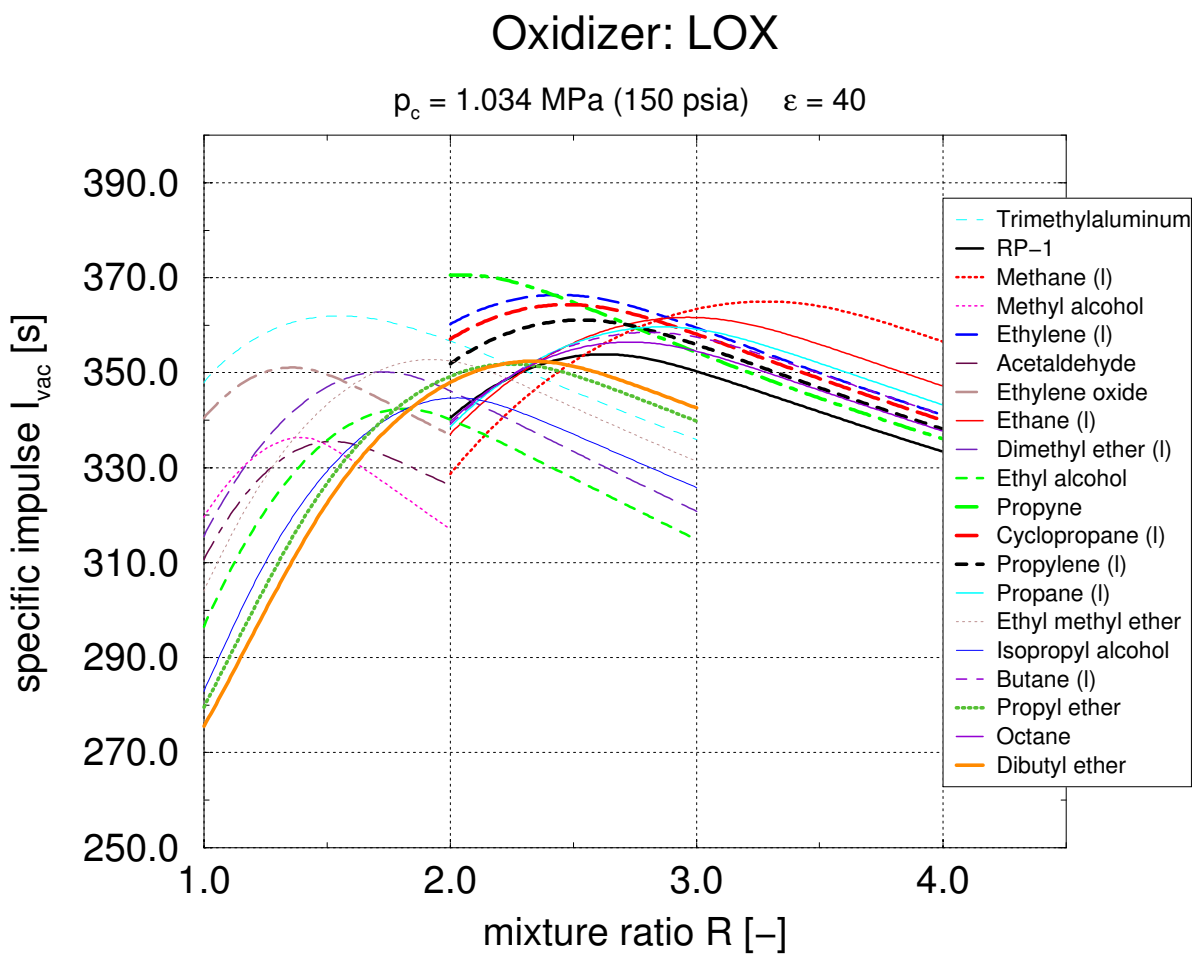

Figure 1: Vacuum impulse of propellant-combinations using LOX as oxidizer

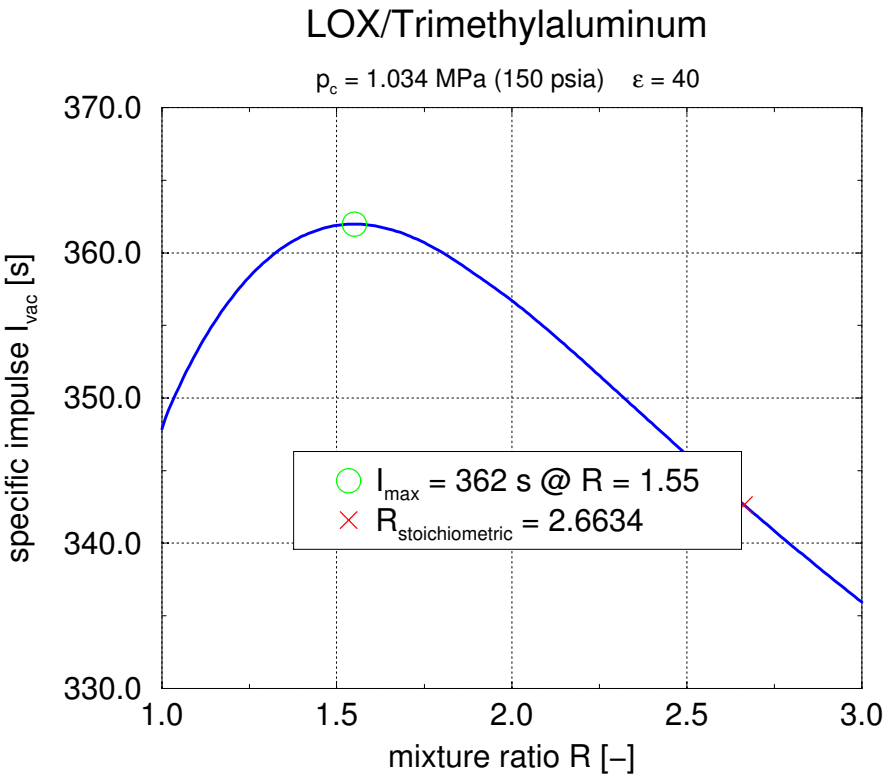

Figure 2: Theoretical Isp-performance of LOX/Trimethylaluminium

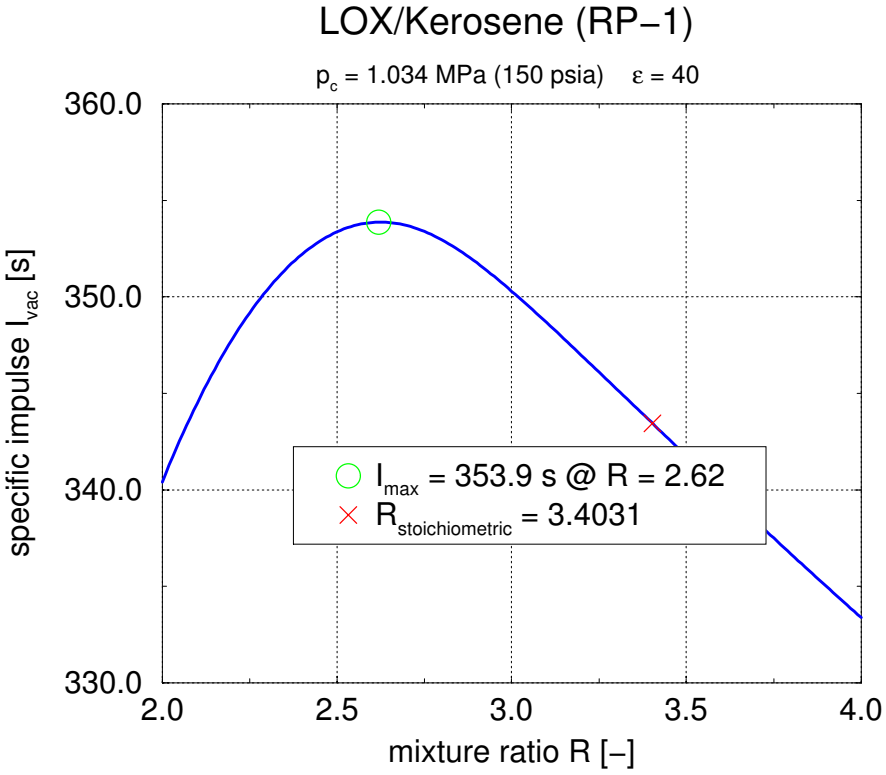

Figure 3: Theoretical Isp-performance of LOX/RP-1

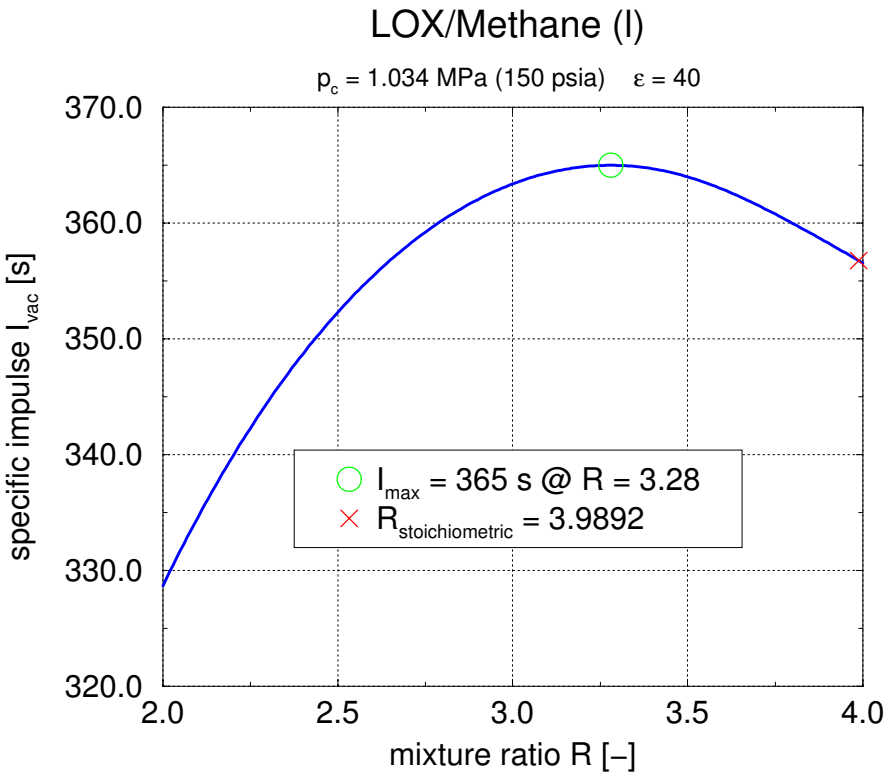

Figure 4: Theoretical Isp-performance of LOX/Methane

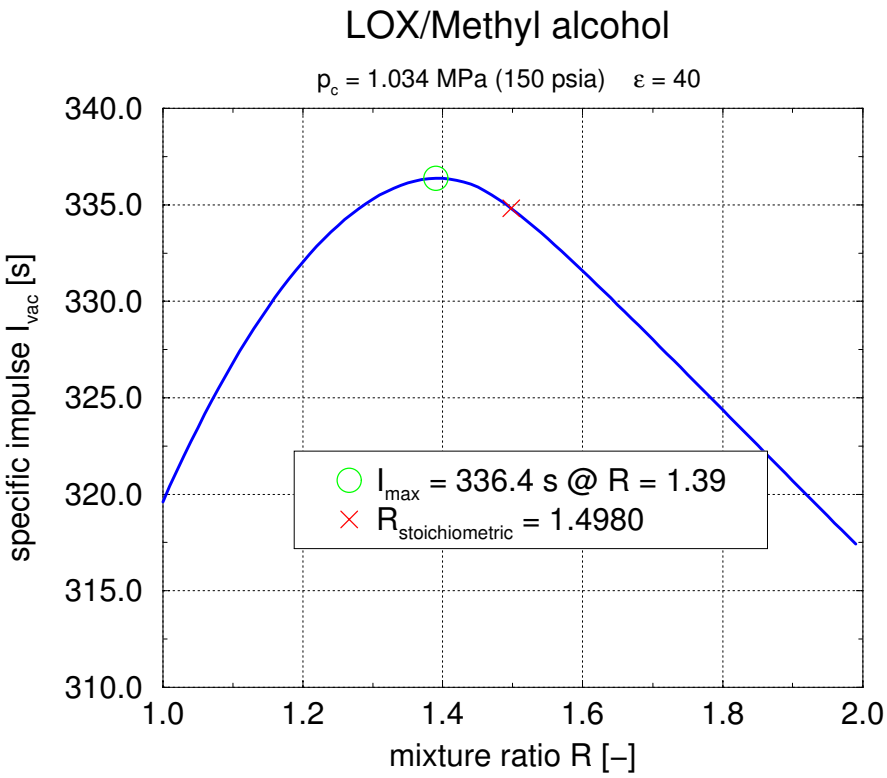

Figure 5: Theoretical Isp-performance of LOX/Methanol

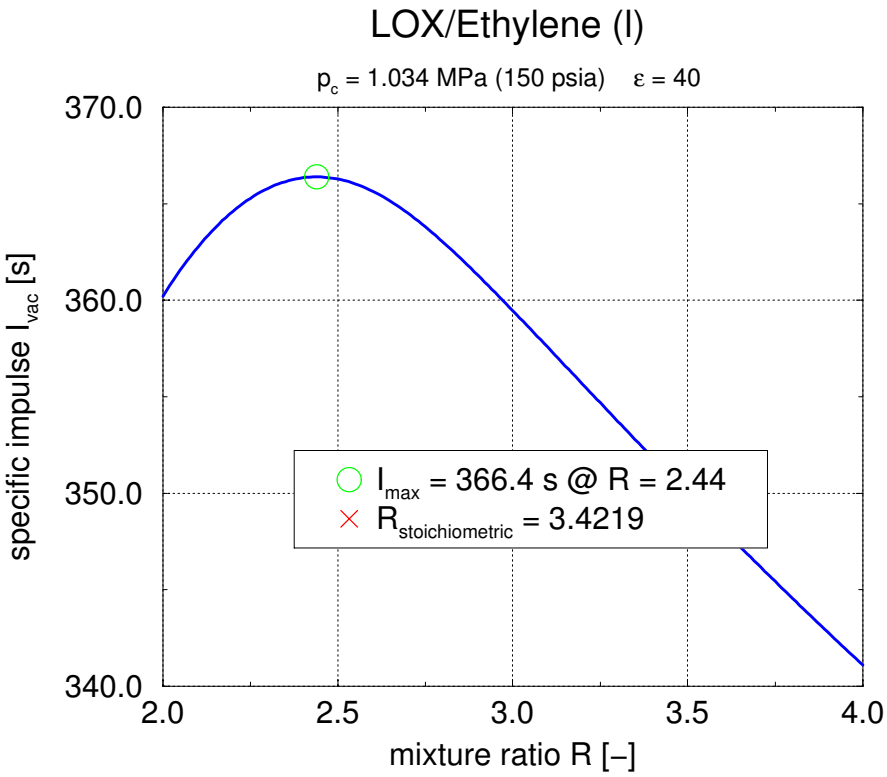

Figure 6: Theoretical Isp-performance of LOX/Ethylene

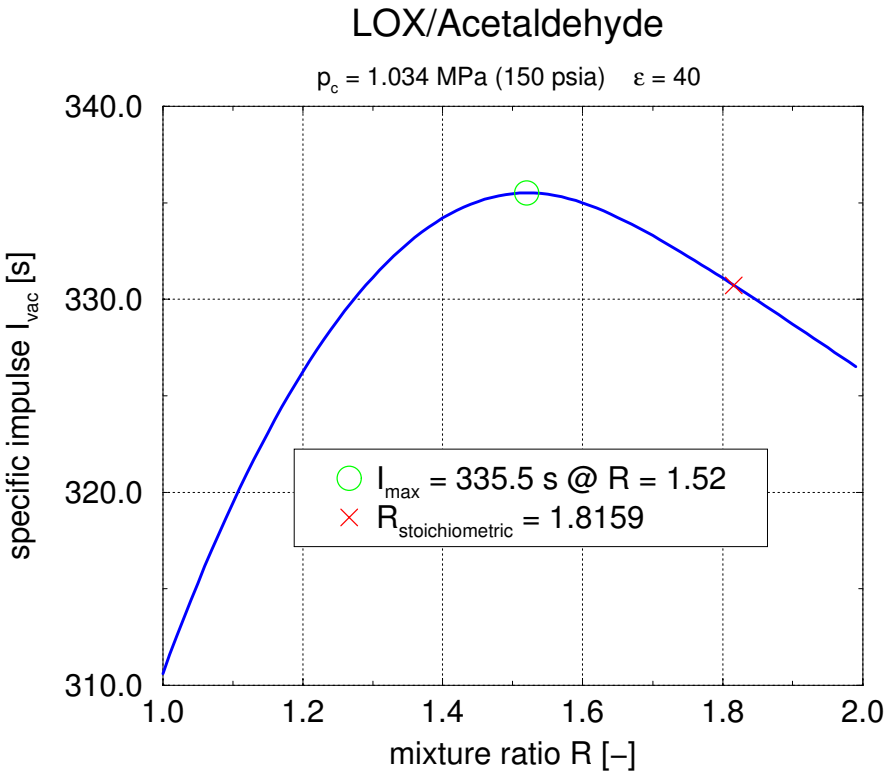

Figure 7: Theoretical Isp-performance of LOX/Acetaldehyde

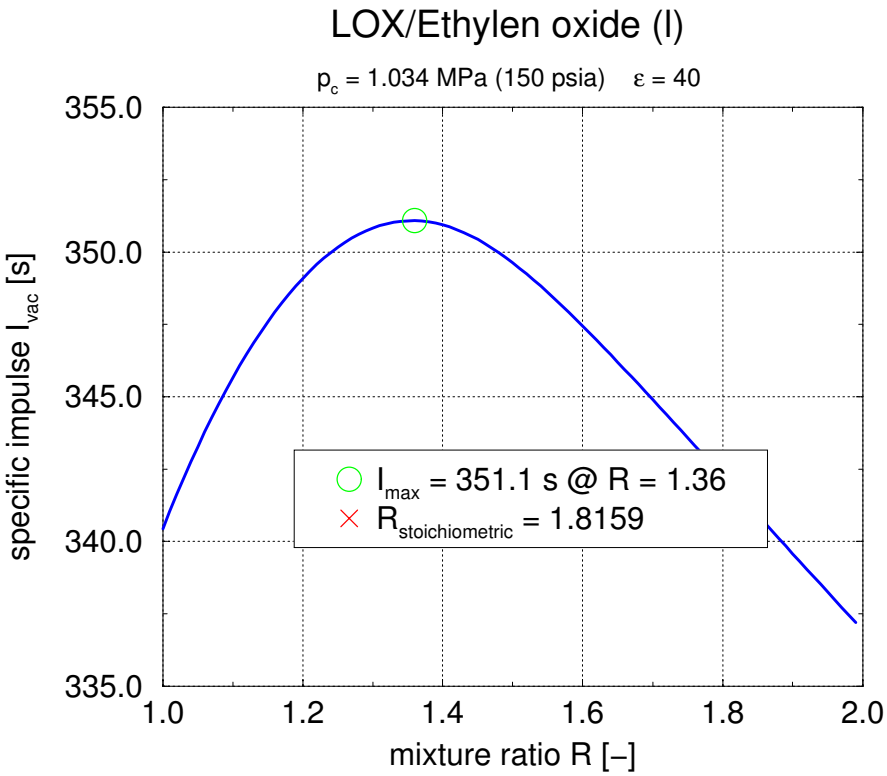

Figure 8: Theoretical Isp-performance of LOX/Ethylene oxide

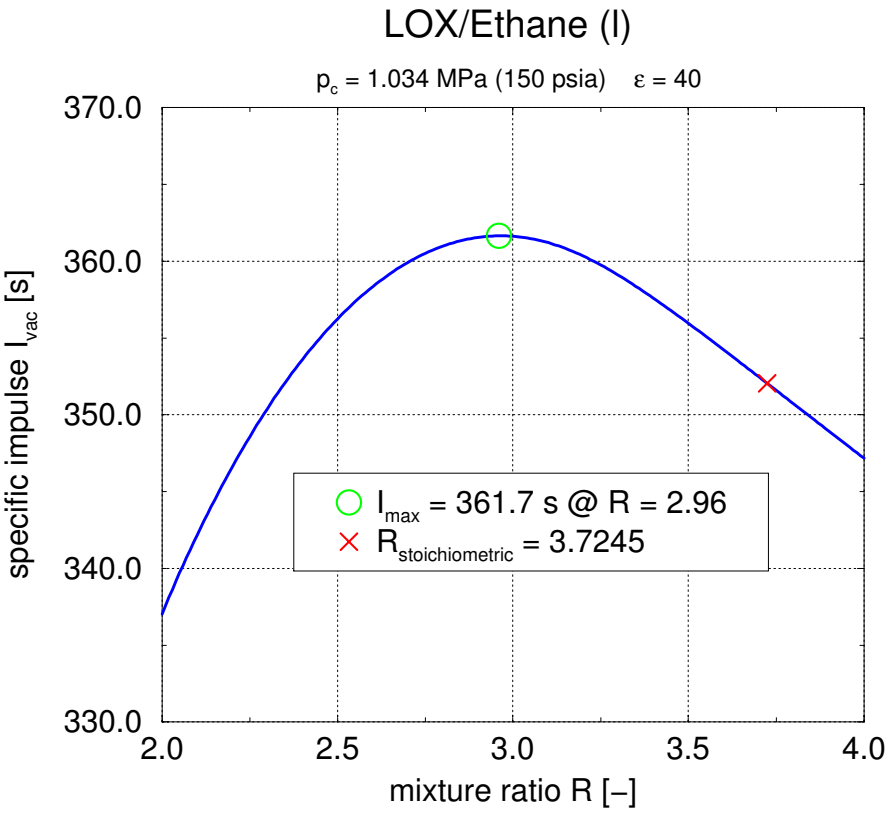

Figure 9: Theoretical Isp-performance of LOX/Ethane

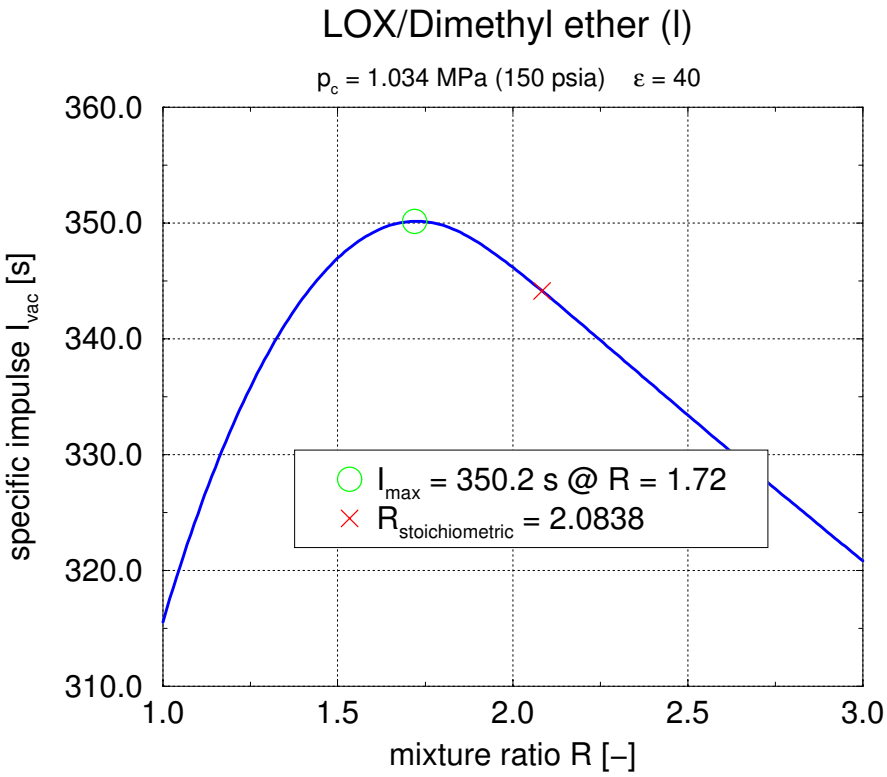

Figure 10: Theoretical Isp-performance of LOX/Dimethyl ether

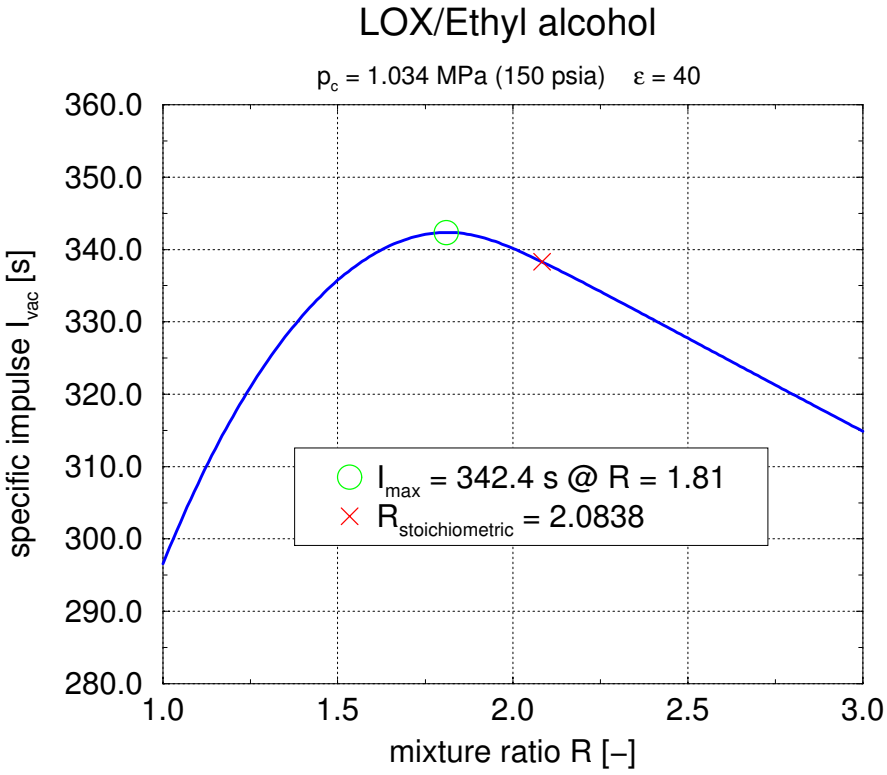

Figure 11: Theoretical Isp-performance of LOX/Ethanol

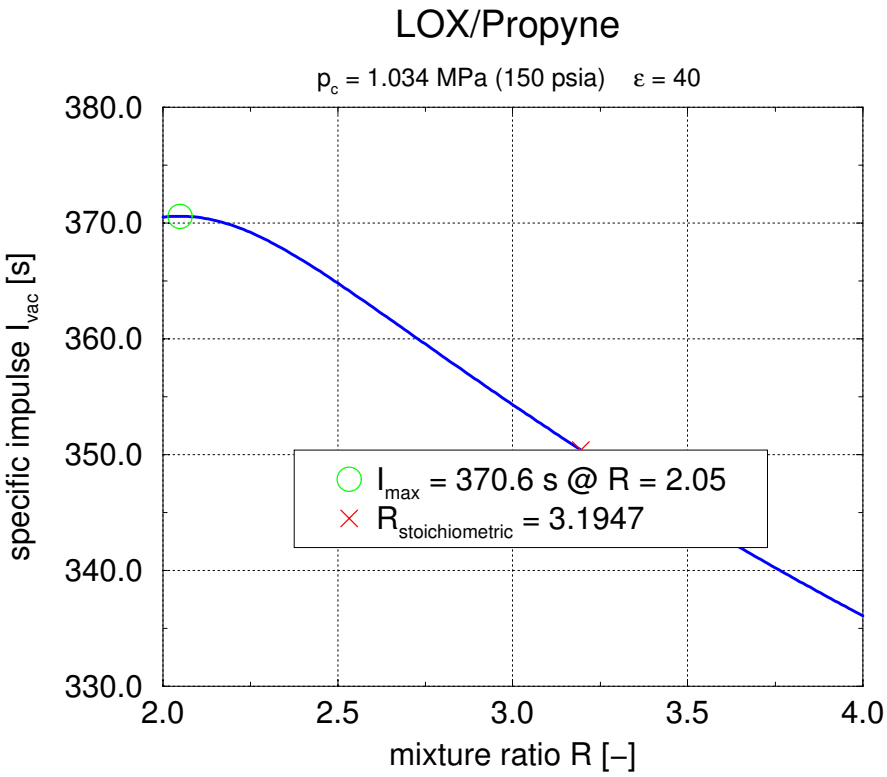

Figure 12: Theoretical Isp-performance of LOX/Propyne

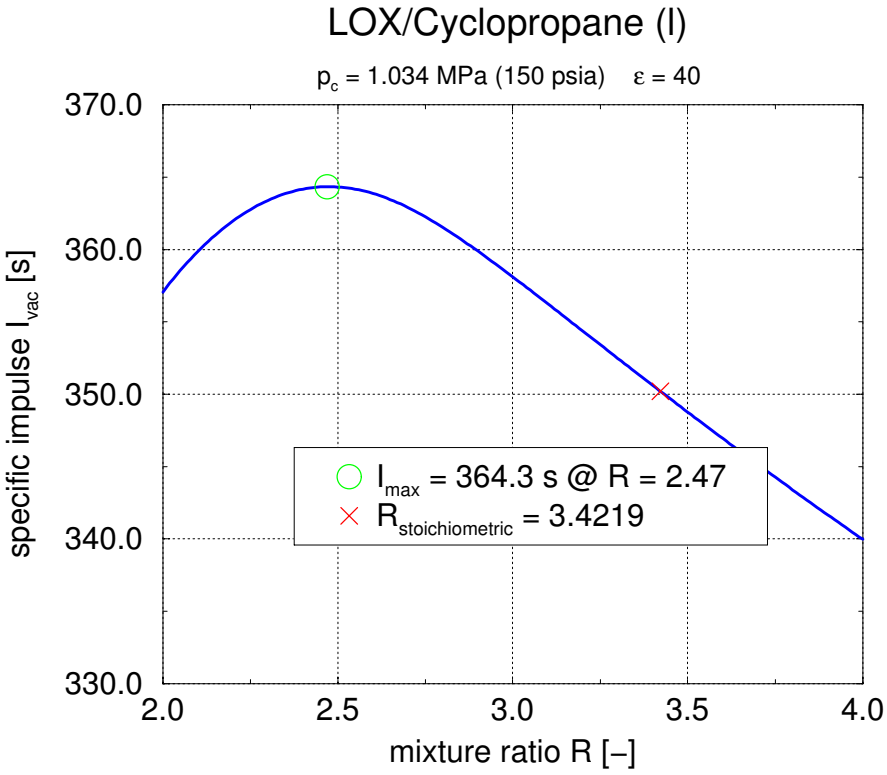

Figure 13: Theoretical Isp-performance of LOX/Cyclopropane

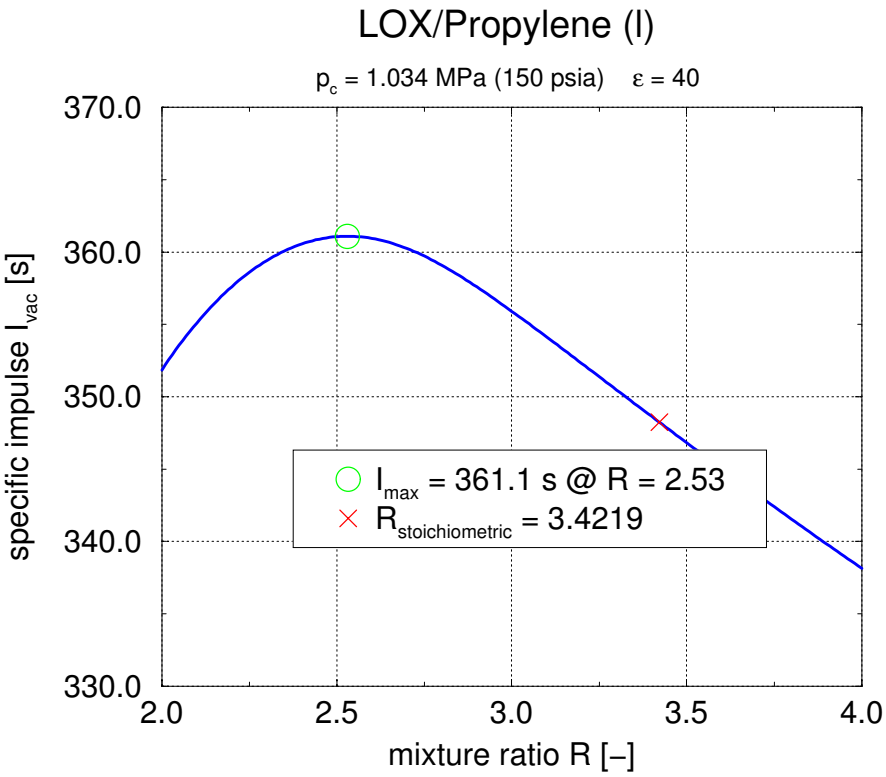

Figure 14: Theoretical Isp-performance of LOX/Propylene

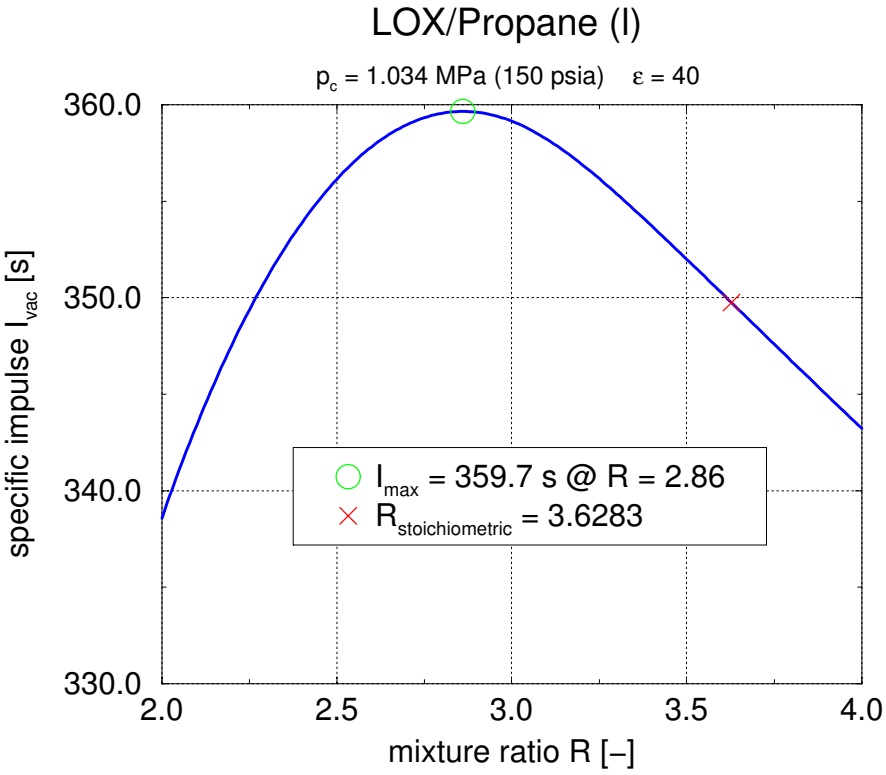

Figure 15: Theoretical Isp-performance of LOX/Propane

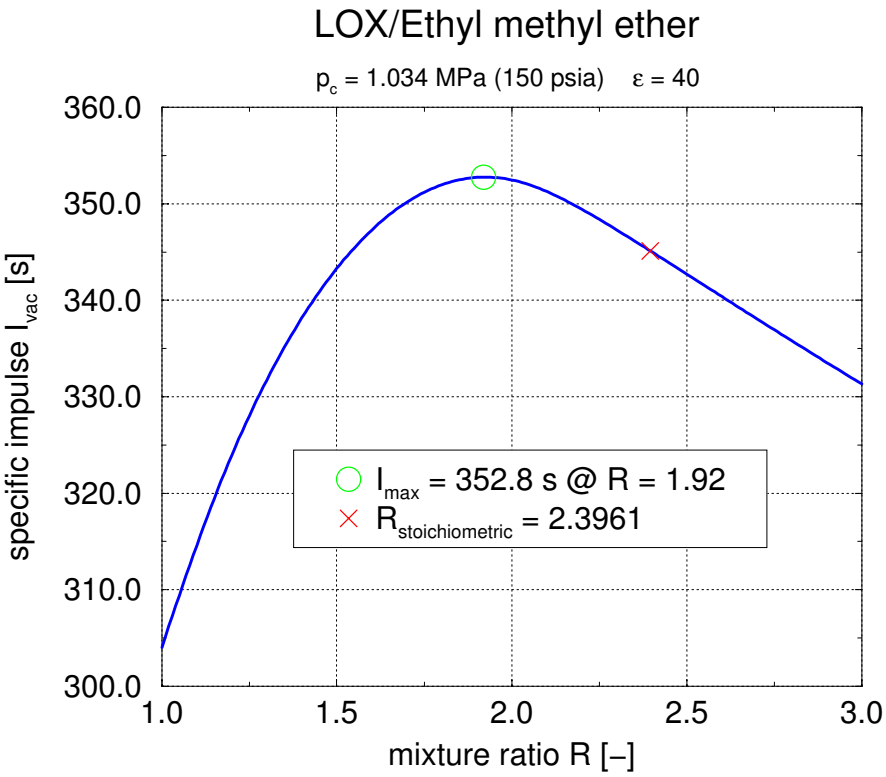

Figure 16: Theoretical Isp-performance of LOX/Ethyl methyl ether

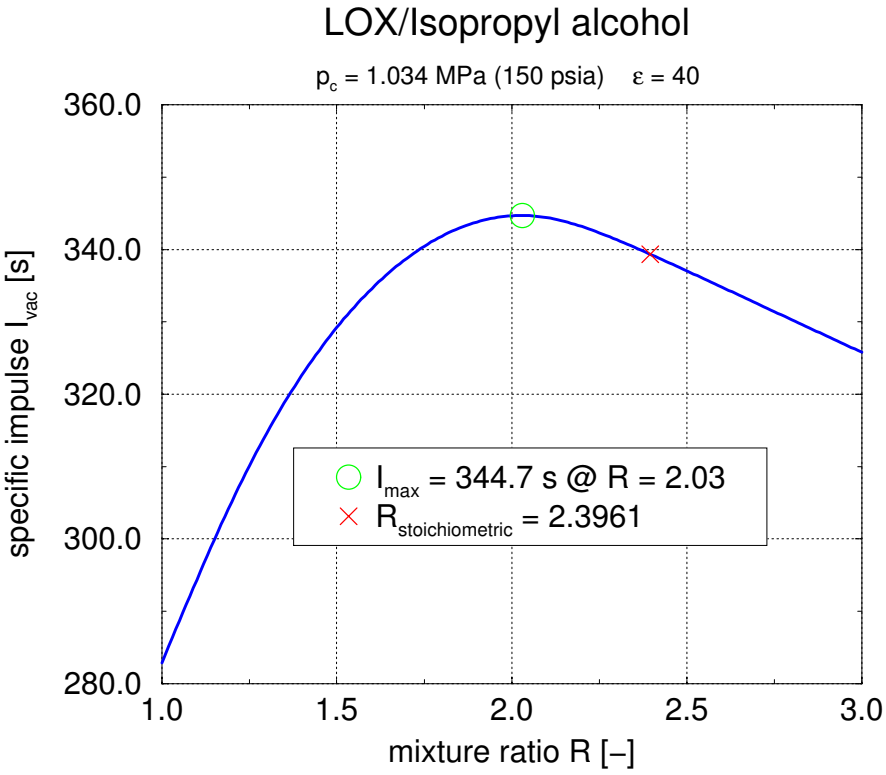

Figure 17: Theoretical Isp-performance of LOX/Isopropyl alcohol

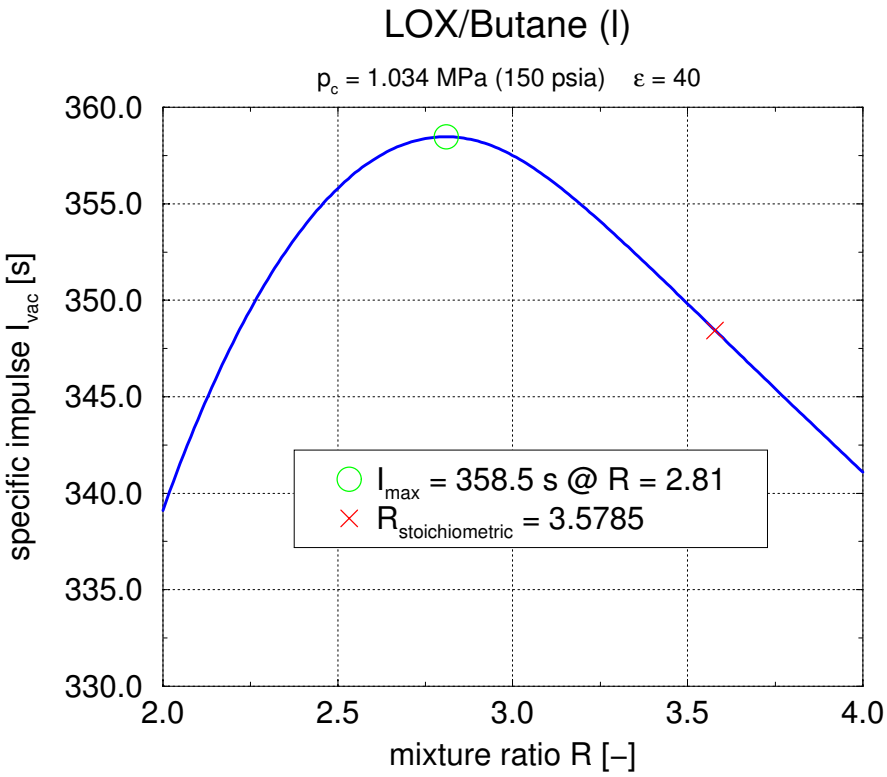

Figure 18: Theoretical Isp-performance of LOX/Butane

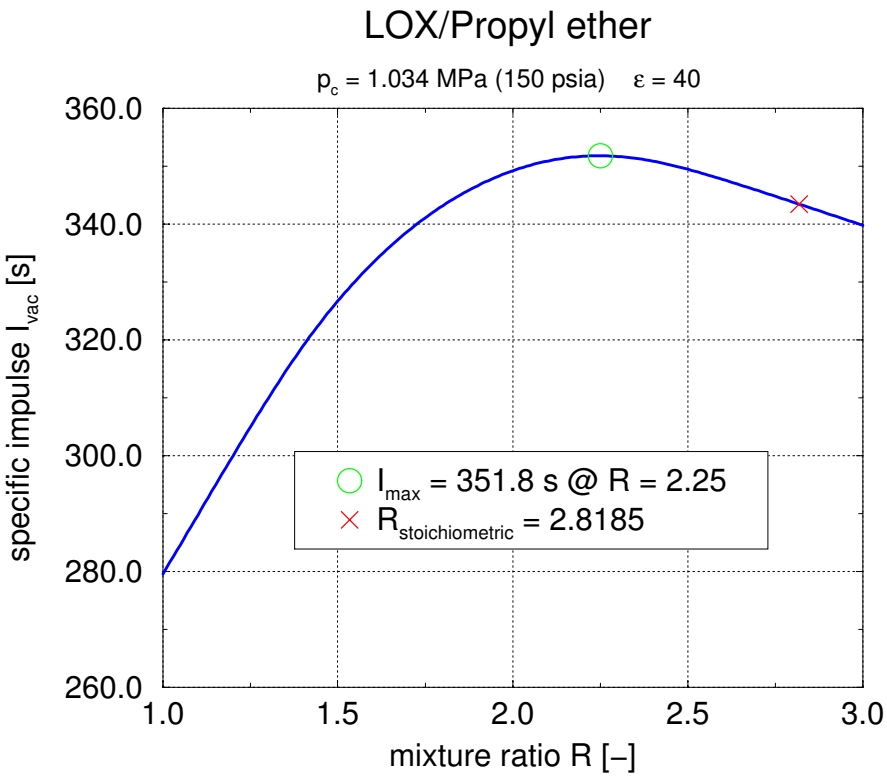

Figure 19: Theoretical Isp-performance of LOX/Propyl ether

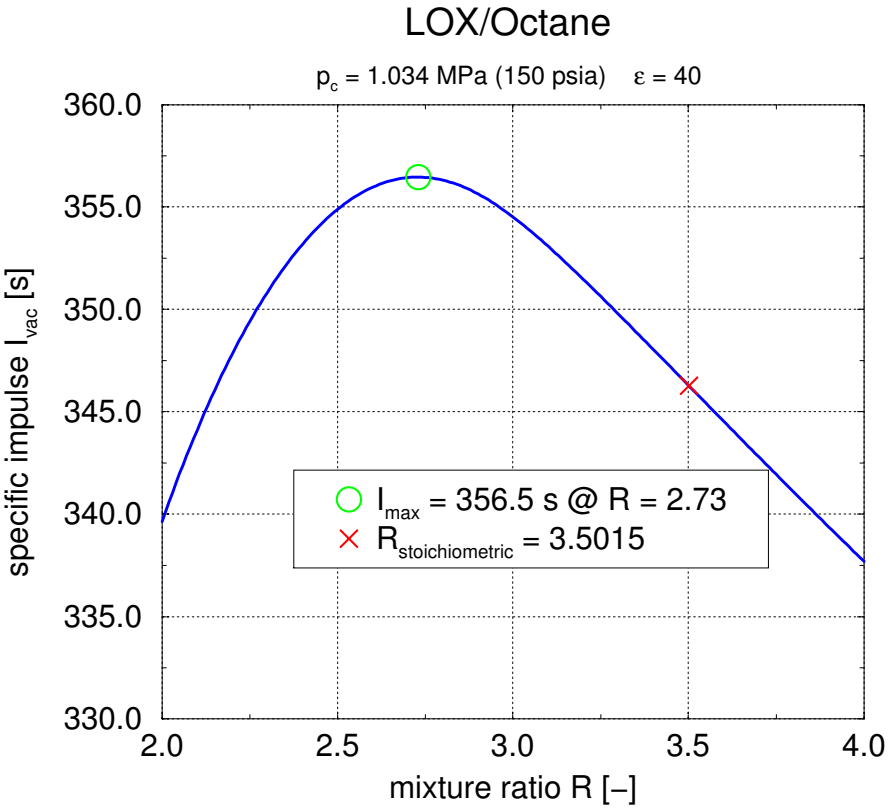

Figure 20: Theoretical Isp-performance of LOX/Octane

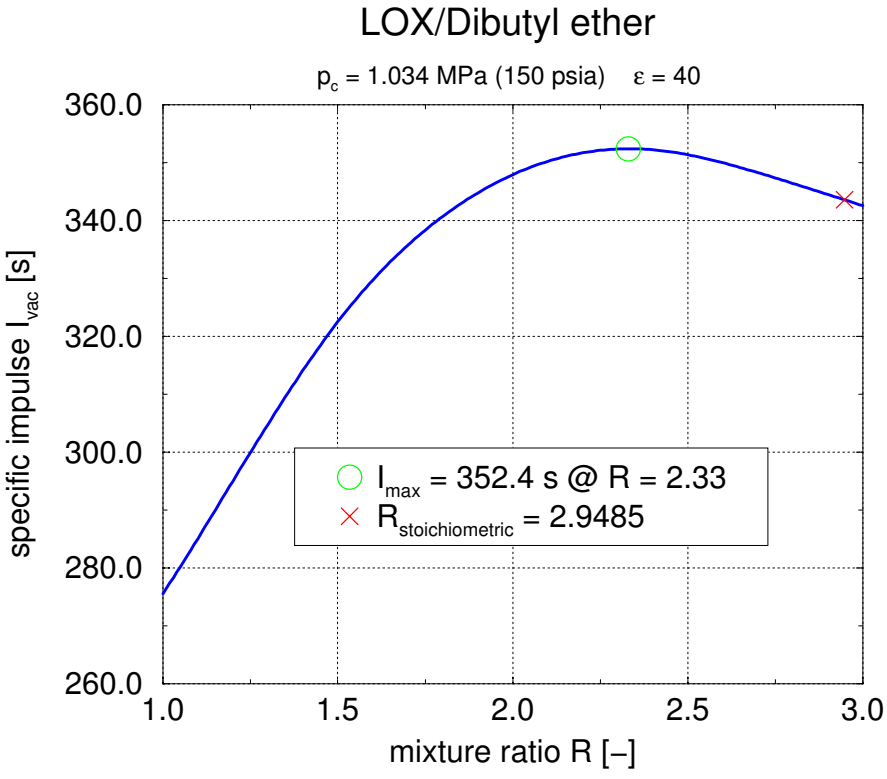

Figure 21: Theoretical Isp-performance of LOX/Dibutyl ether

3.2 Comparison of specific impulse for propellant-combinations using 90% H_2O_2 as oxidizer

Table 9 and Figure 22 give an overview over the results of the theoretical Isp-performance analysis of propellant-combinations using a 90% H_2O_2 solution as oxidizer. Figure 23 to Figure 41 show the respective specific vacuum impulses of each propellant combination.

The mixture ratio is varied in steps of 0.01 to find the mixture ratio leading to the maximum values of I_{vac} (labeled "R_{opt}" in Table 9).

Fuel	R_{stoich} *[-]*	R_{opt} *[-]*	I_{vac} *[s]*	T_c *[K]*
Trimethylaluminium	6.292	5.63	325	2863
Kerosene (RP-1)	8.039	7.96	314.5	2690
Methane (l)	9.423	9.37	316.1	2624
Methyl alcohol	3.539	3.53	304.6	2545
Ethylene (l)	8.083	7.83	321.2	2757
Acetaldehyde	4.29	4.27	307.5	2648
Ethylen oxide (l)	4.29	4.19	317.9	2754
Ethane (l)	8.798	8.73	316.2	2658
Dimethy ether (l)	4.922	4.89	313.6	2656
Ethyl alcohol	4.922	4.91	308.2	2601
Propyne	7.547	7	325	2842
Cyclopropane (l)	8.083	7.88	320.1	2745
Propylene (l)	8.083	7.93	318.3	2726
Propane (l)	8.571	8.5	315.8	2668
Ethyl methyl ether	5.66	5.61	314.8	2675
Isopropyl alcohol	5.66	5.64	309.5	2621
Butane (l)	8.453	8.38	315.5	2673
Propyl ether	6.658	6.61	313.6	2670
Octane	8.271	8.2	315	2679
Dibutyl ether	6.965	6.91	313.9	2674

Table 9: Performance of propellant-combinations using 90% H_2O_2 as oxidizer

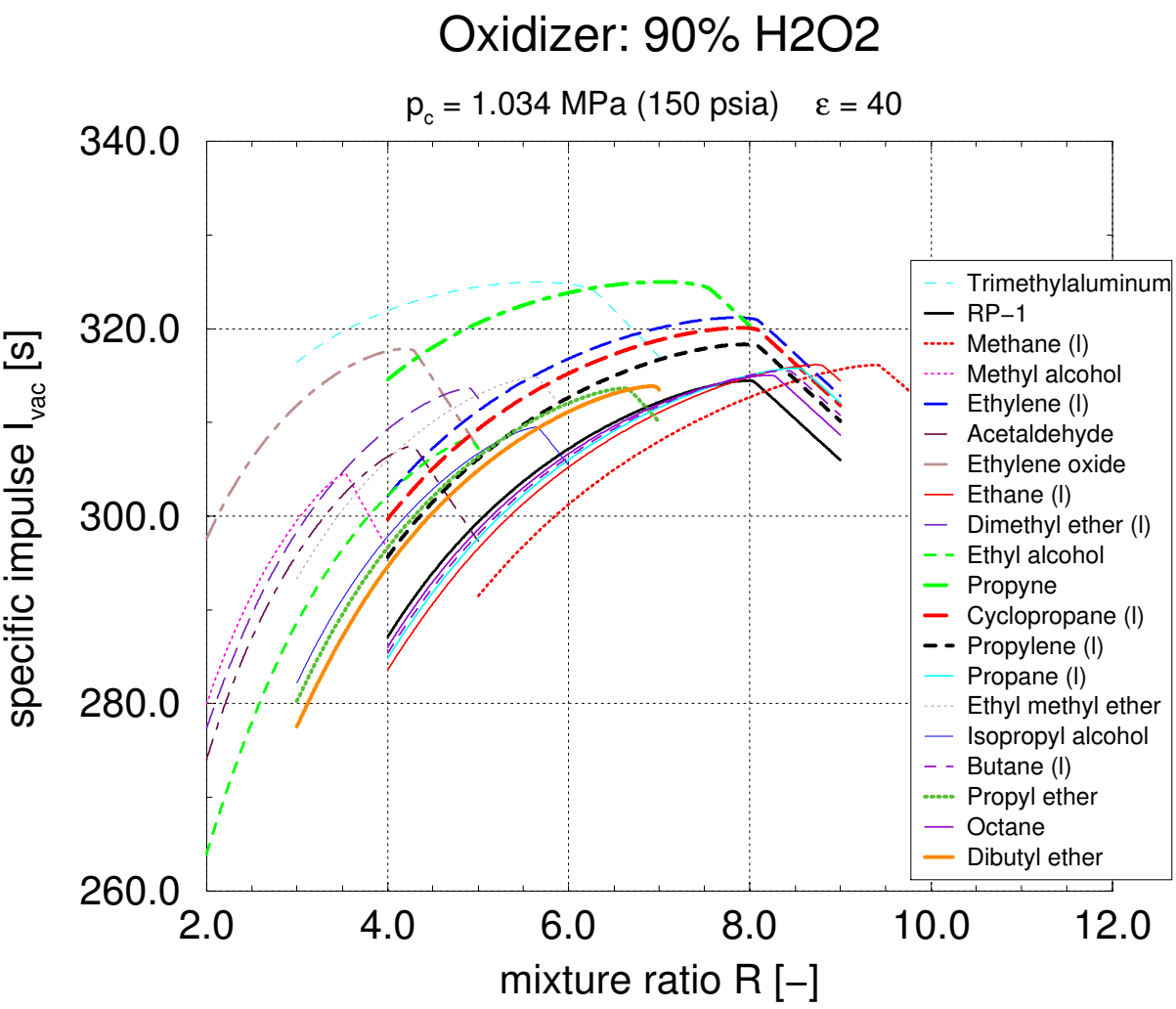

Figure 22: Vacuum impulse of propellant-combinations using H_2O_2 as oxidizer

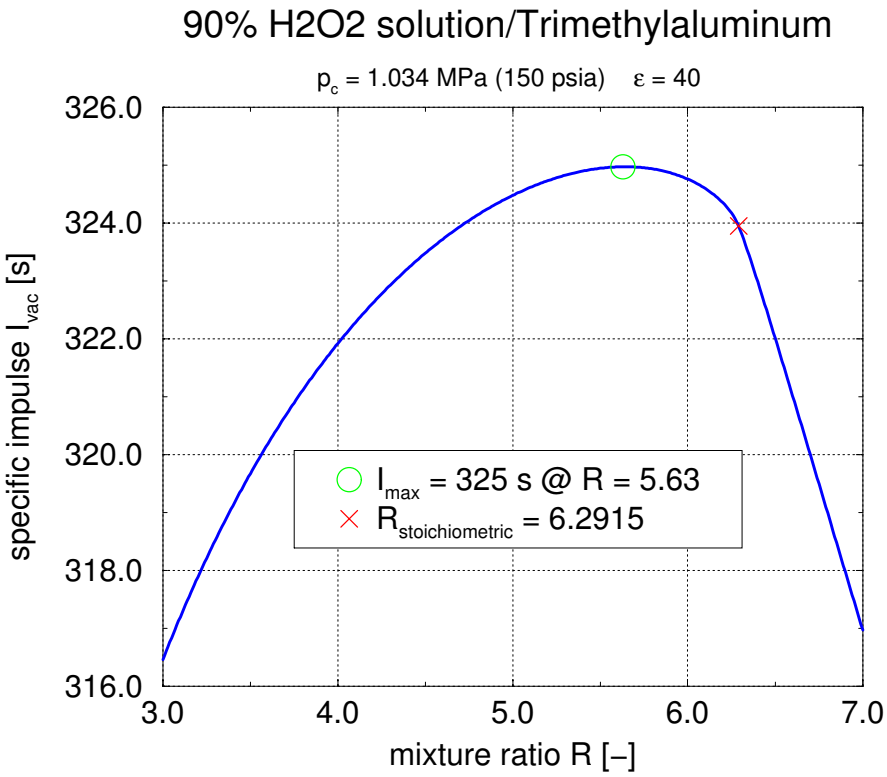

Figure 23: Theoretical Isp-performance of H2O2/Trimethylaluminum

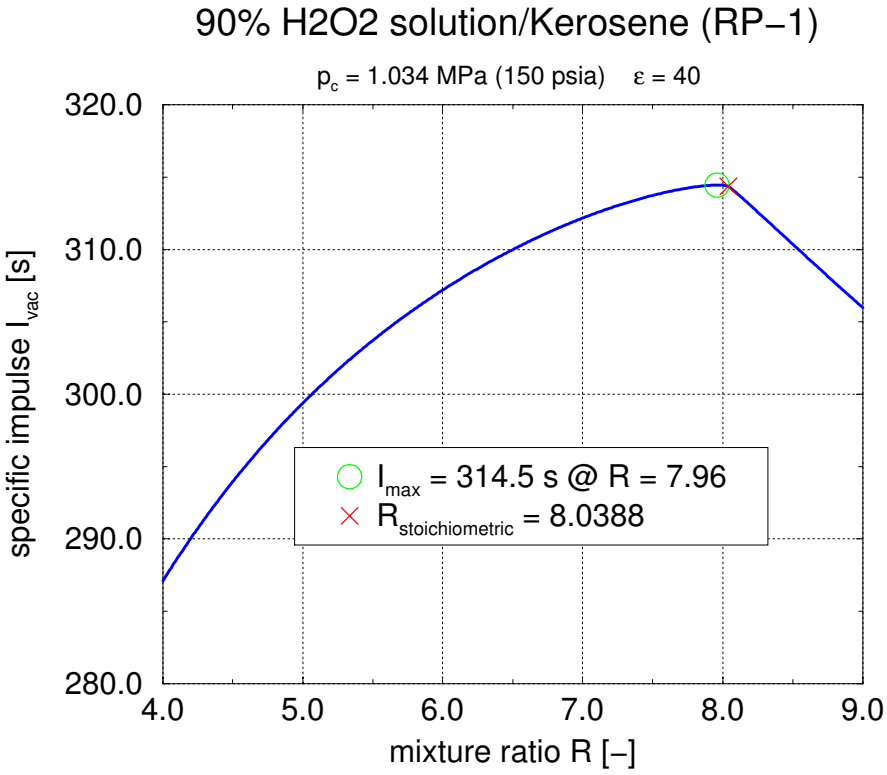

Figure 24: Theoretical Isp-performance of H2O2/RP-1

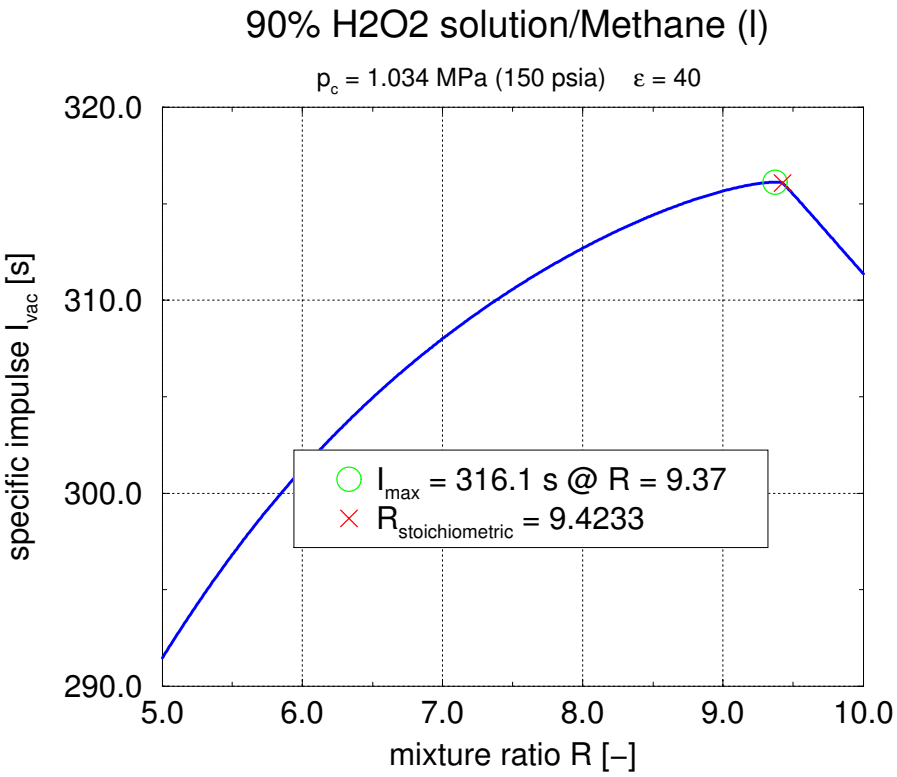

Figure 25: Theoretical Isp-performance of H2O2/Methane

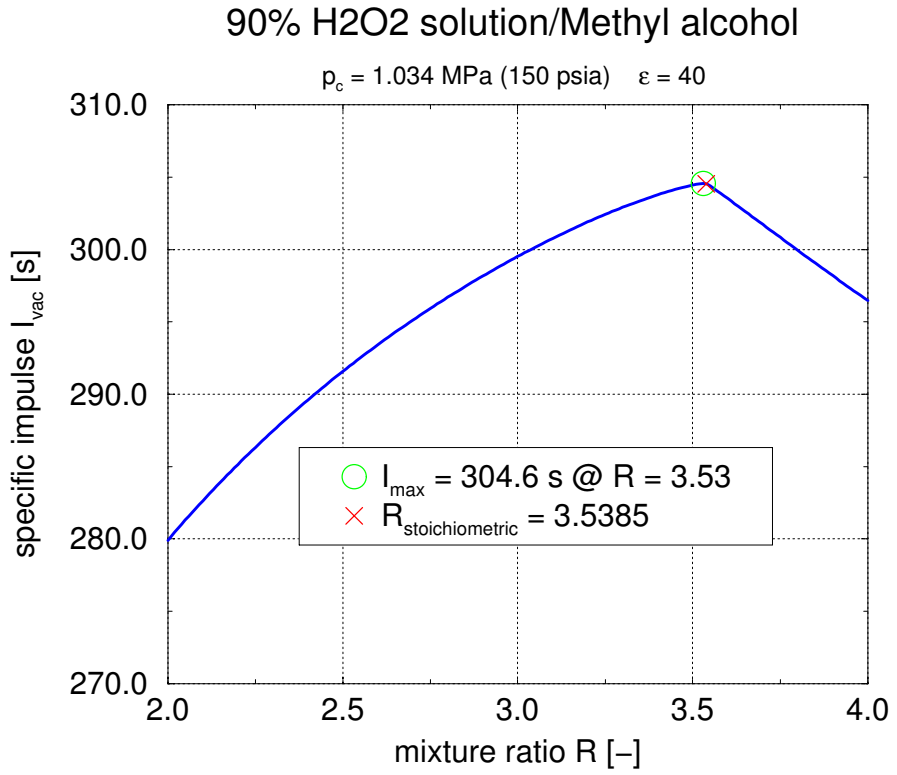

Figure 26: Theoretical Isp-performance of H2O2/Methanol

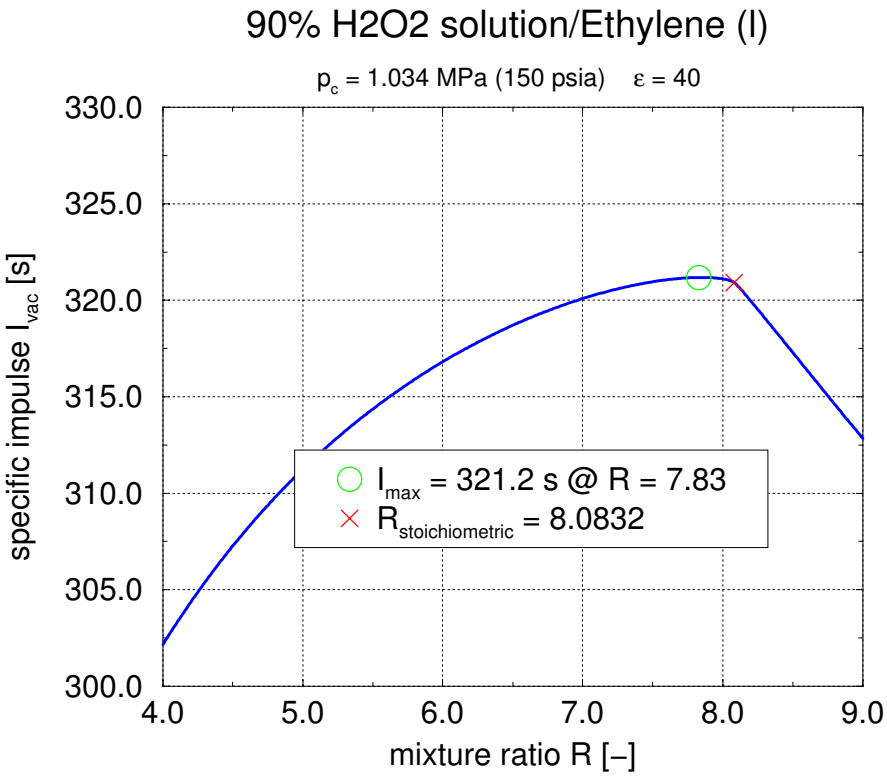

Figure 27: Theoretical Isp-performance of H2O2/Ethylene

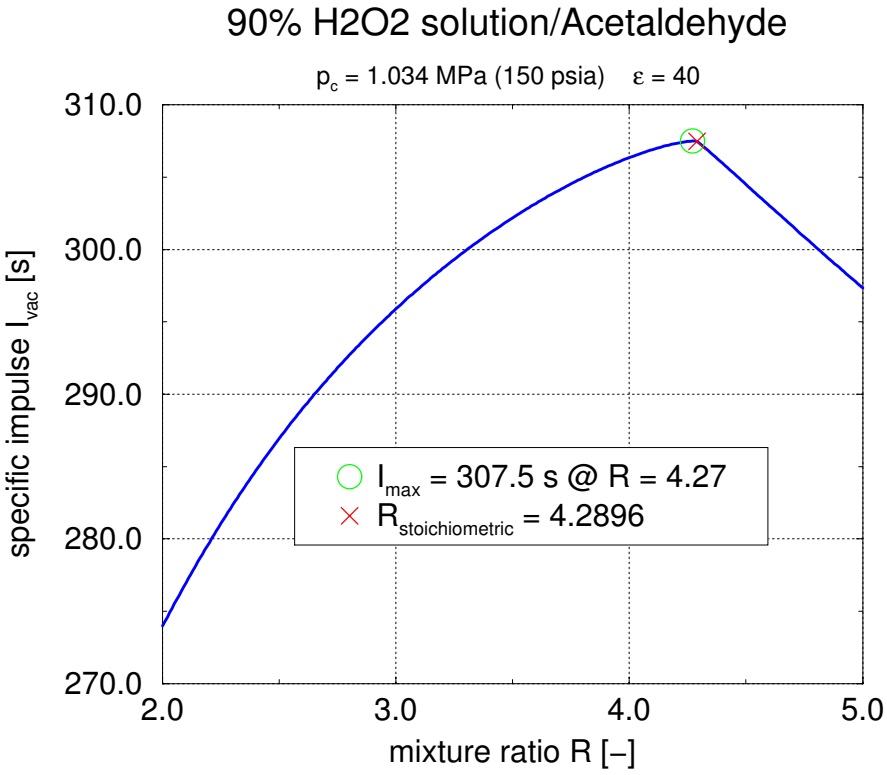

Figure 28: Theoretical Isp-performance of H2O2/Acetaldehyde

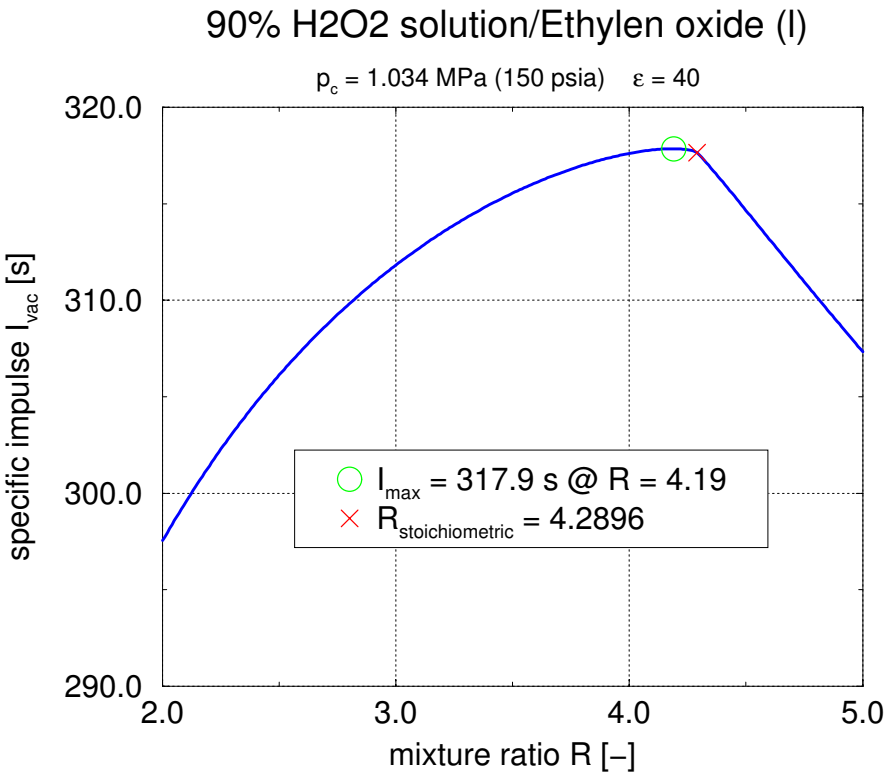

Figure 29: Theoretical Isp-performance of H2O2/Ethylene oxide

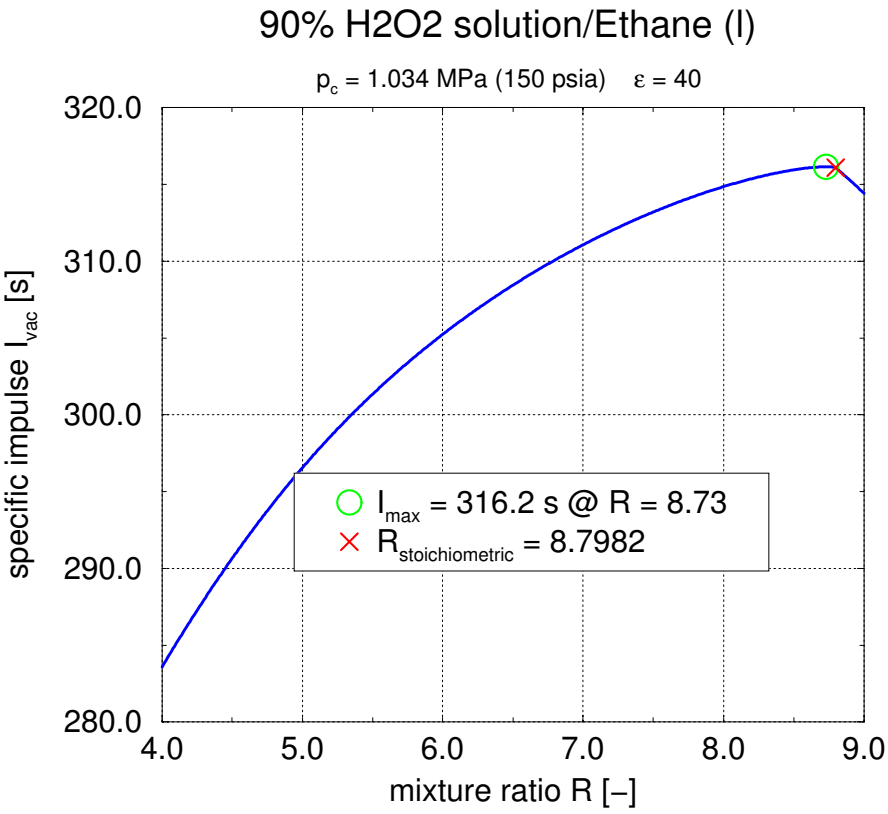

Figure 30: Theoretical Isp-performance of H2O2/Ethane

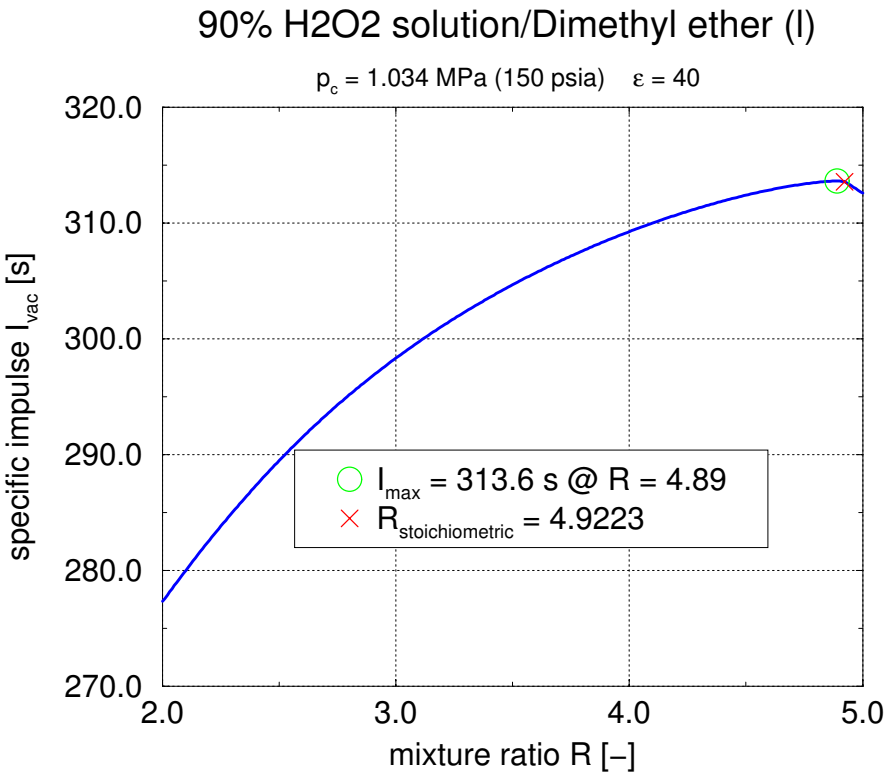

Figure 31: Theoretical Isp-performance of H2O2/Dimethyl ether

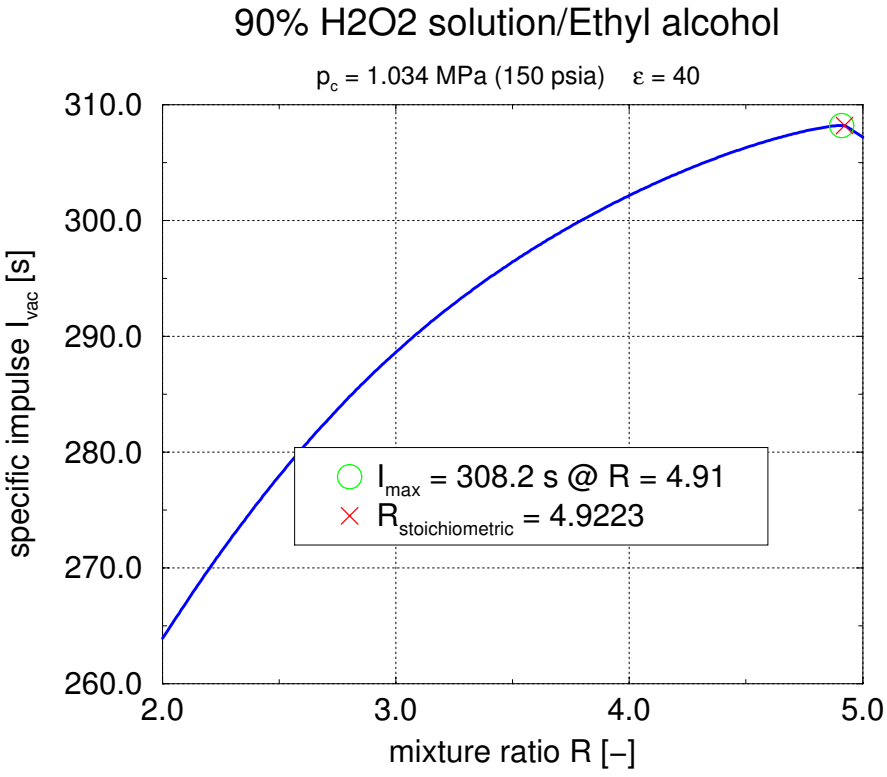

Figure 32: Theoretical Isp-performance of H2O2/Ethanol

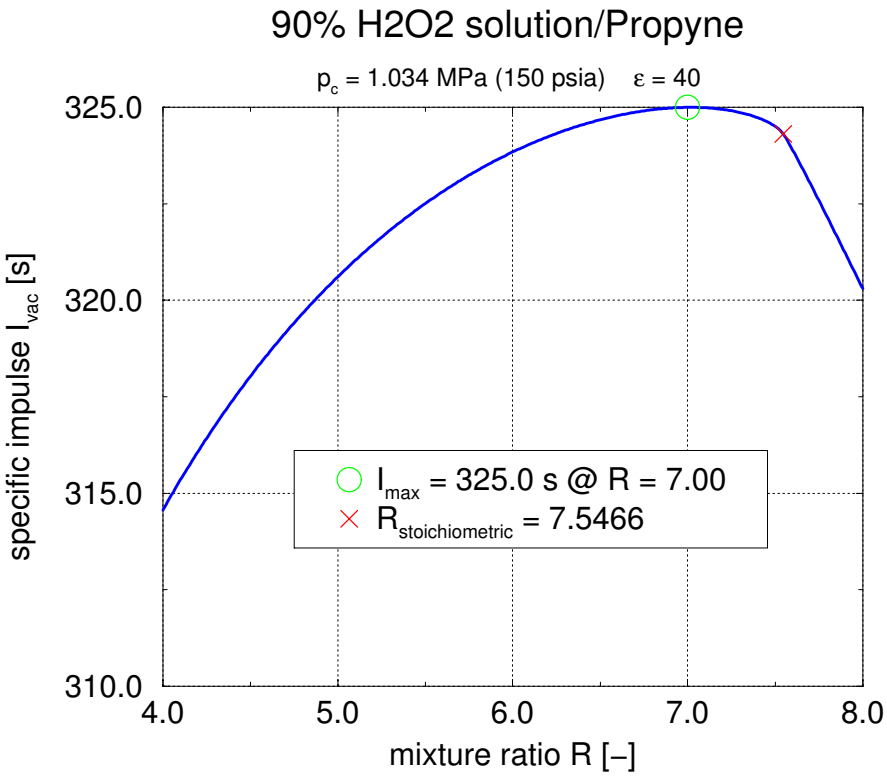

Figure 33: Theoretical Isp-performance of H2O2/Propyne

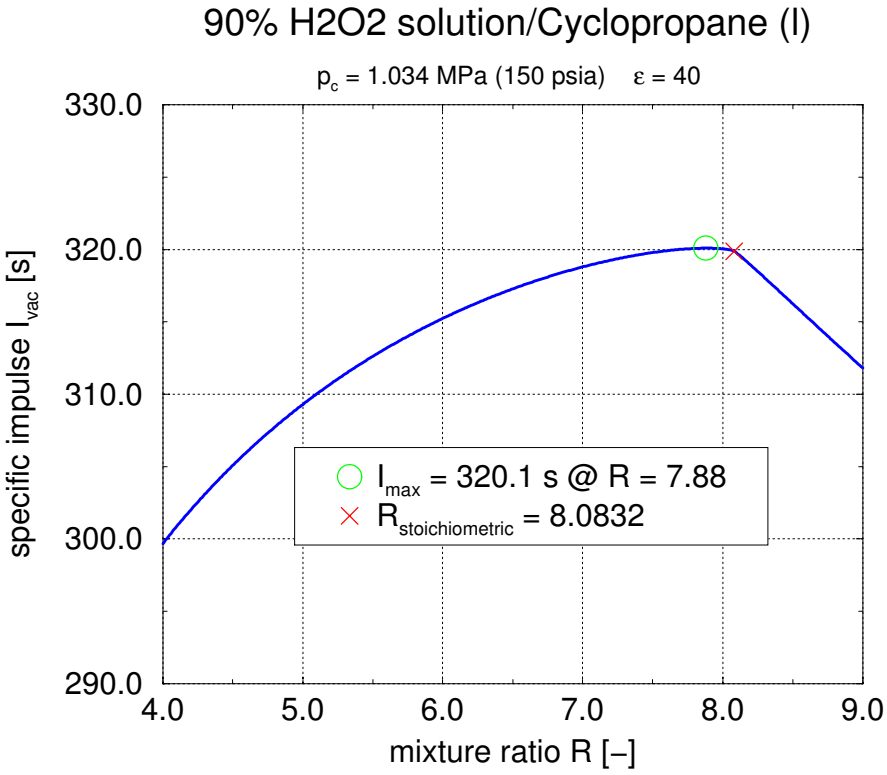

Figure 34: Theoretical Isp-performance of H2O2/Cyclopropane

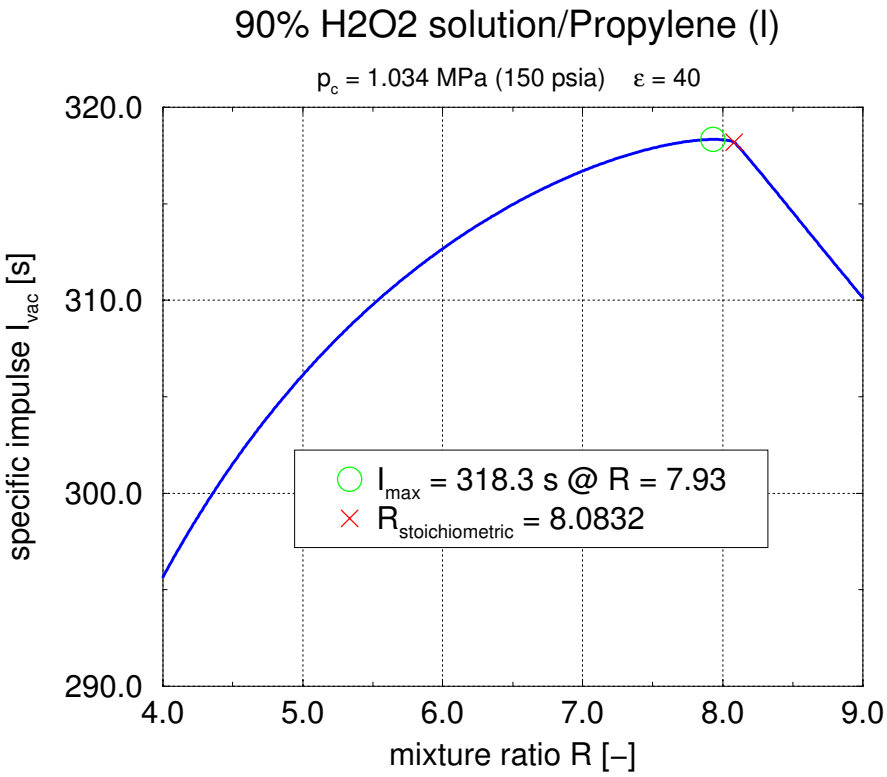

Figure 35: Theoretical Isp-performance of H2O2/Propylene

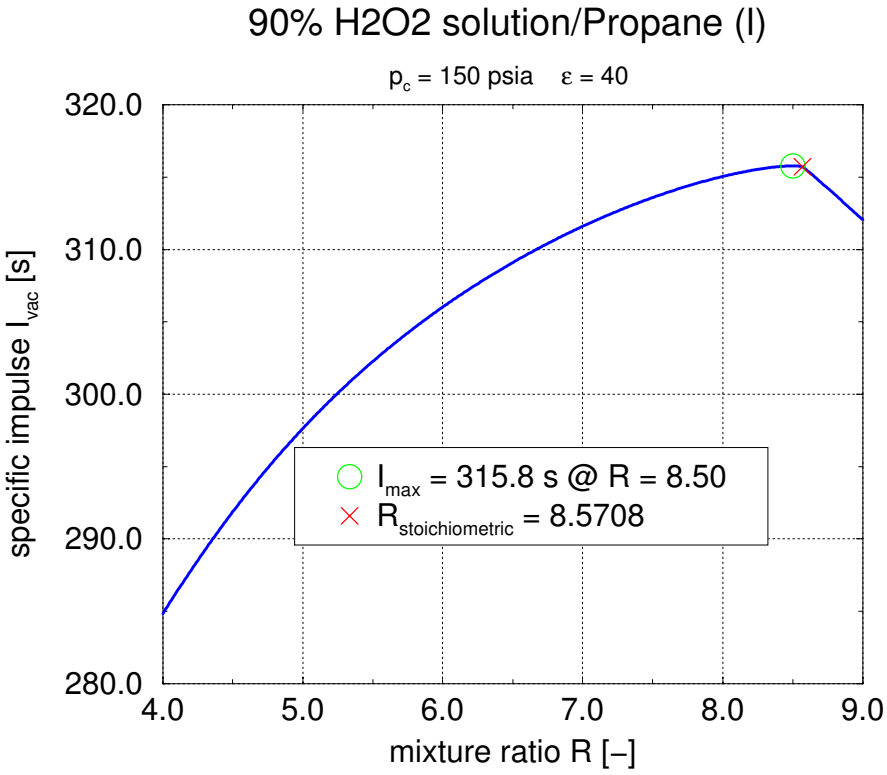

Figure 36: Theoretical Isp-performance of H2O2/Propane

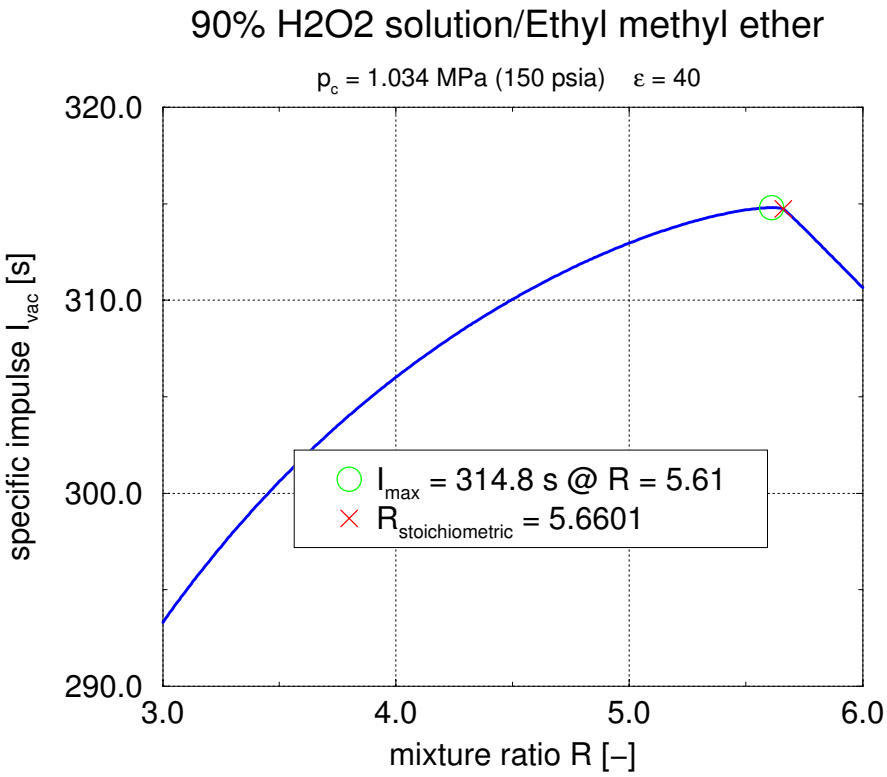

Figure 37: Theoretical Isp-performance of H2O2/Ethyl methyl ether

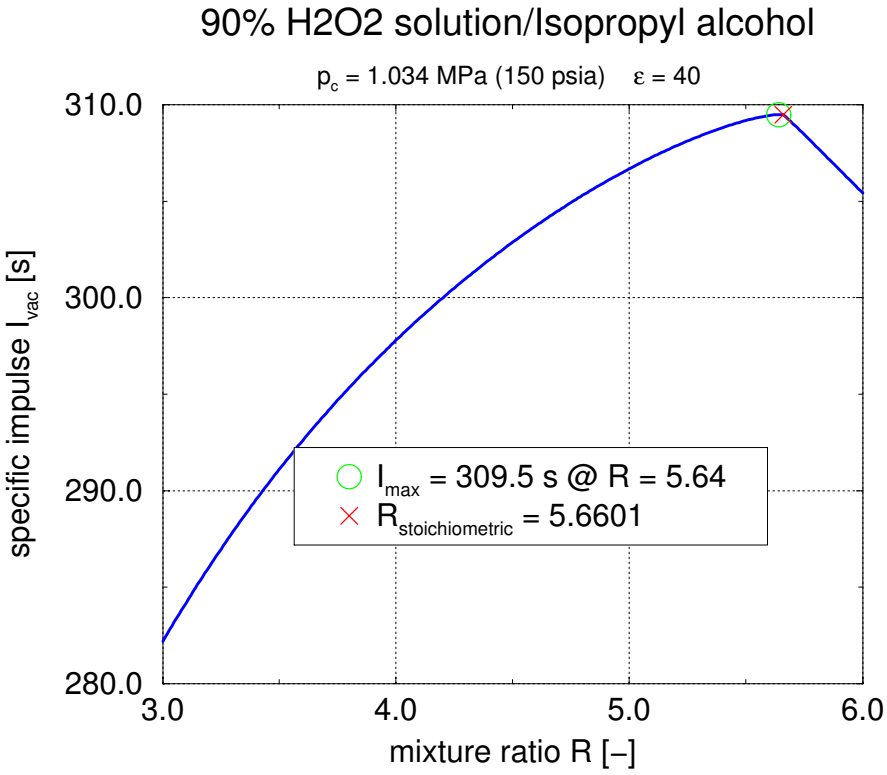

Figure 38: Theoretical Isp-performance of H2O2/Isopropyl alcohol

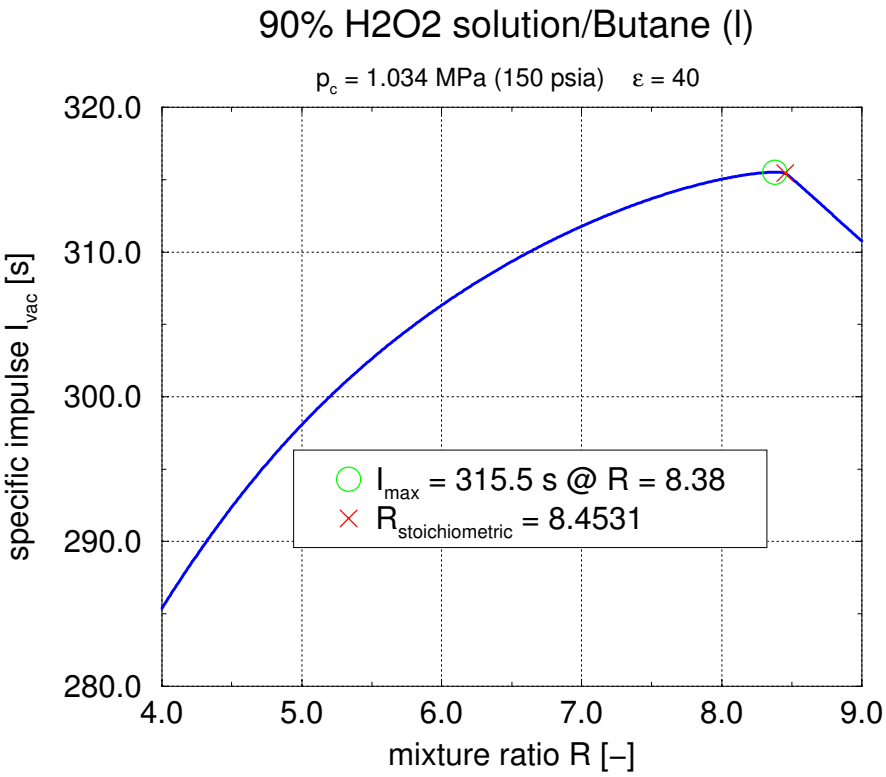

Figure 39: Theoretical Isp-performance of H2O2/Butane

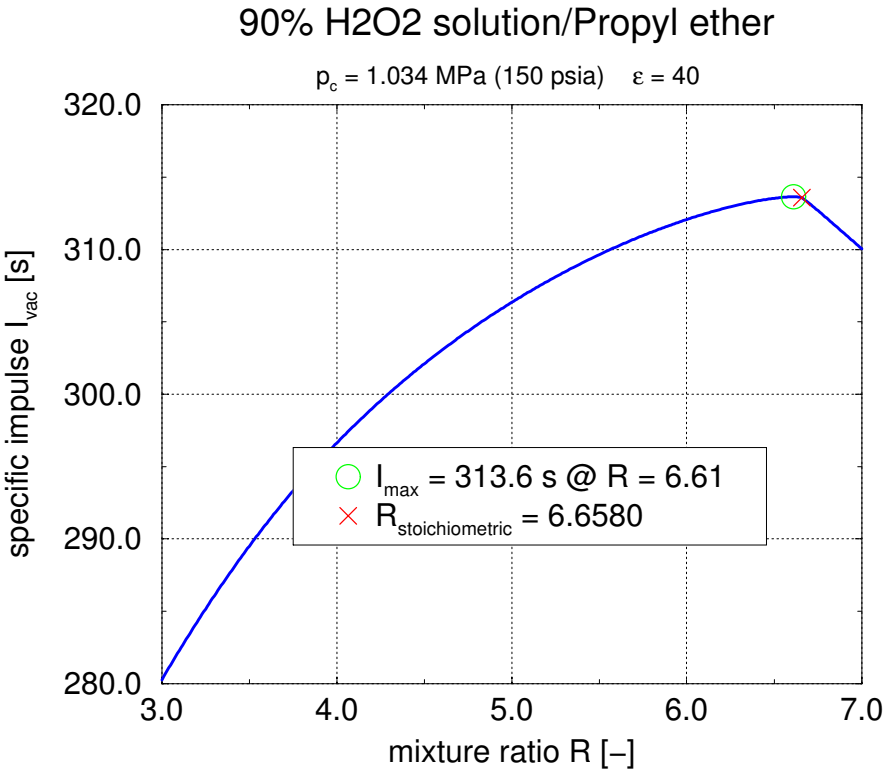

Figure 40: Theoretical Isp-performance of H2O2/Propyl ether

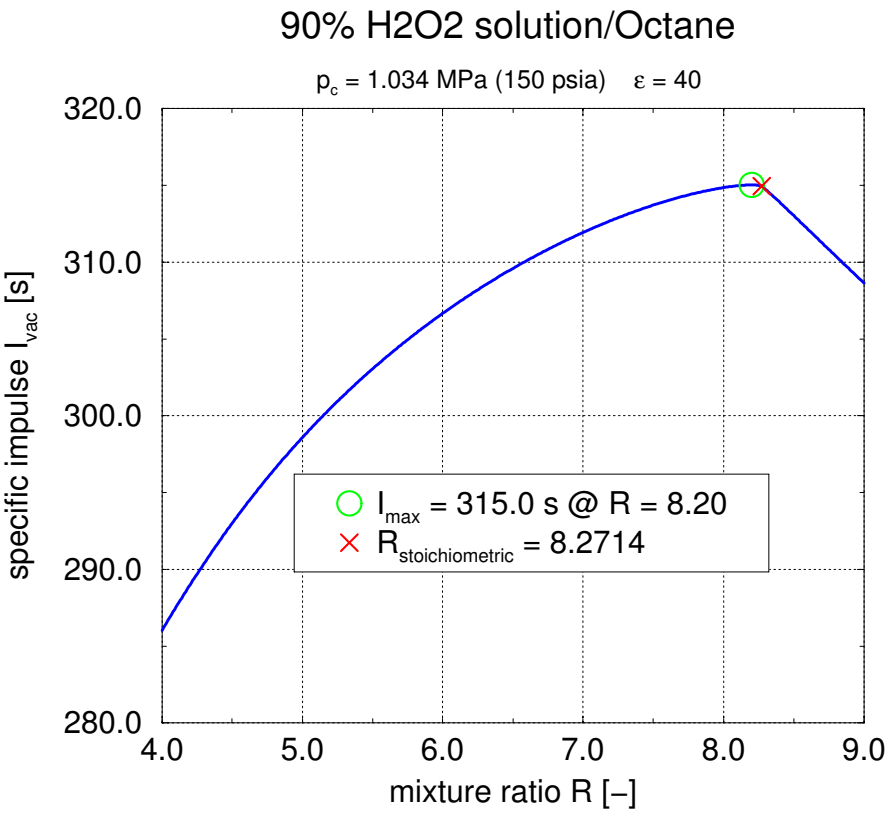

Figure 41: Theoretical Isp-performance of H2O2/Octane

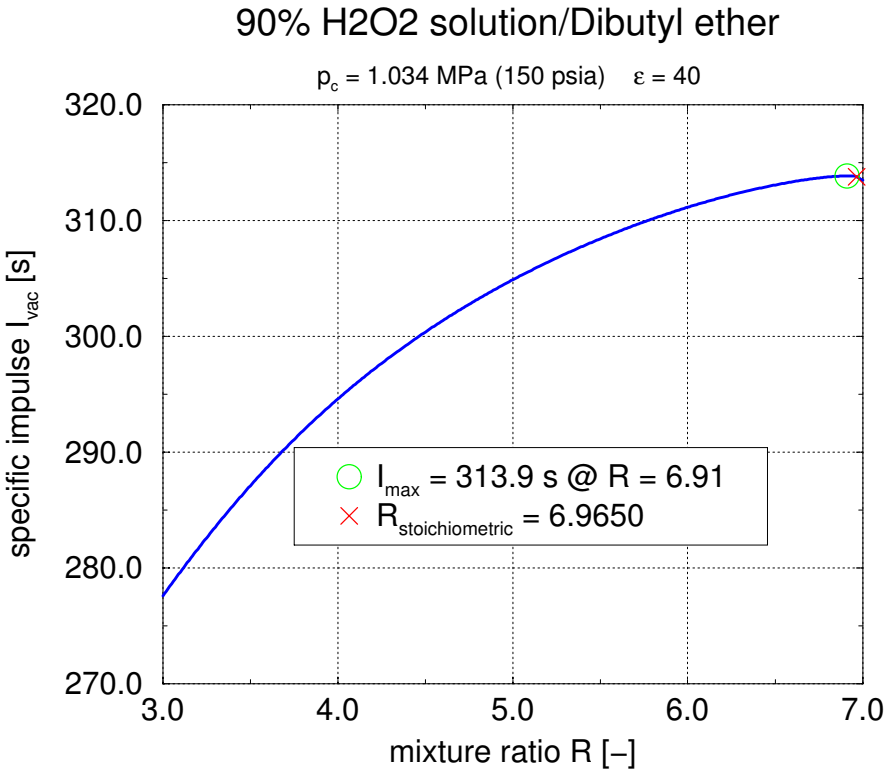

Figure 42: Theoretical Isp-performance of H2O2/Dibutyl ether

3.3 Comparison of the product of mean tank density and specific impulse for propellant-combinations using LOX as oxidizer

Figure 43 gives an overview over the results of the density and impulse analysis of propellant-combinations using liquid oxygen (LOX) as oxidizer.

Figure 44 to Figure 63 show the respective products of mean tank densities and specific vacuum impulses of each propellant-combination.

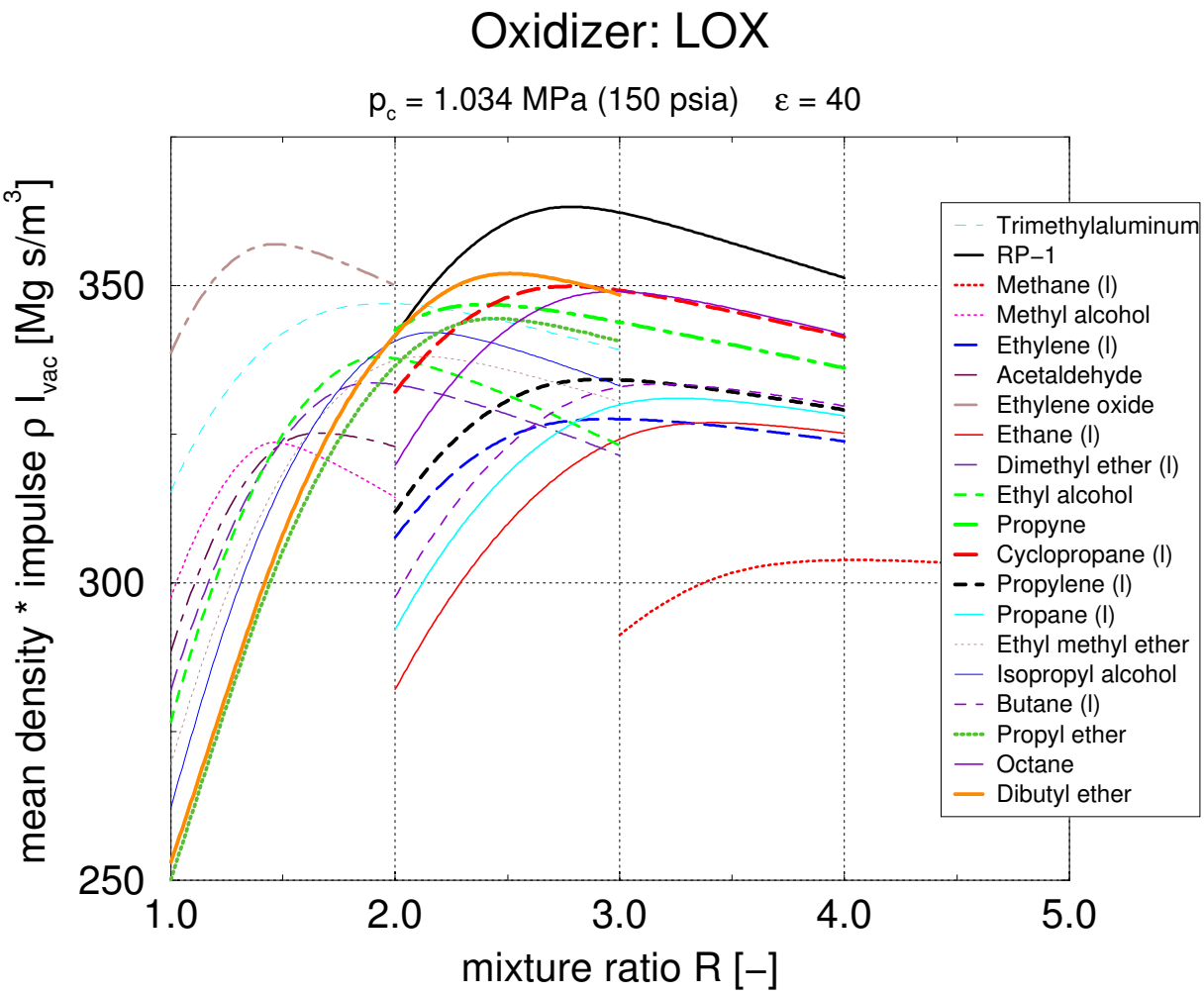

Figure 43: Mean density times vacuum impulse of propellant-combinations using LOX as oxidizer

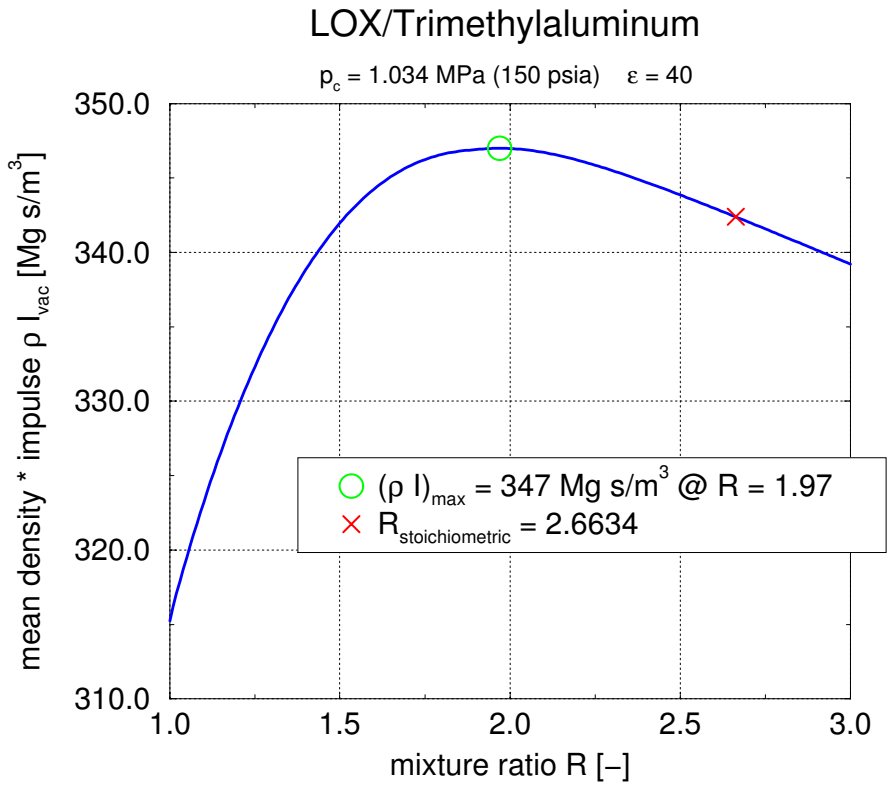

Figure 44: Density and impulse product of LOX/Trimethylaluminium

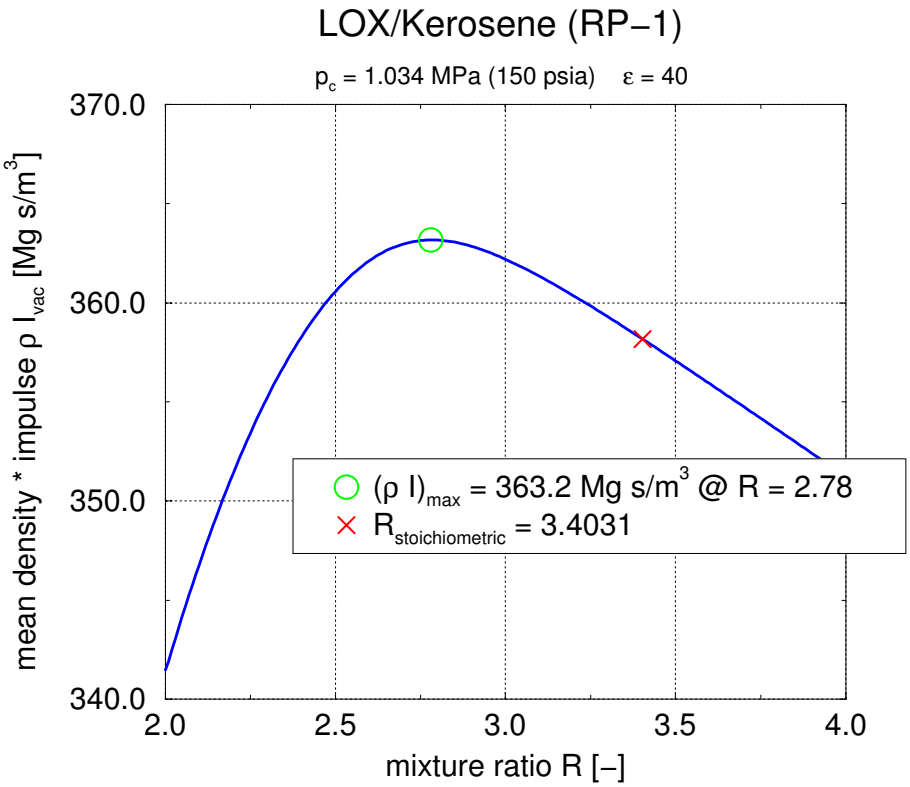

Figure 45: Density and impulse product of LOX/RP-1

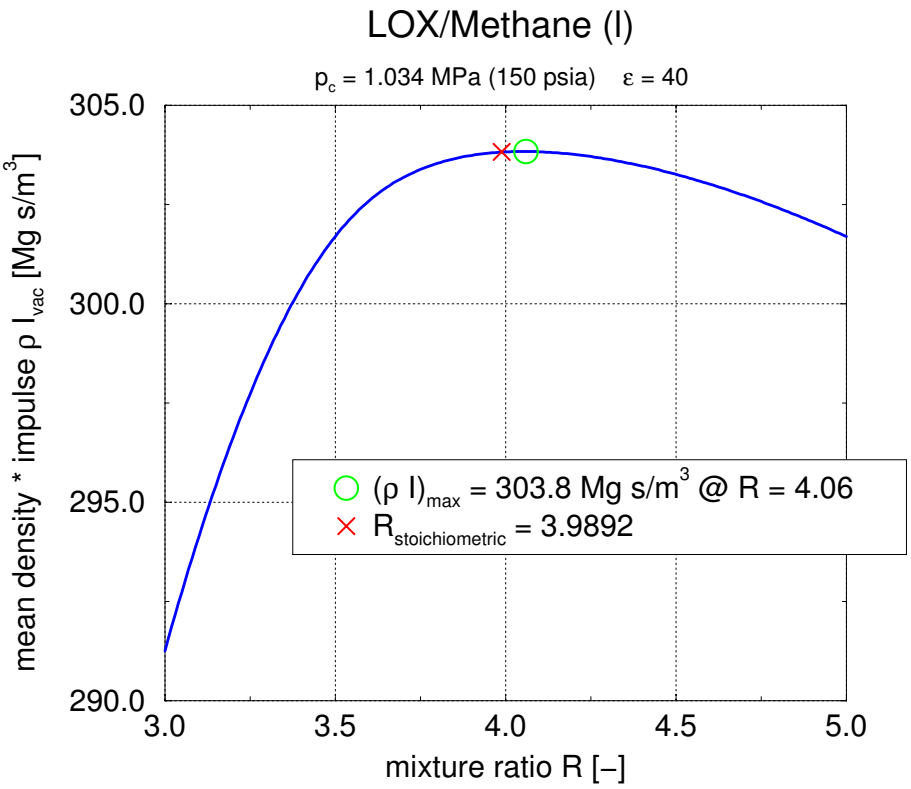

Figure 46: Density and impulse product of LOX/Methane

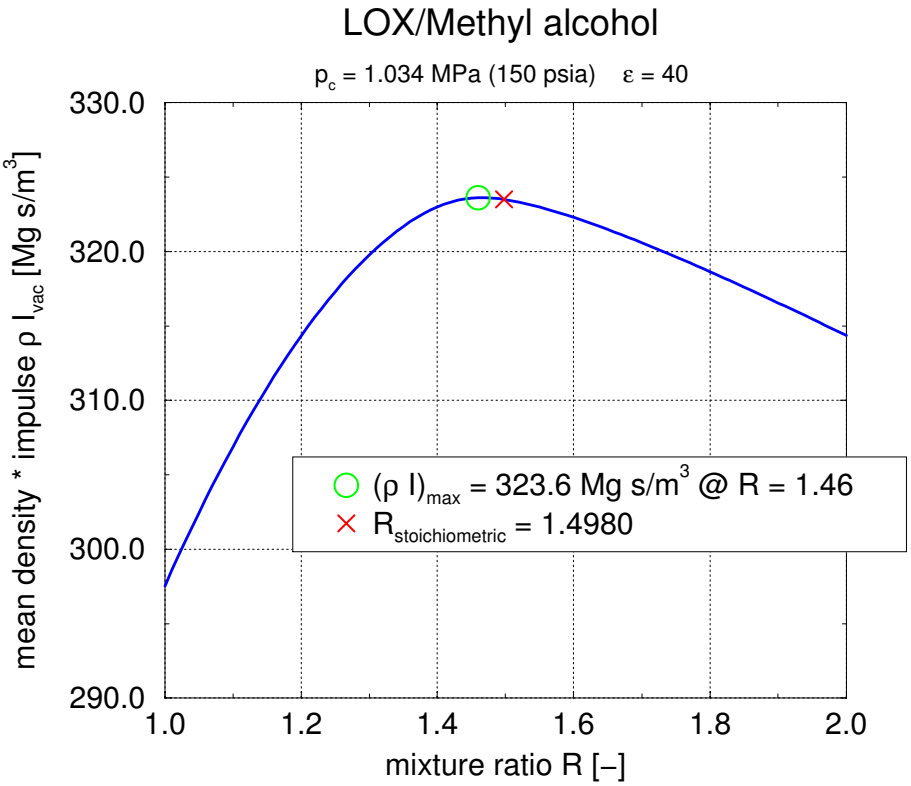

Figure 47: Density and impulse product of LOX/Methanol

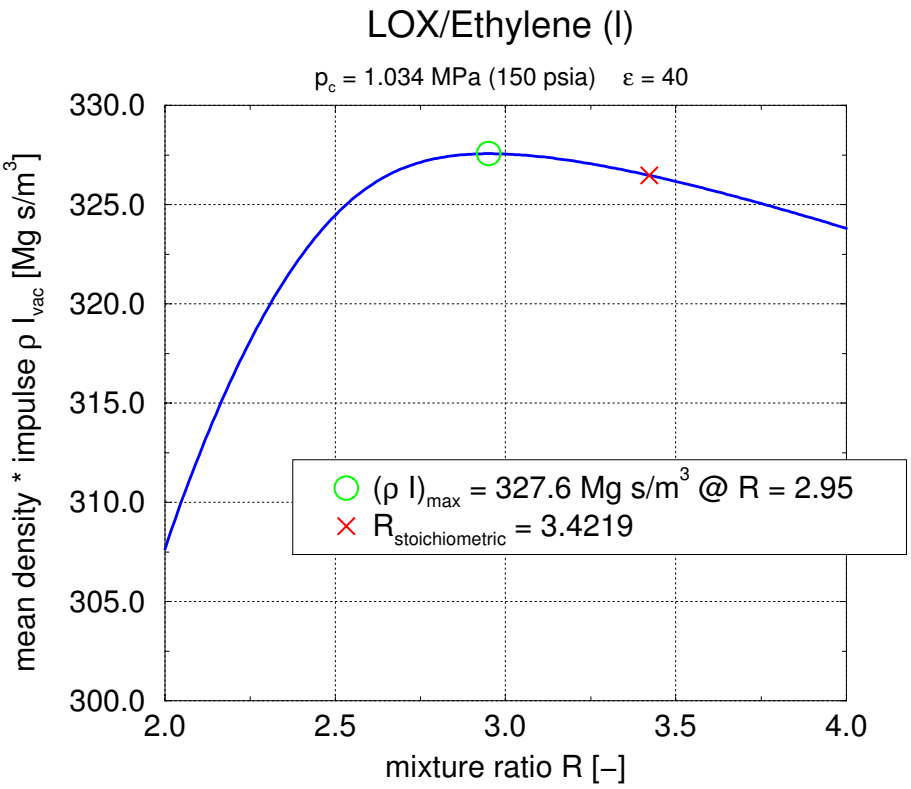

Figure 48: Density and impulse product of LOX/Ethylene

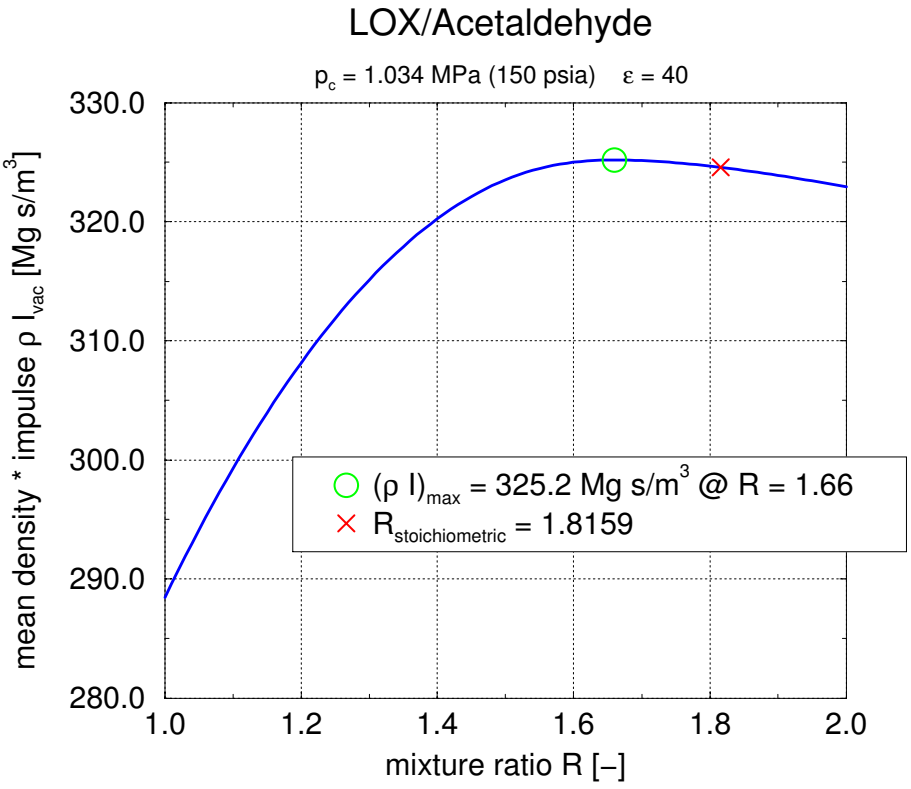

Figure 49: Density and impulse product of LOX/Acetaldehyde

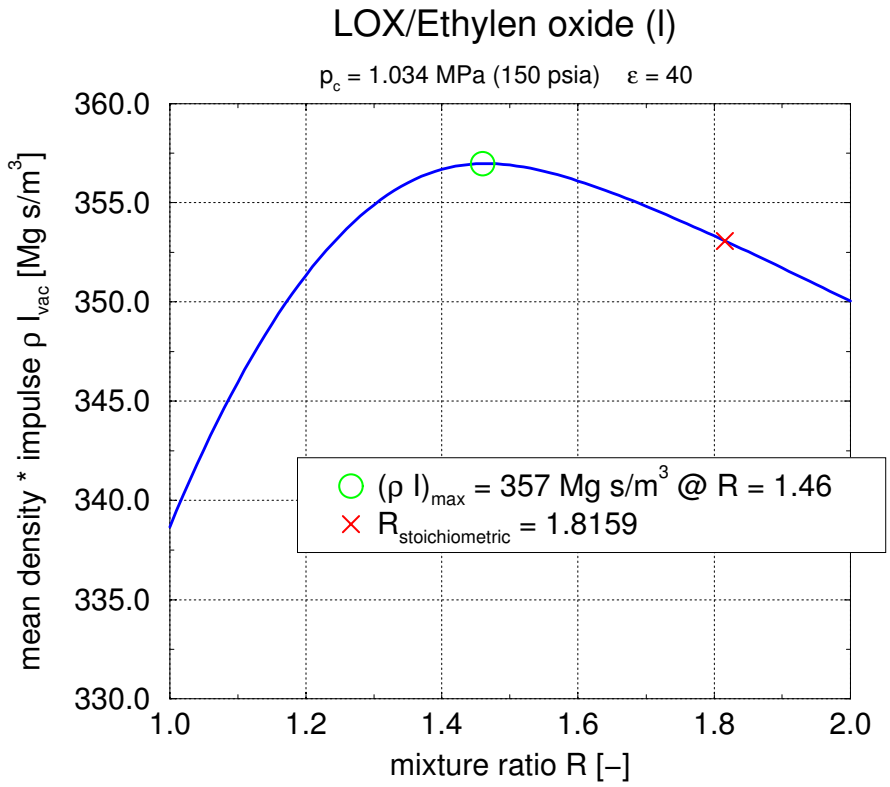

Figure 50: Density and impulse product of LOX/Ethylene oxide

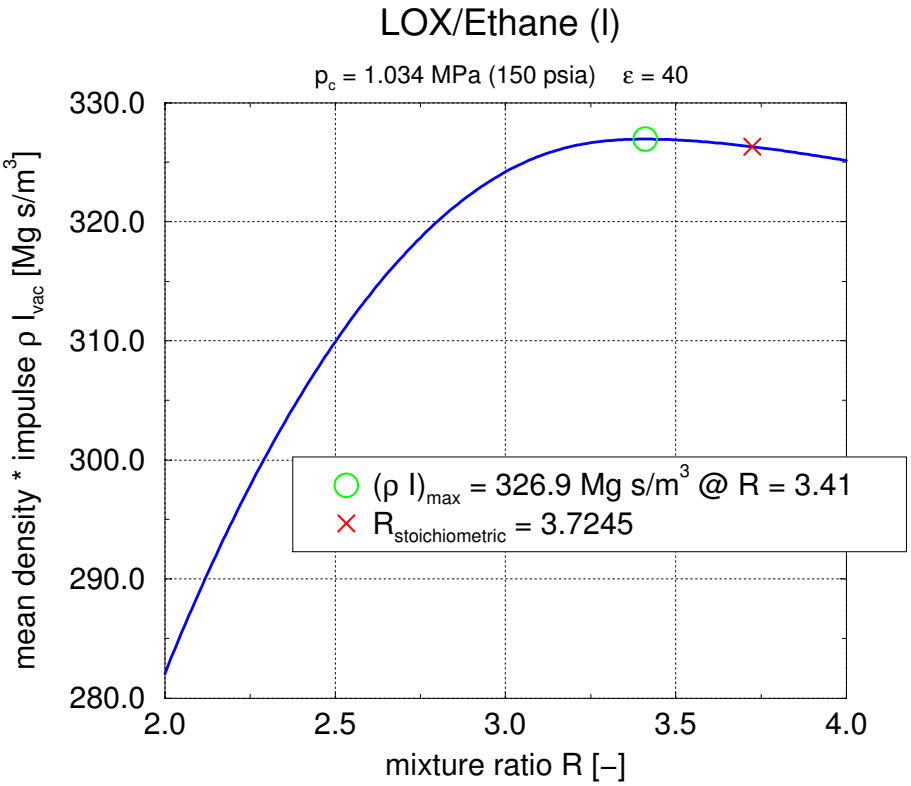

Figure 51: Density and impulse product of LOX/Ethane

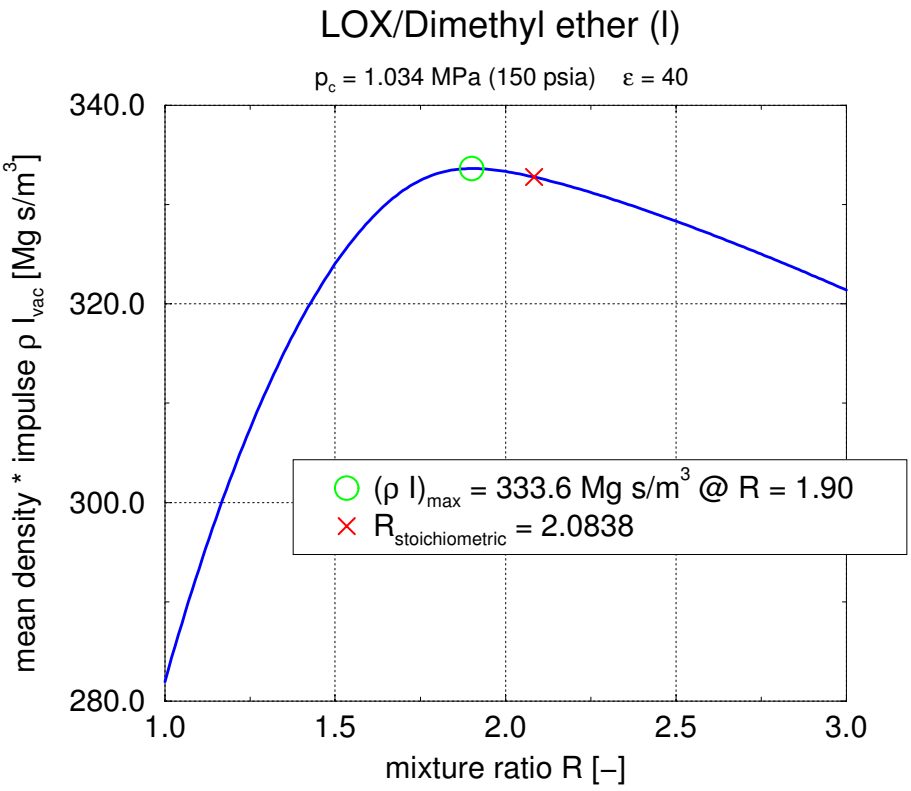

Figure 52: Density and impulse product of LOX/Dimethyl ether

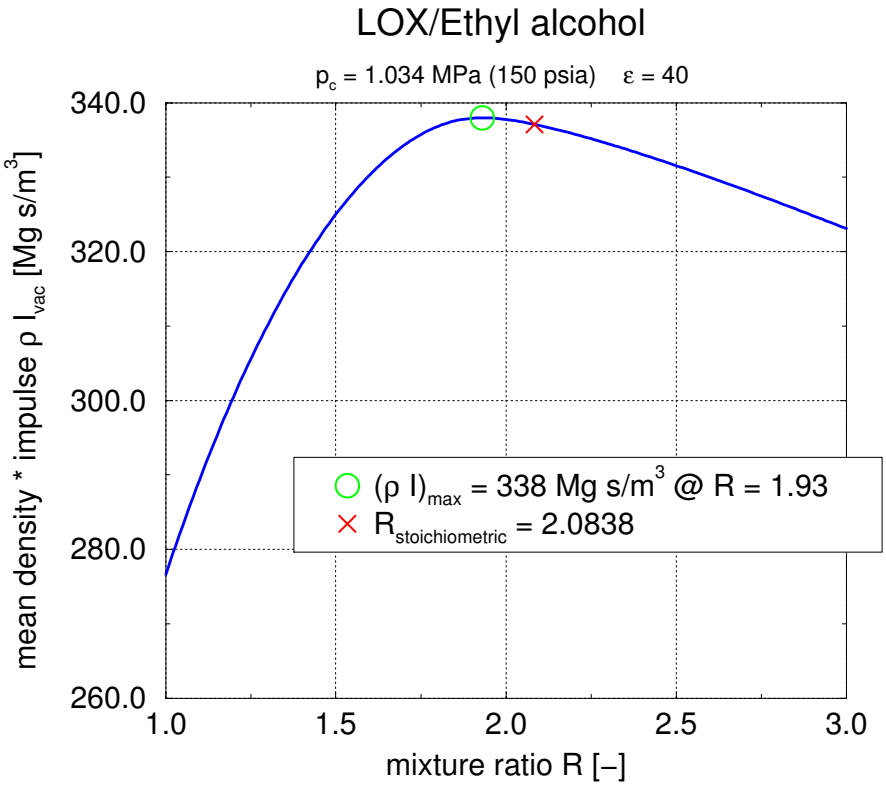

Figure 53: Density and impulse product of LOX/Ethanol

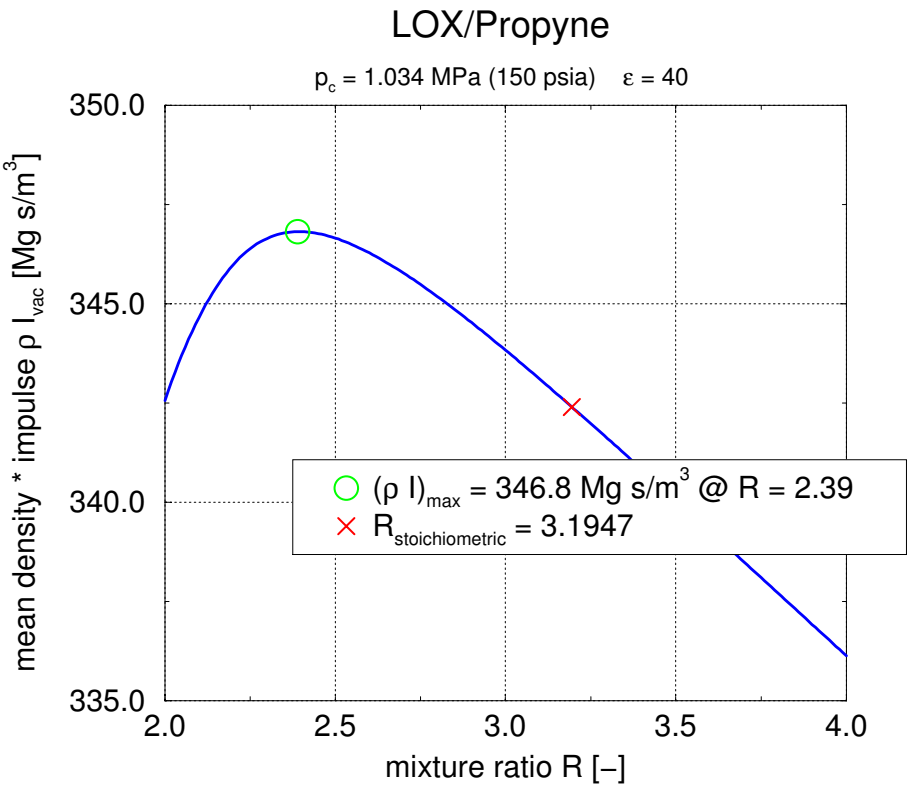

Figure 54: Density and impulse product of LOX/Propyne

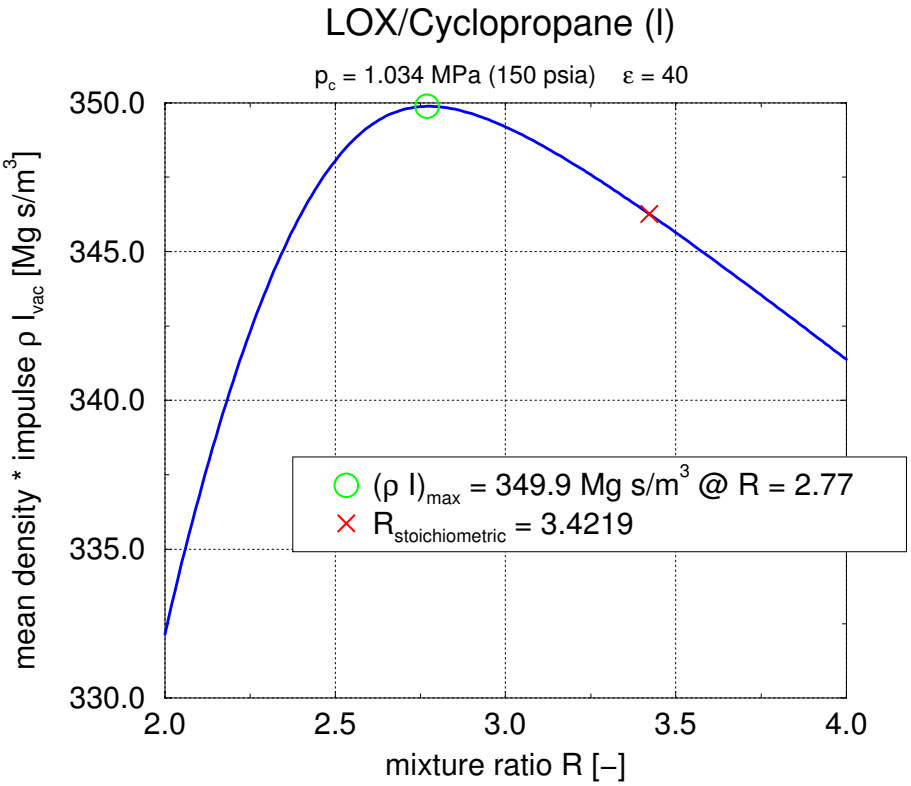

Figure 55: Density and impulse product of LOX/Cyclopropane

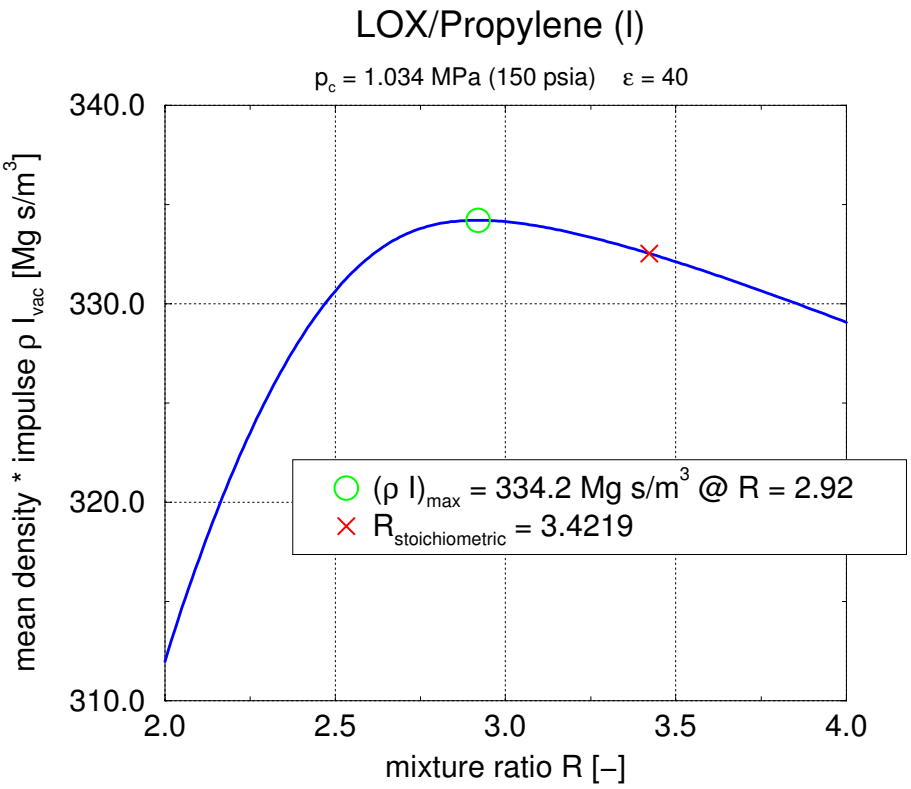

Figure 56: Density and impulse product of LOX/Propylene

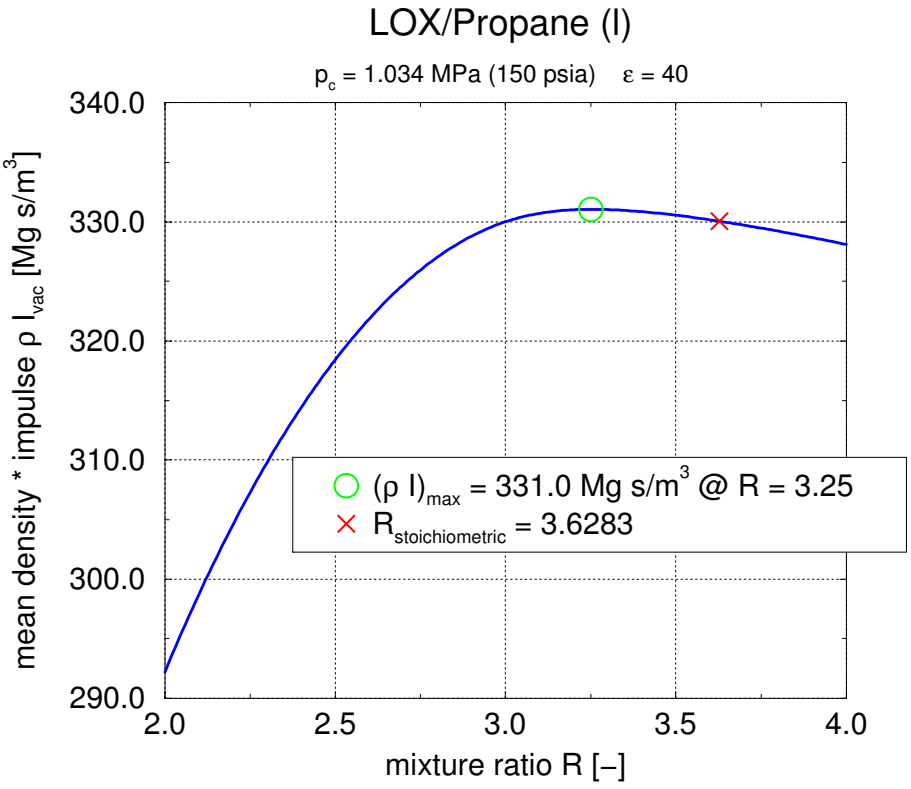

Figure 57: Density and impulse product of LOX/Propane

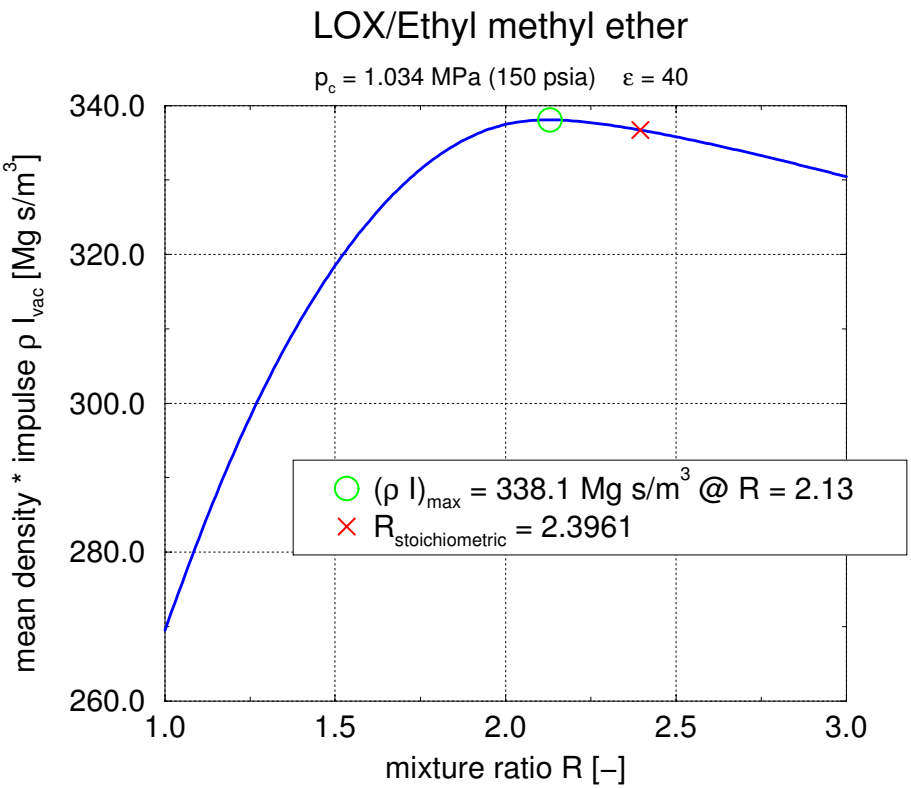

Figure 58: Density and impulse product of LOX/Ethyl methyl ether

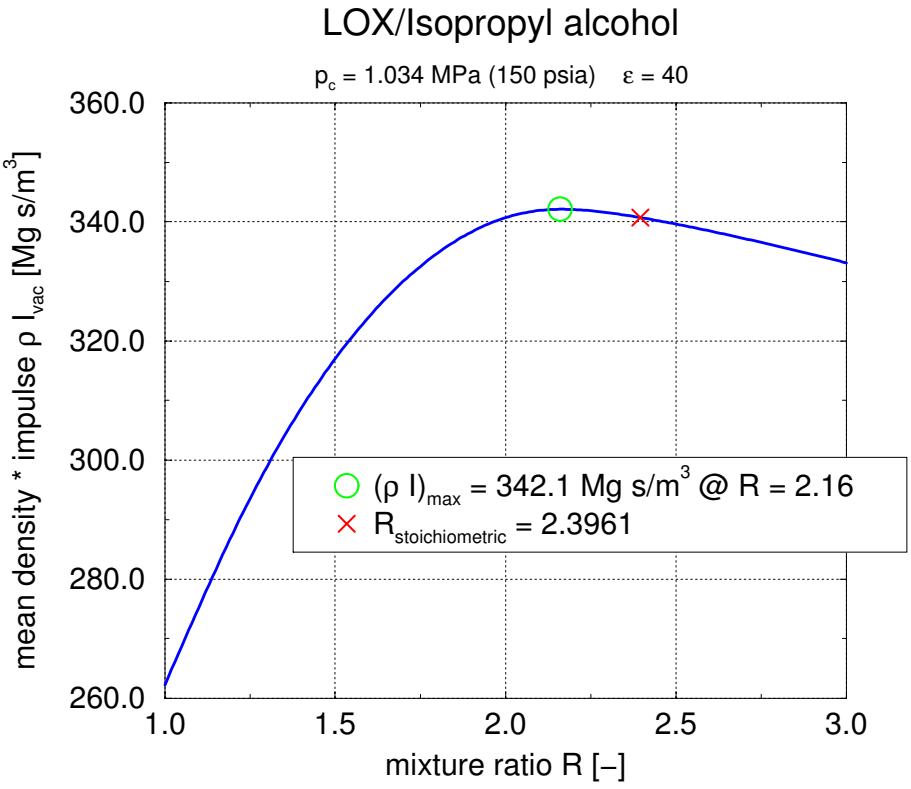

Figure 59: Density and impulse product of LOX/Isopropyl alcohol

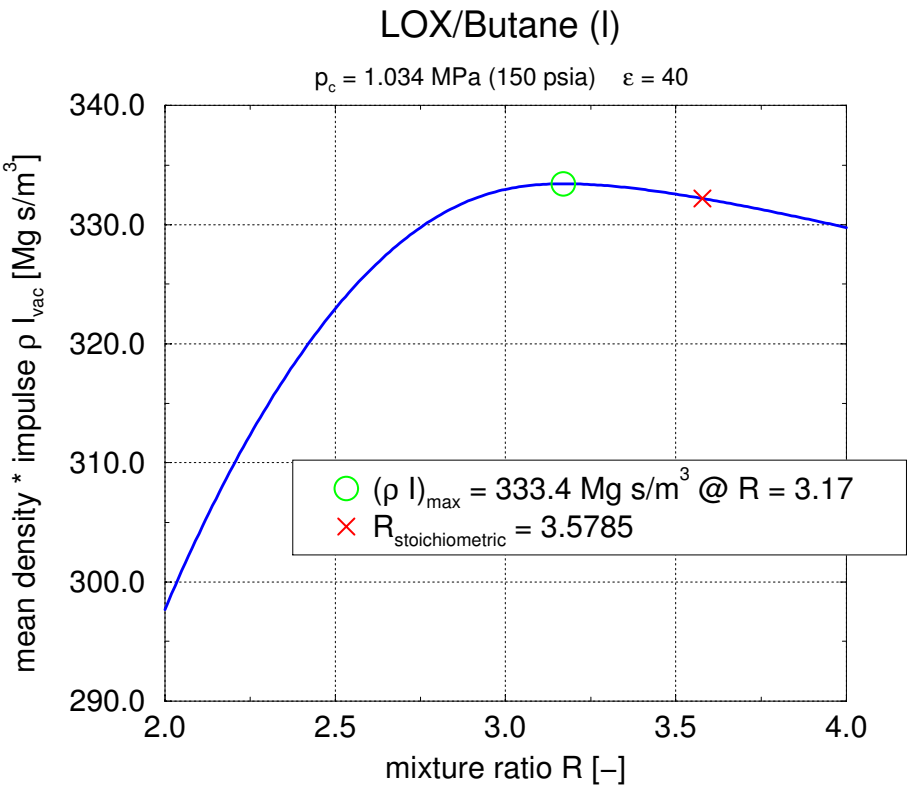

Figure 60: Density and impulse product of LOX/Butane

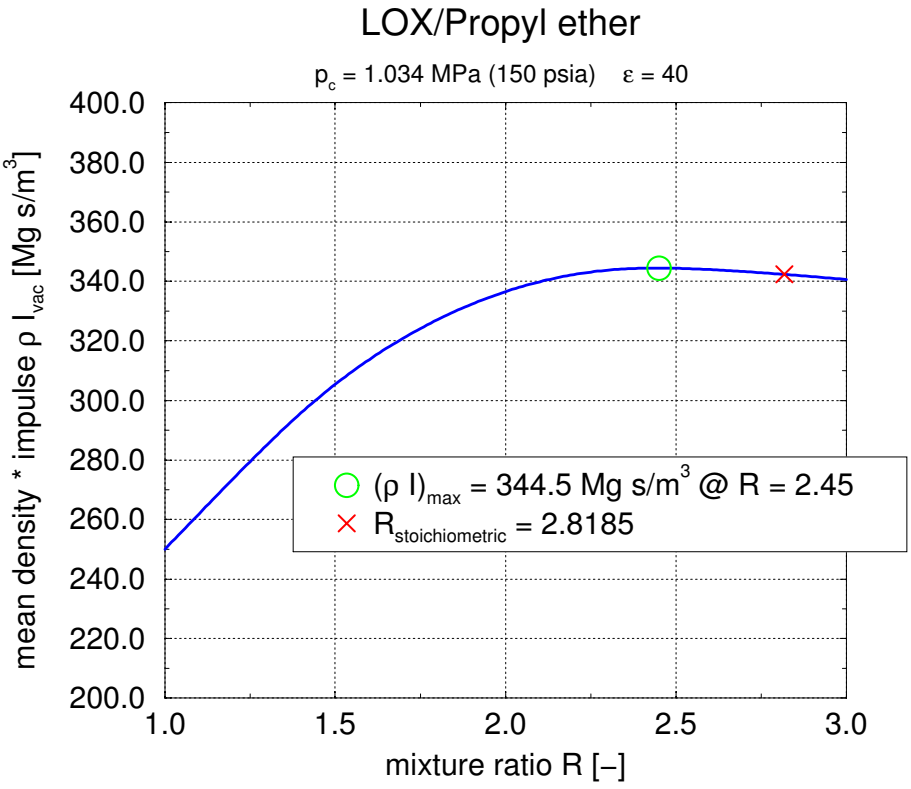

Figure 61: Density and impulse product of LOX/Propyl ether

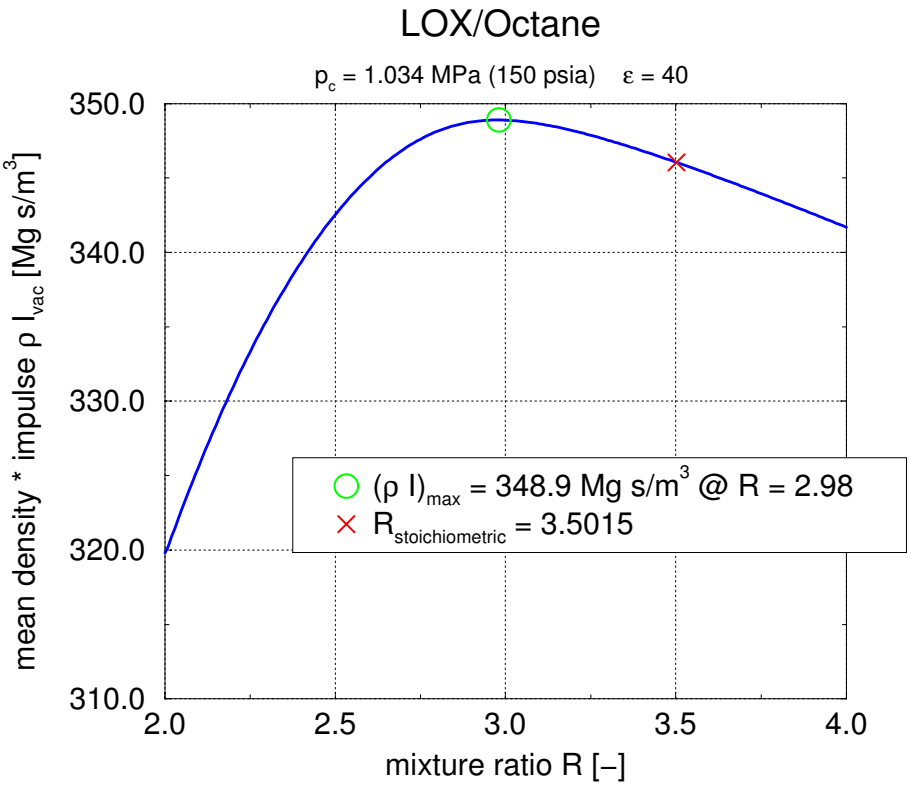

Figure 62: Density and impulse product of LOX/Octane

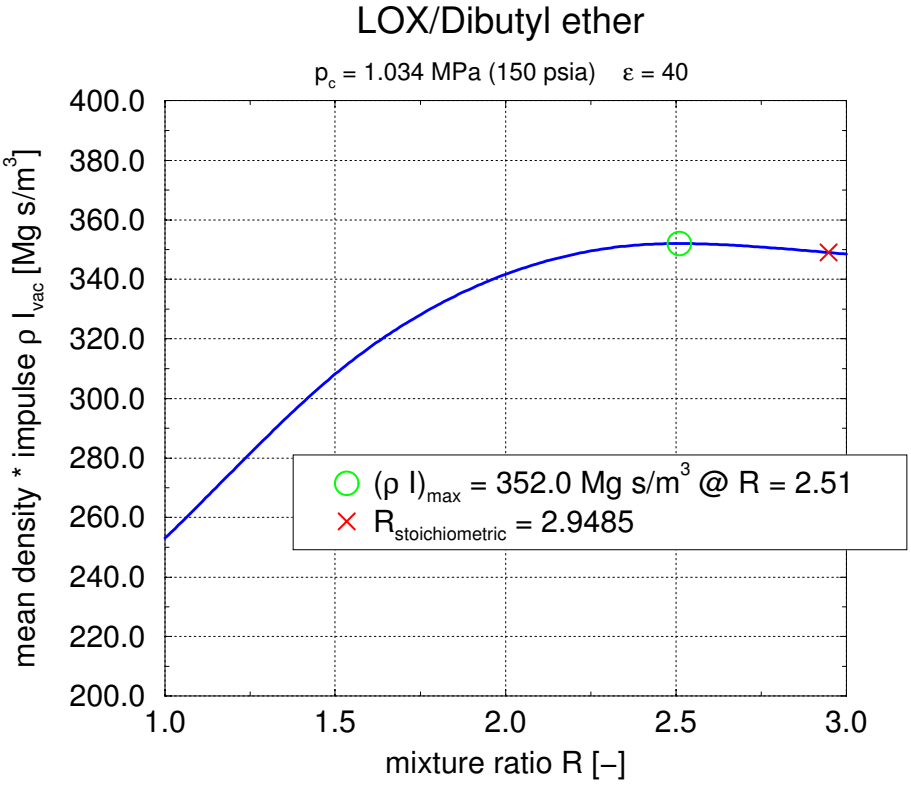

Figure 63: Density and impulse product of LOX/Dibutyl ether

3.4 Comparison of the theoretical c*-performance for propellant-combinations using LOX as oxidizer

Figure 64 gives an overview over the results of the theoretical c*-performance analysis of propellant-combinations using liquid oxygen (LOX) as oxidizer.

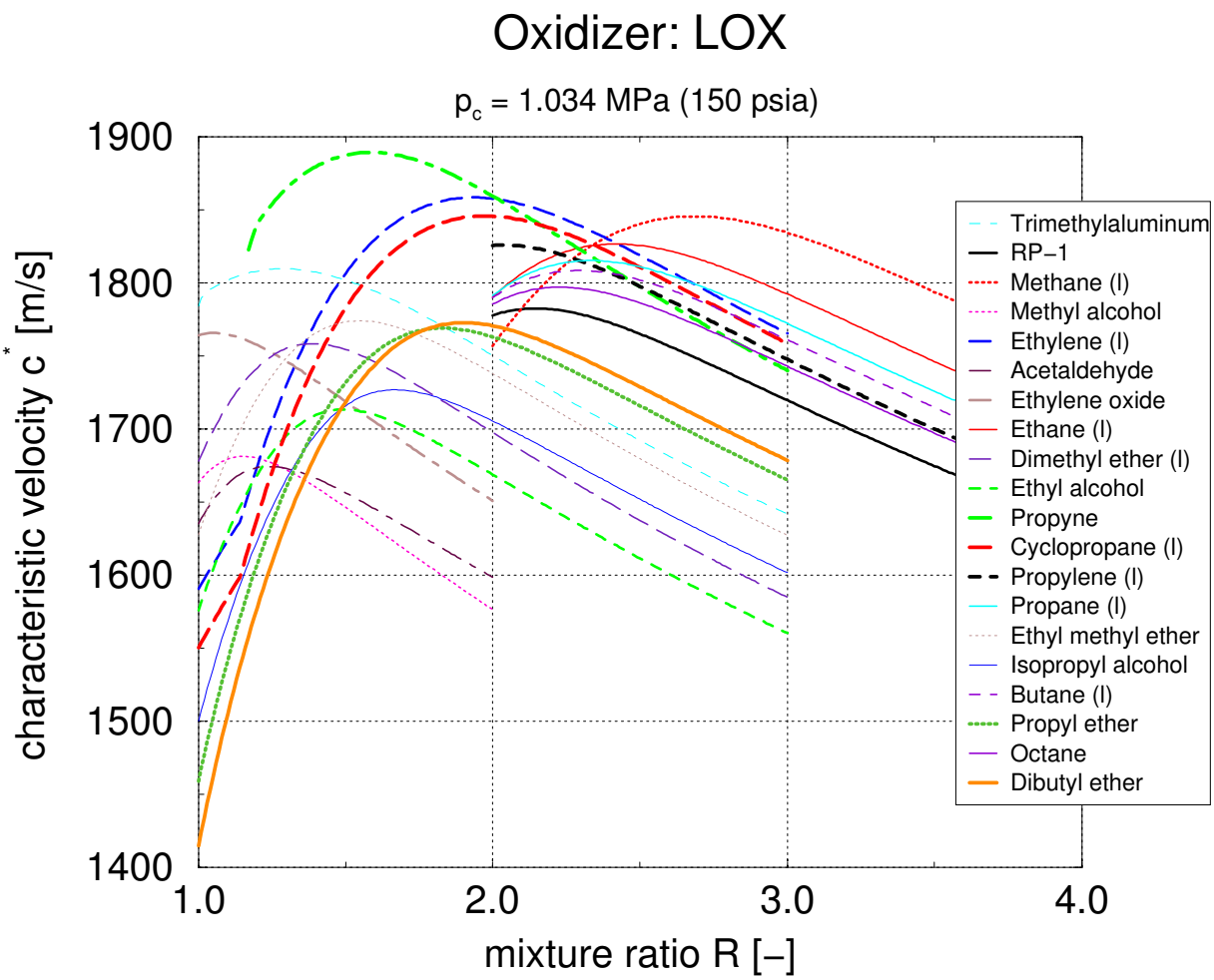

Figure 64: Theoretical characteristic velocity of propellant-combinations using LOX as oxidizer

3.5 Comparison of the theoretical c*-performance for propellant-combinations using 90% H_2O_2 as oxidizer

Figure 65 gives an overview over the results of the theoretical c*-performance analysis of propellant-combinations using a 90% H_2O_2 solution as oxidizer.

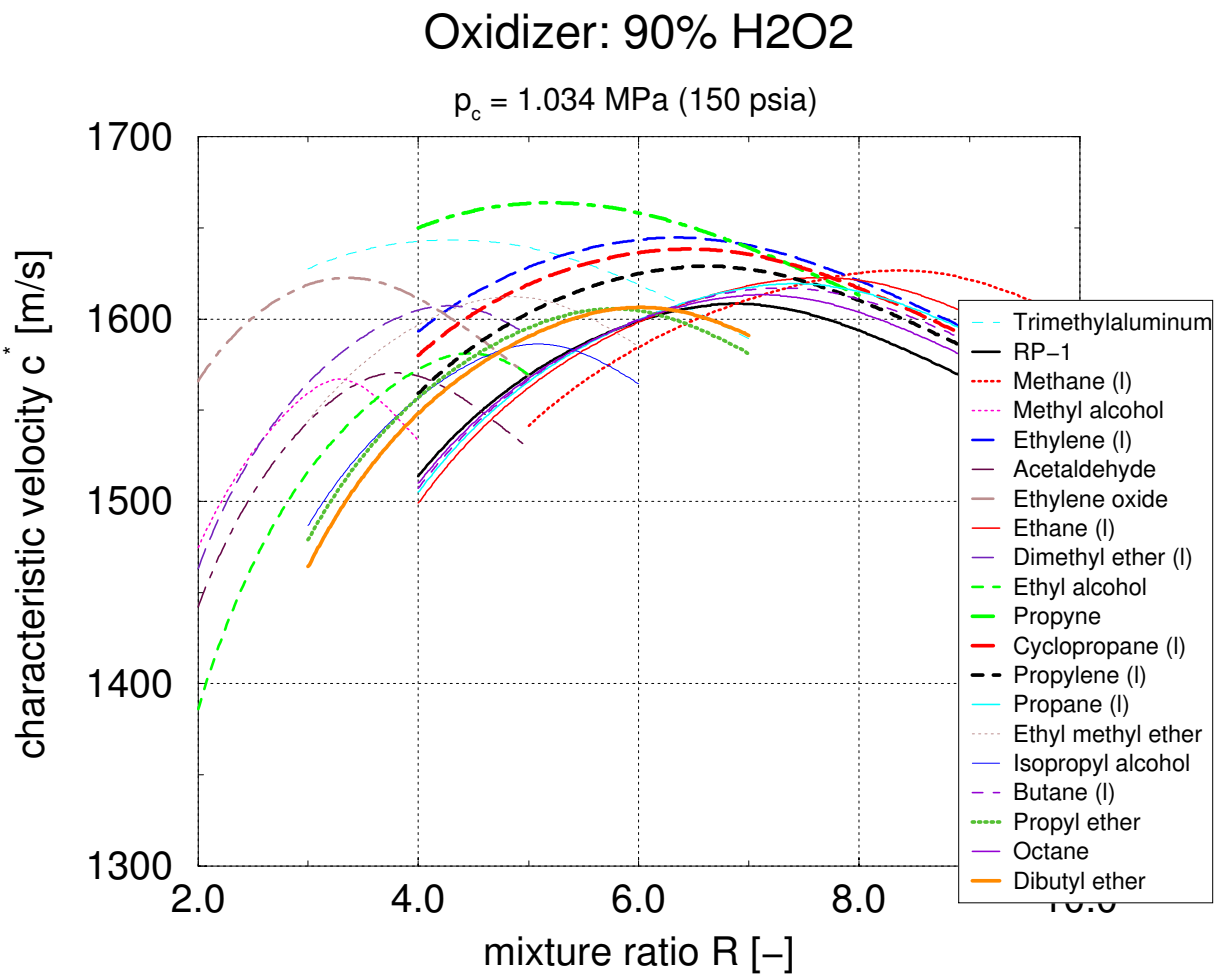

Figure 65: Theoretical characteristic velocity of propellant-combinations using H_2O_2 as oxidizer

3.6 Comparison of the product of mean tank density and specific impulse for propellant-combinations using 90% H_2O_2 as oxidizer

Figure 66 gives an overview over the results of the density and impulse analysis of propellant-combinations using a 90% H_2O_2 solution as oxidizer. Figure 67 to Figure 86 show the respective products of mean tank densities and specific vacuum impulses of each propellant-combination.

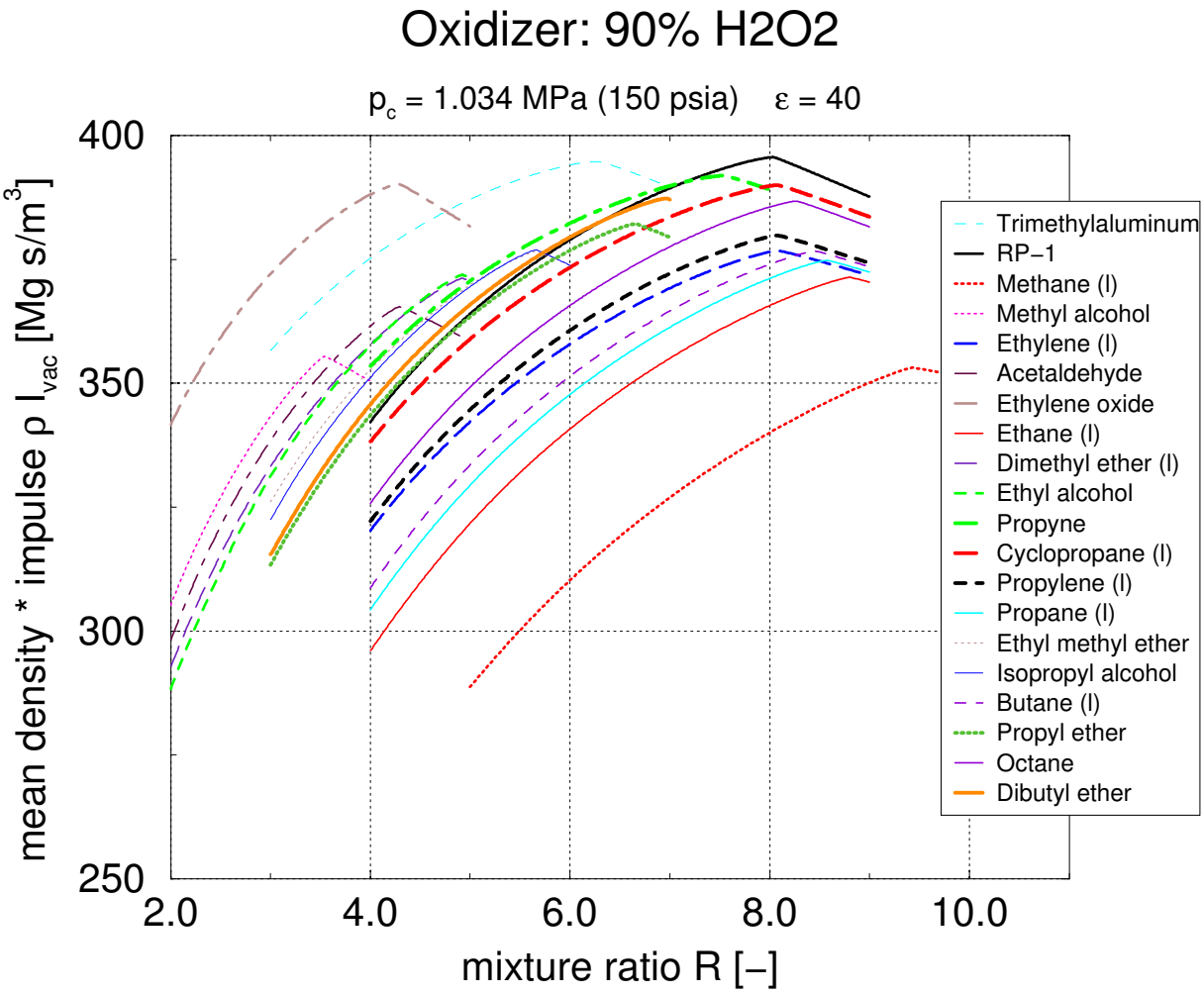

Figure 66: Mean density times vacuum impulse of propellant-combinations using H_2O_2 as oxidizer

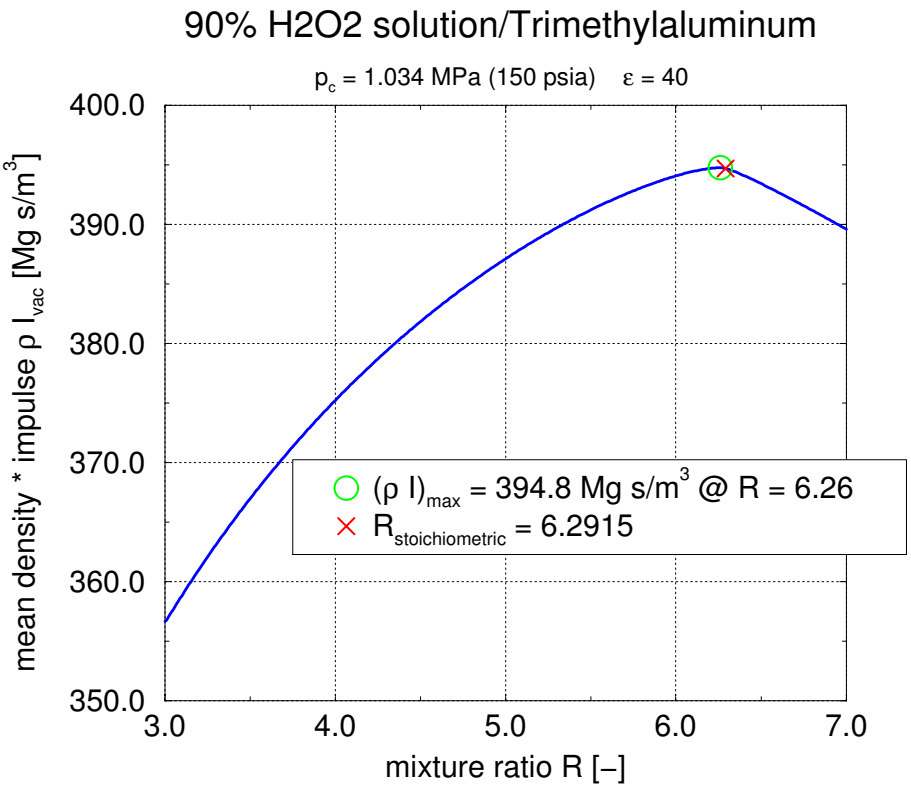

Figure 67: Density and impulse product of H2O2/Trimethylaluminum

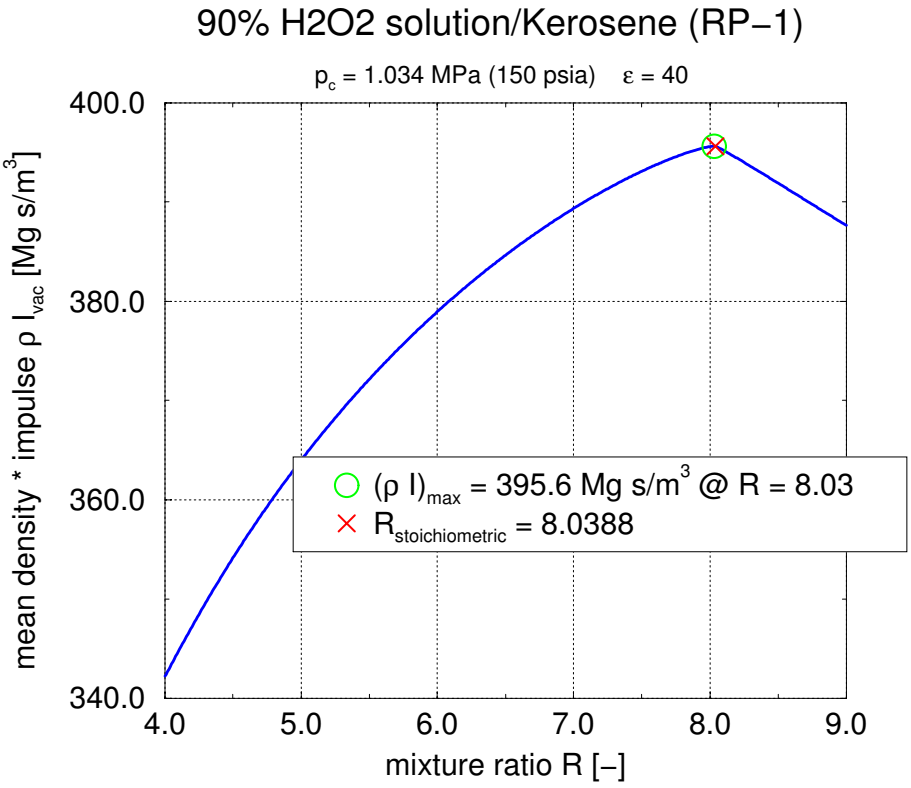

Figure 68: Density and impulse product of H2O2/RP-1

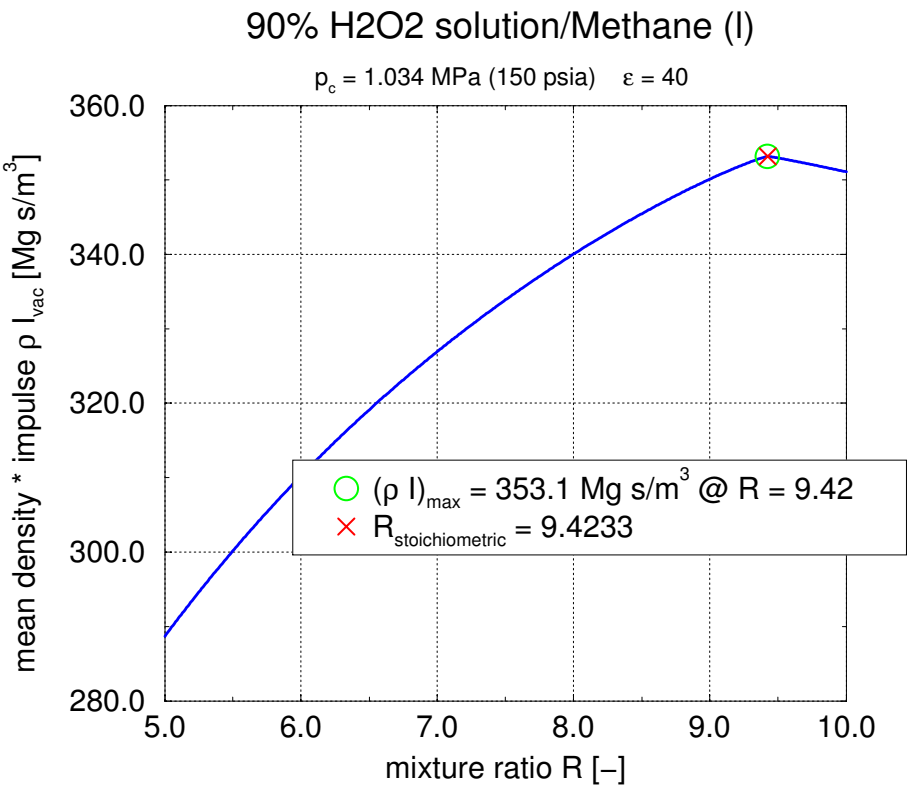

Figure 69: Density and impulse product of H2O2/Methane

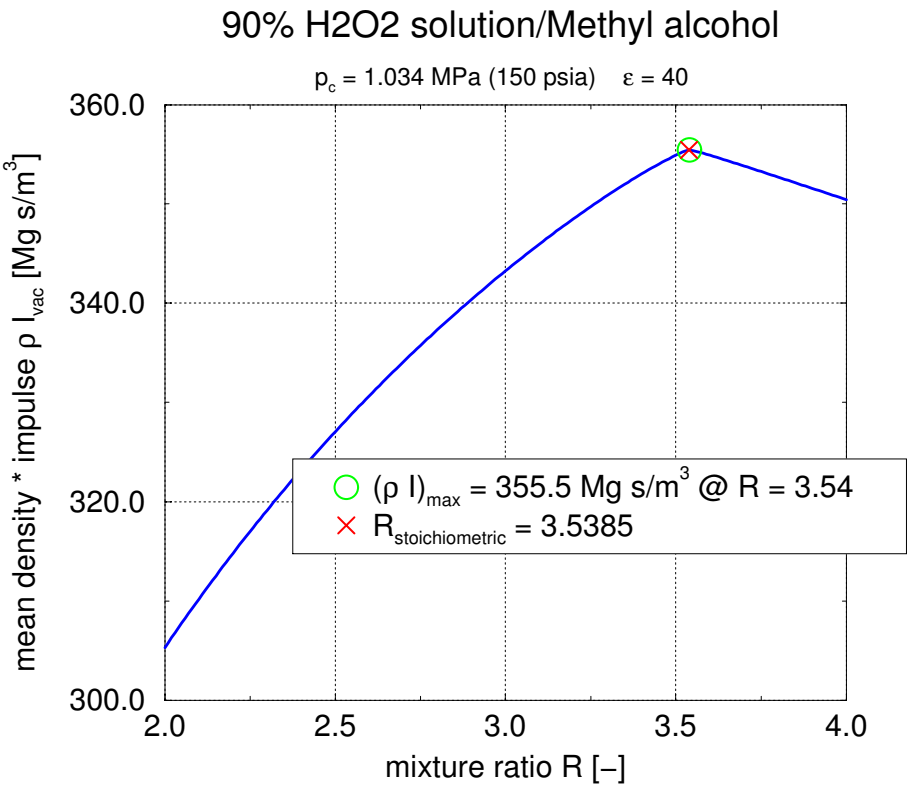

Figure 70: Density and impulse product of H2O2/Methanol

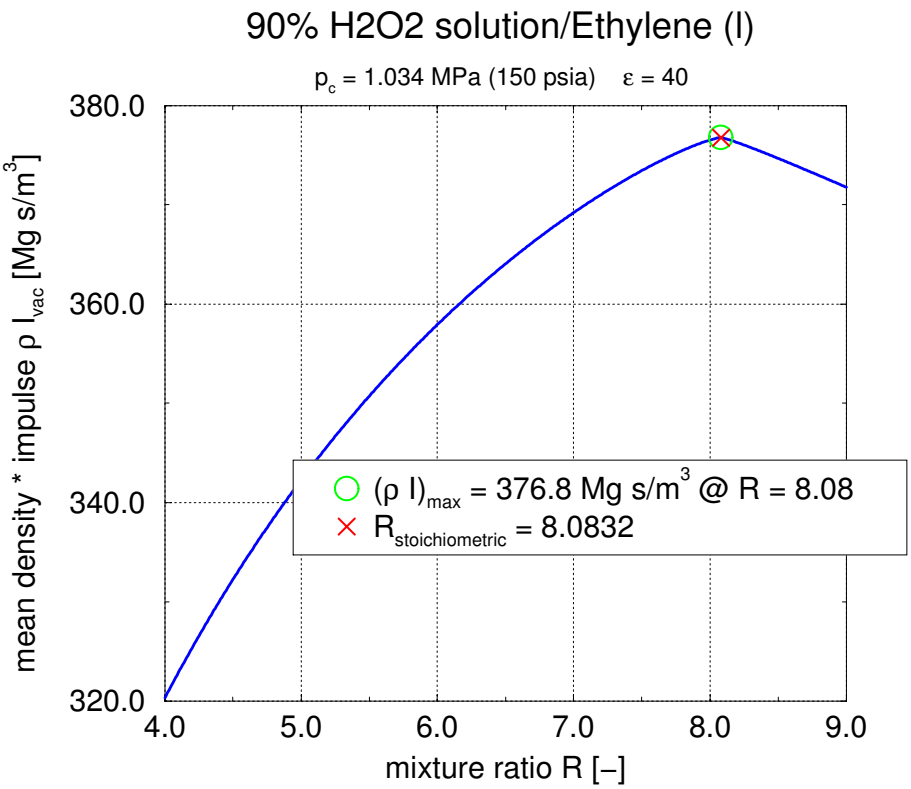

Figure 71: Density and impulse product of H2O2/Ethylene

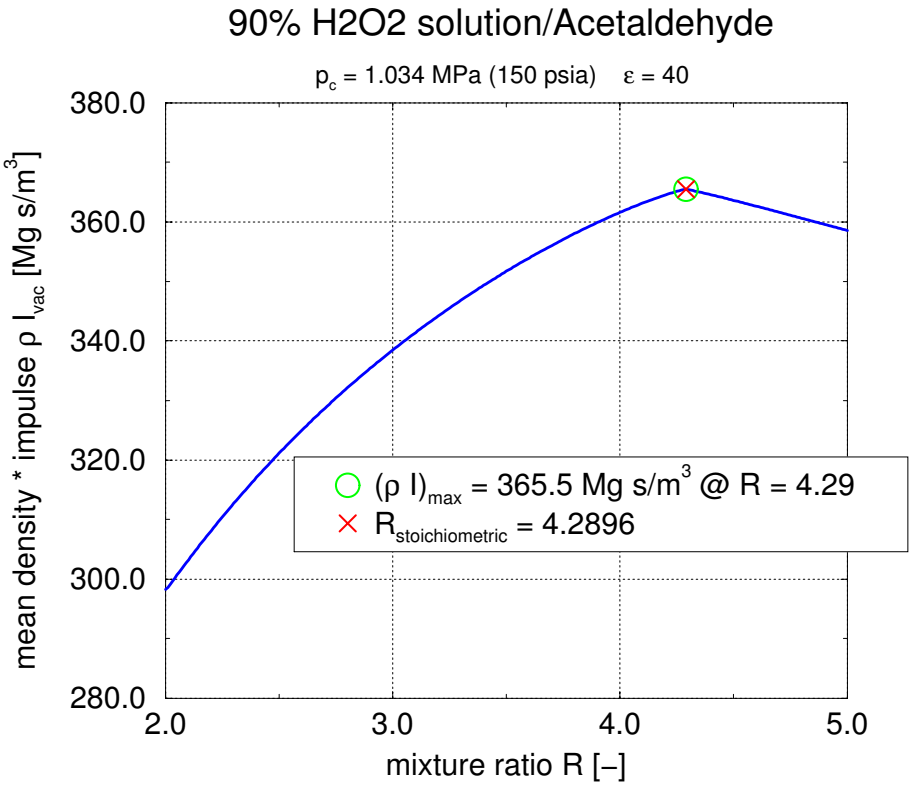

Figure 72: Density and impulse product of H2O2/Acetaldehyde

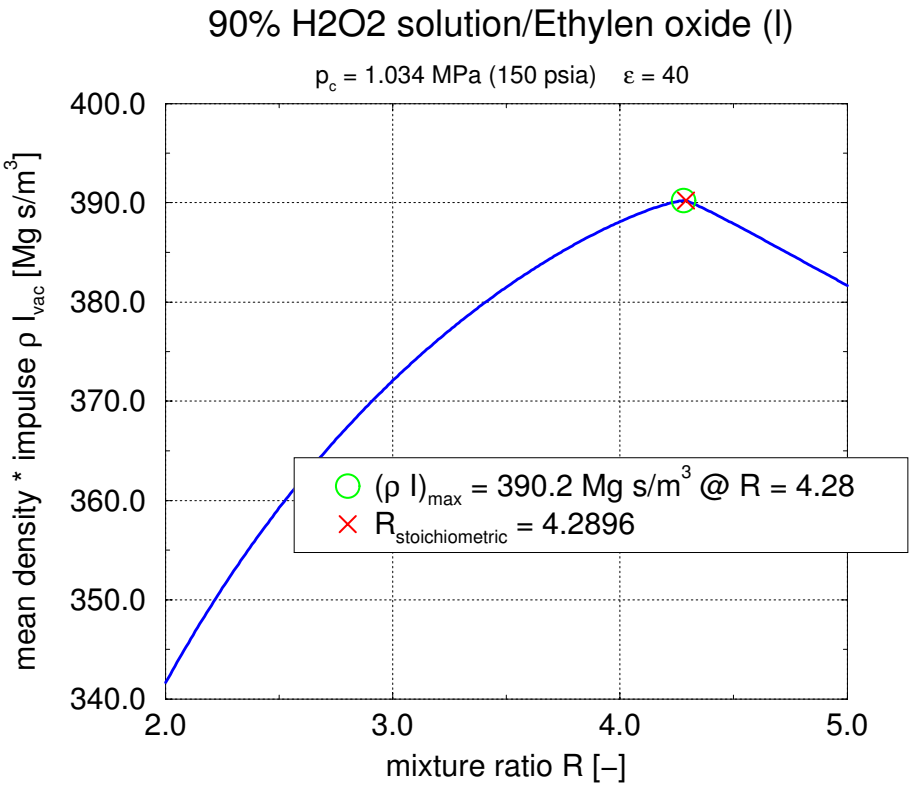

Figure 73: Density and impulse product of H2O2/Ethylene oxide

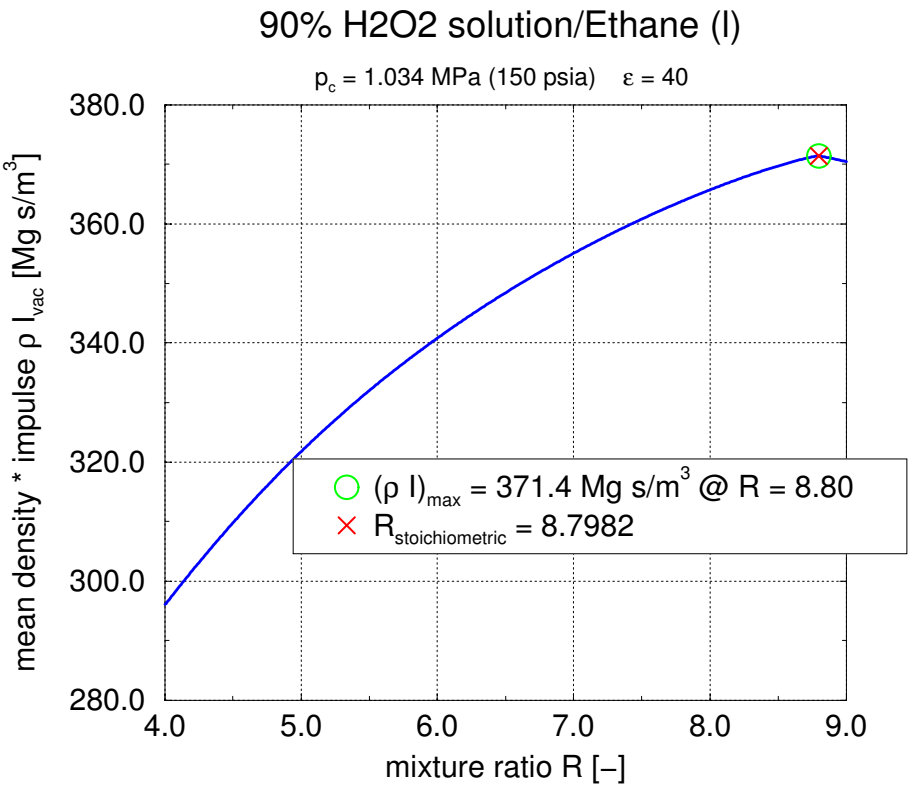

Figure 74: Density and impulse product of H2O2/Ethane

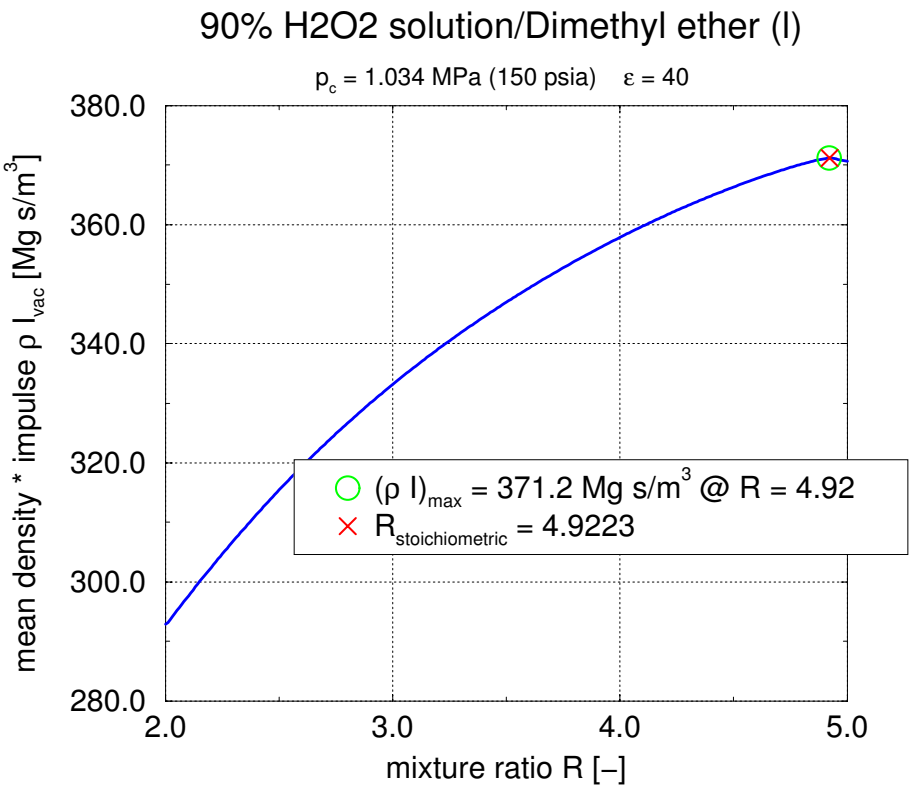

Figure 75: Density and impulse product of H2O2/Dimethyl ether

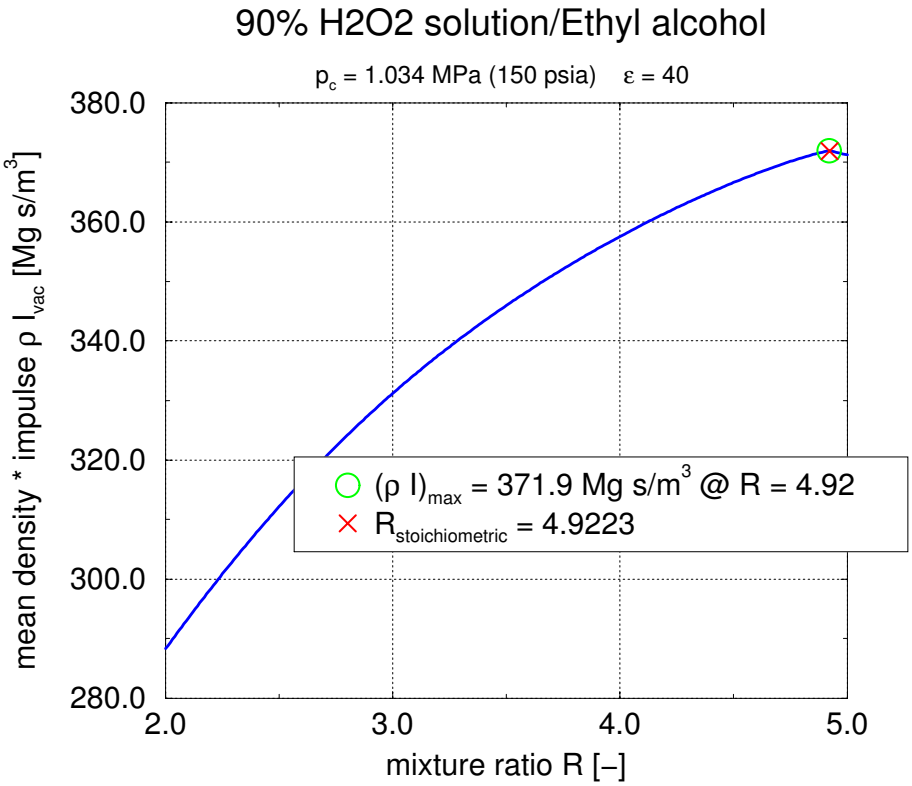

Figure 76: Density and impulse product of H2O2/Ethanol

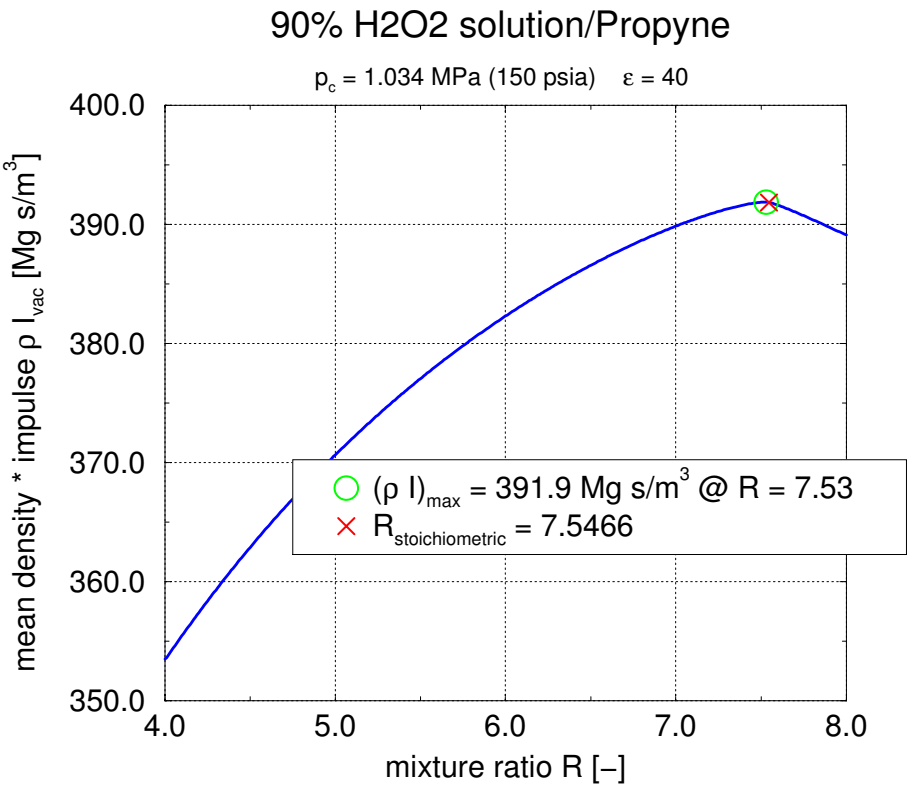

Figure 77: Density and impulse product of H2O2/Propyne

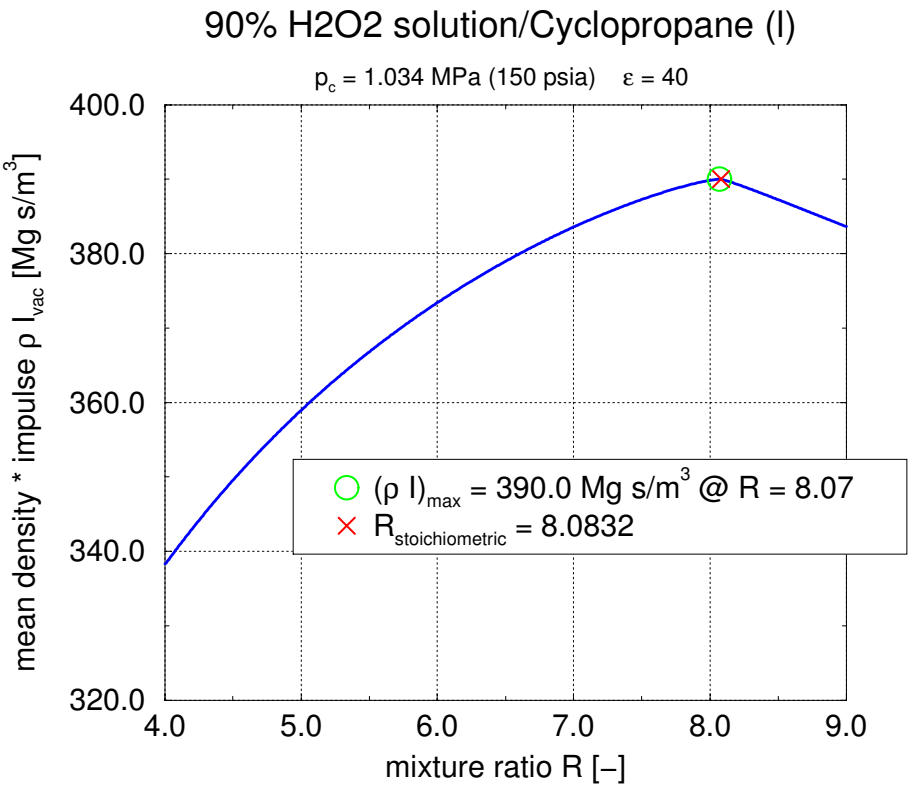

Figure 78: Density and impulse product of H2O2/Cyclopropane

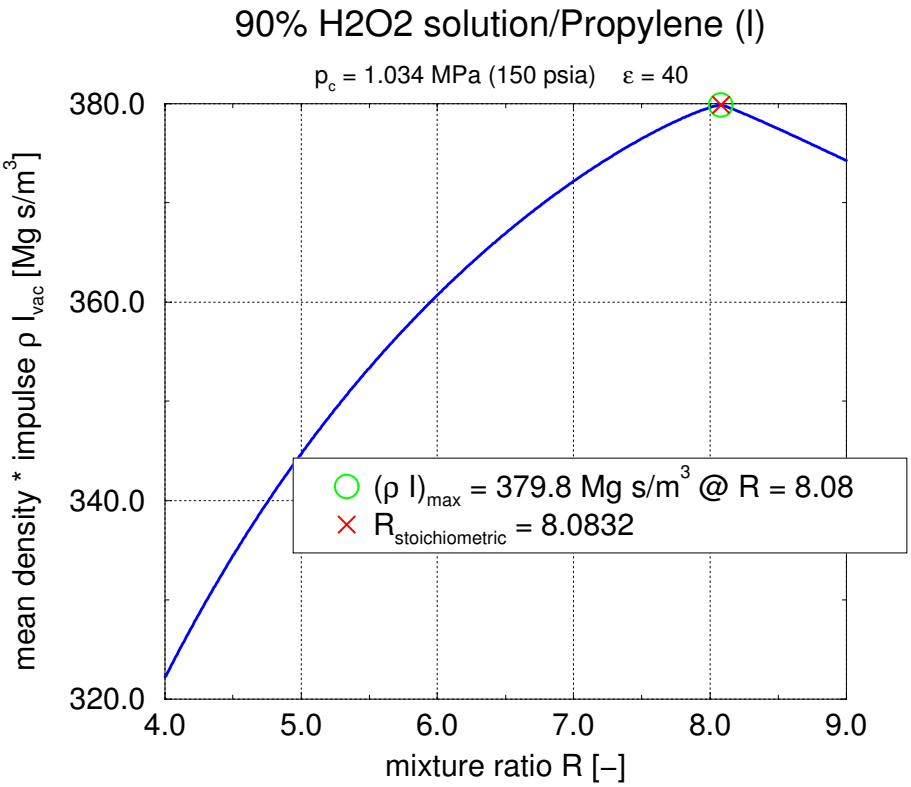

Figure 79: Density and impulse product of H2O2/Propylene

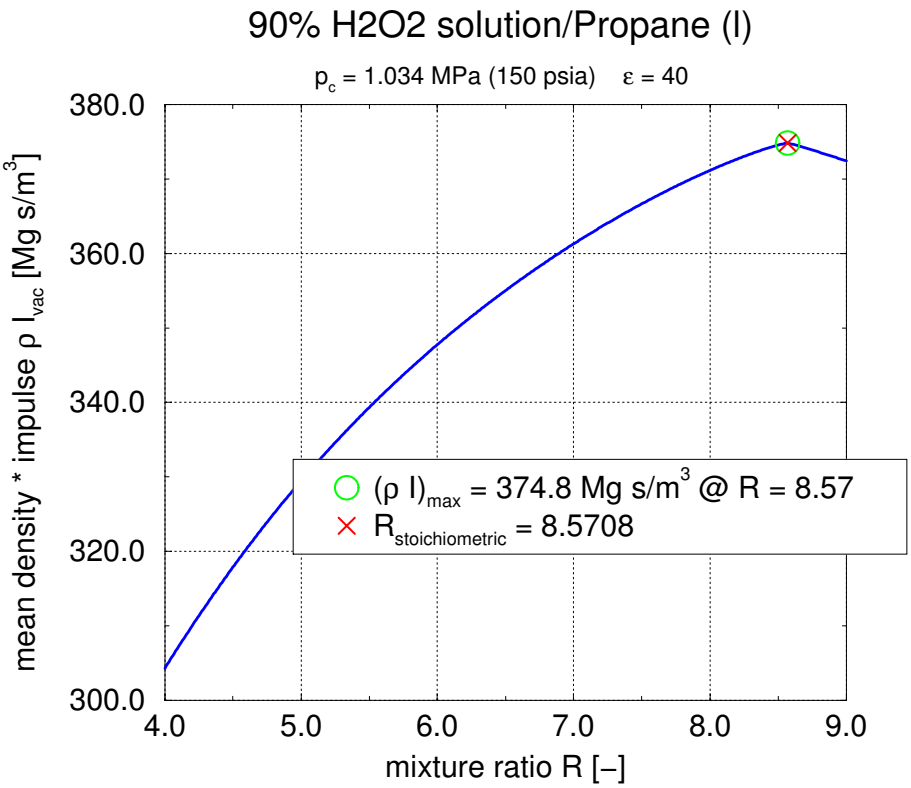

Figure 80: Density and impulse product of H2O2/Propane

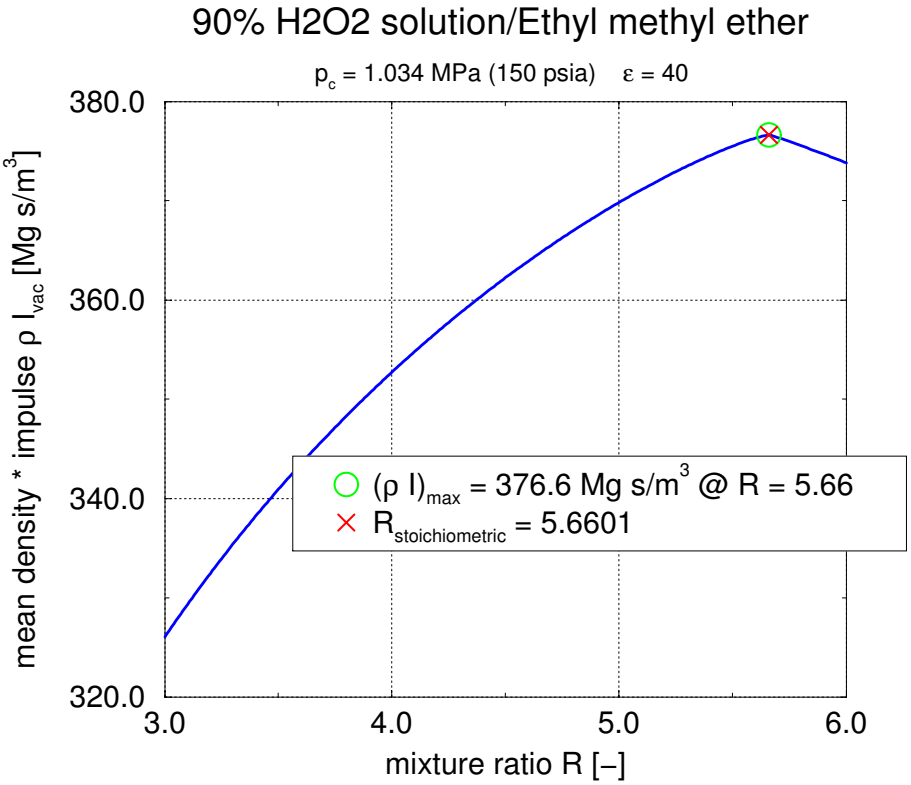

Figure 81: Density and impulse product of H2O2/Ethyl methyl ether

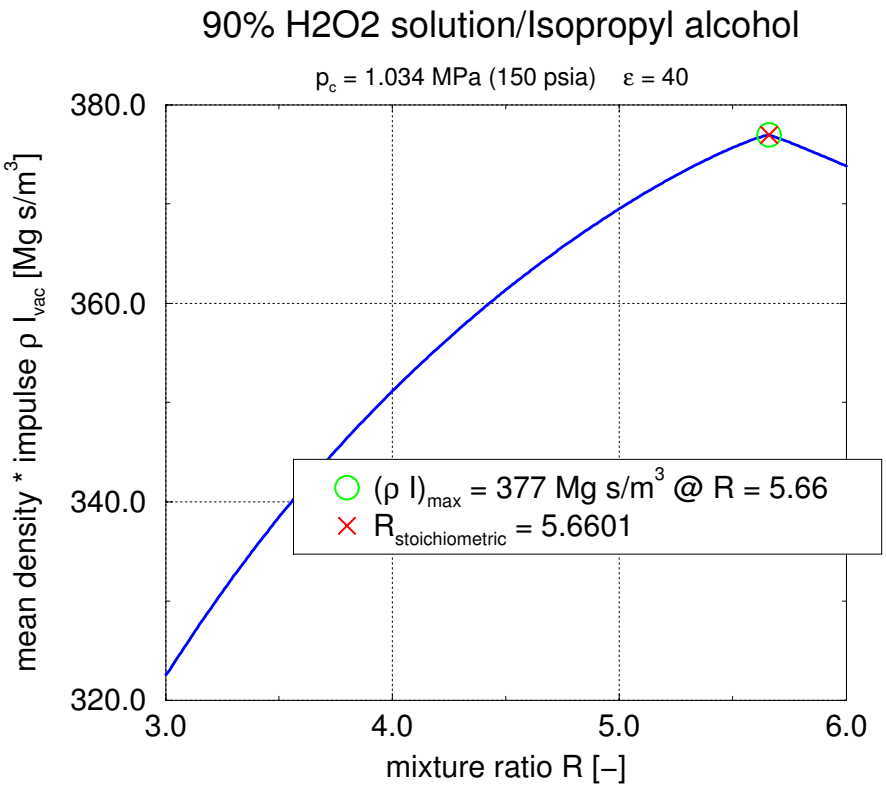

Figure 82: Density and impulse product of H2O2/Isopropyl alcohol

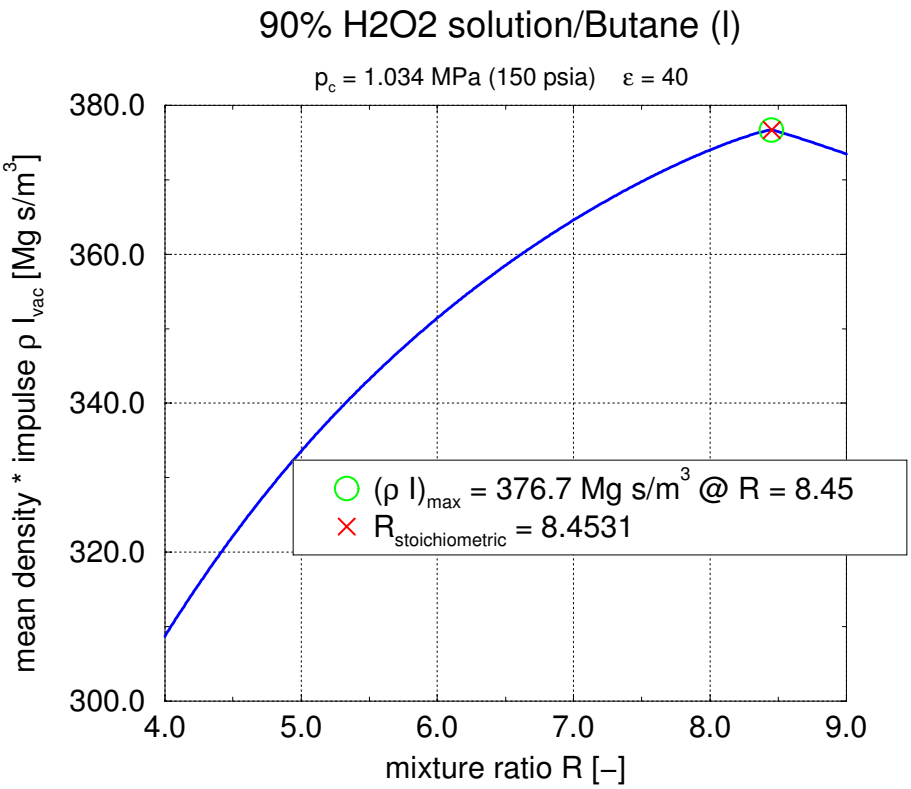

Figure 83: Density and impulse product of H2O2/Butane

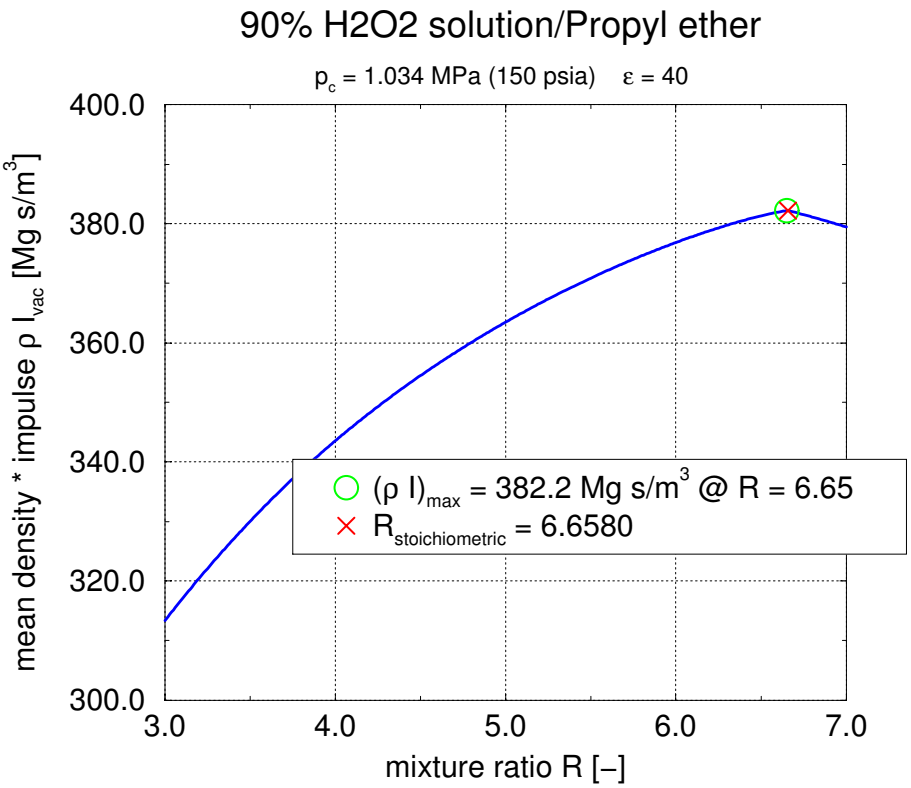

Figure 84: Density and impulse product of H2O2/Propyl ether

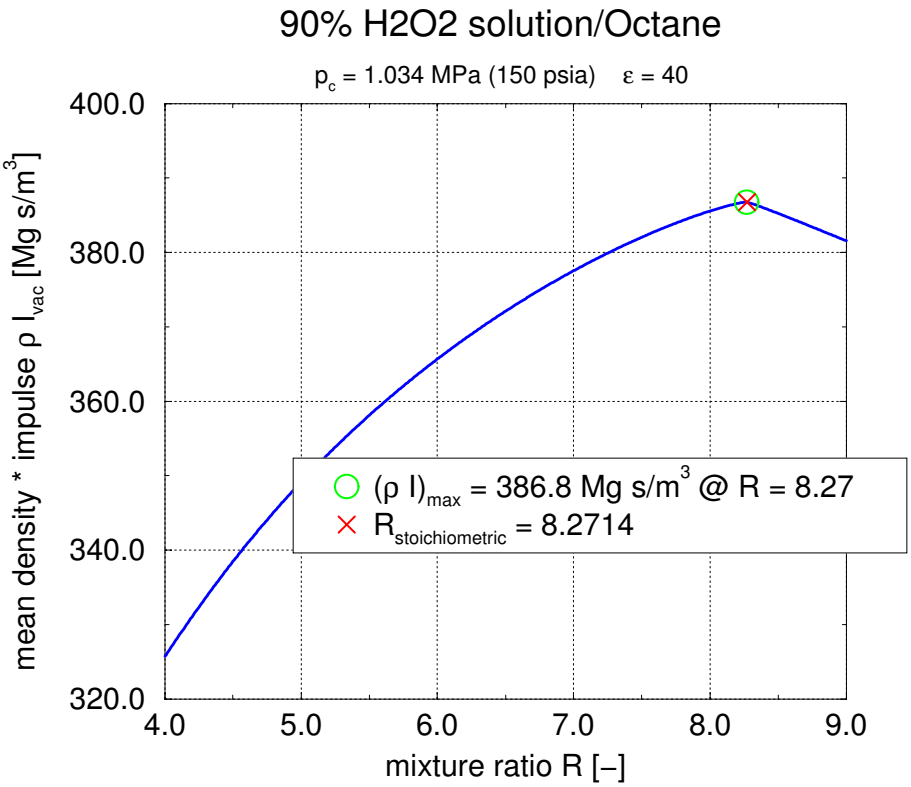

Figure 85: Density and impulse product of H2O2/Octane

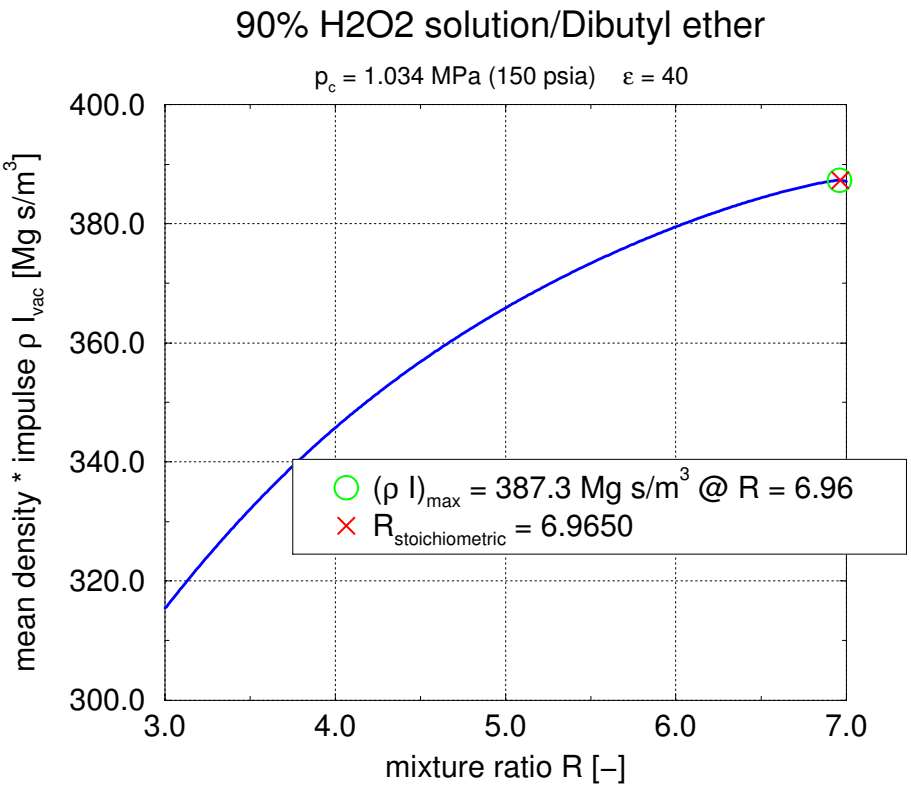

Figure 86: Density and impulse product of H2O2/Dibutyl ether

3.7 Analysis of selected propellant combination's oxidizer rich pre combustion properties

To evaluate the conditions in an oxidizer rich pre combustion chamber or gas generator the following propellant combinations have been examined by using the CEA86 ODE program:

- LOX/Kerosene (RP-1)
- LOX/Methane
- LOX/Dimethyl-ether
- LOX/Ethyl alcohol
- LOX/Propane
- LOX/Isopropyl alcohol

For each combination the following three thermodynamic properties are displayed:

T_c combustion temperature (Figure 87 to Figure 92)

ρ_c density of the gases in the pre combustion chamber (Figure 93 to Figure 98)

c_p specific heat of the gases in the pre combustion chamber (Figure 99 to Figure 104)

The chamber pressure is held constant at p_c = 10 MPa, the mixture ratio R is varied to find an oxygen rich mixture ratio yielding resulting chamber temperatures around Tc ≈ 900 K.

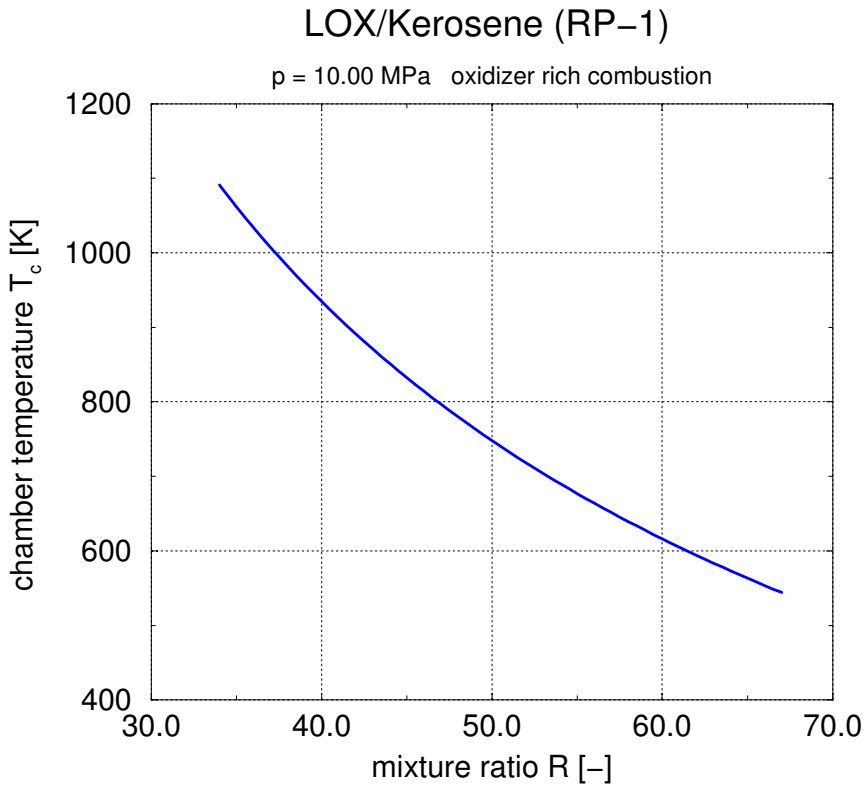

Figure 87: Oxidizer rich preburner temperature for LOX/RP-1

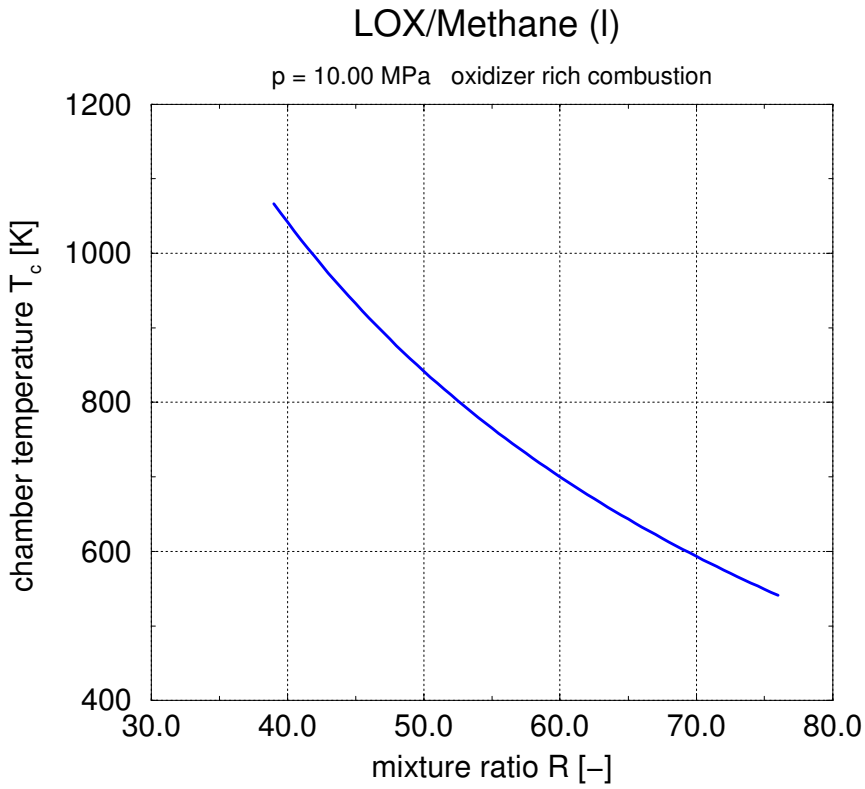

Figure 88: Oxidizer rich preburner temperature for LOX/Methane

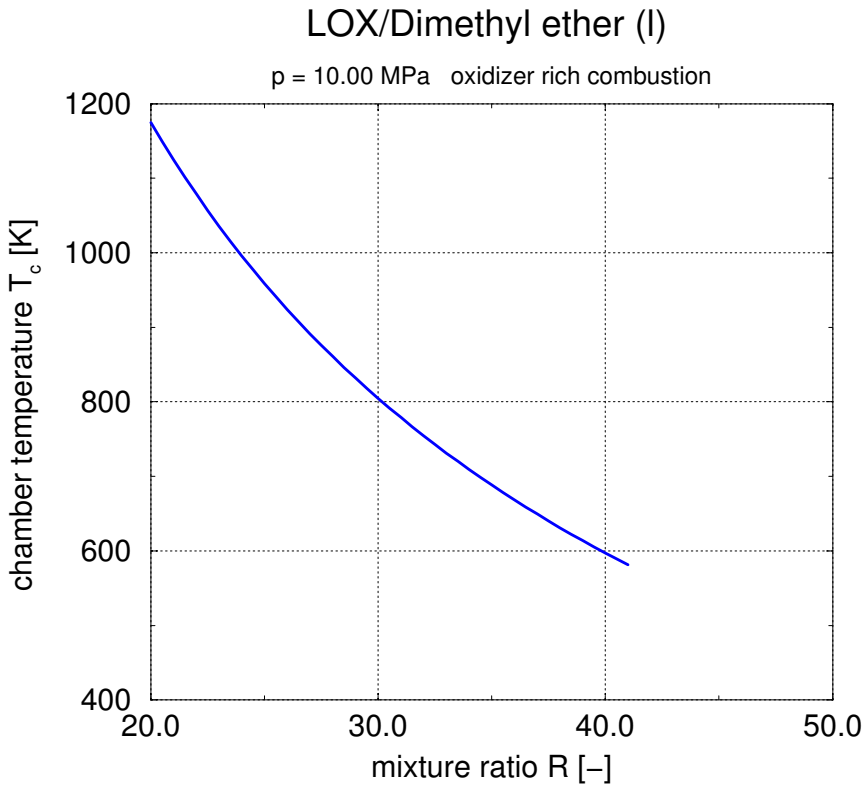

Figure 89: Oxidizer rich preburner temperature for LOX/Dimethyl ether

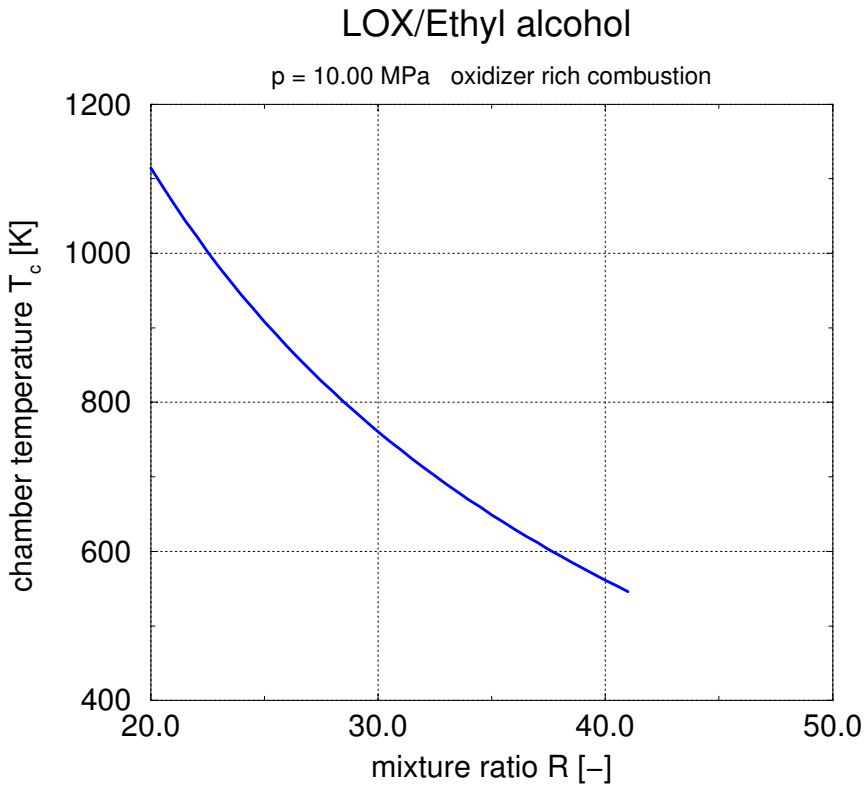

Figure 90: Oxidizer rich preburner temperature for LOX/Ethanol

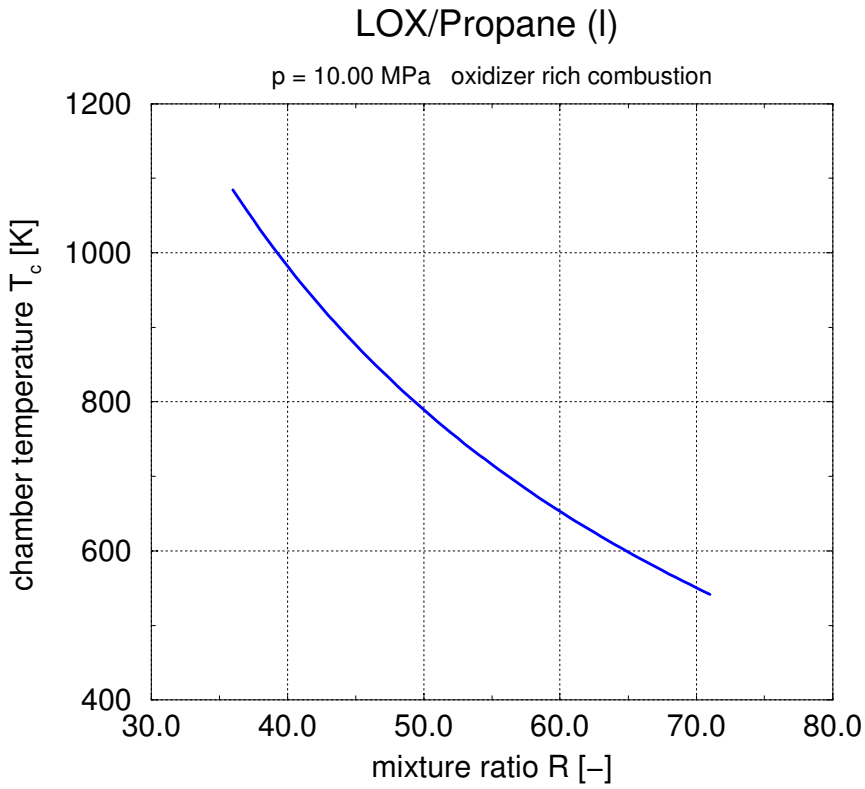

Figure 91: Oxidizer rich preburner temperature for LOX/Propane

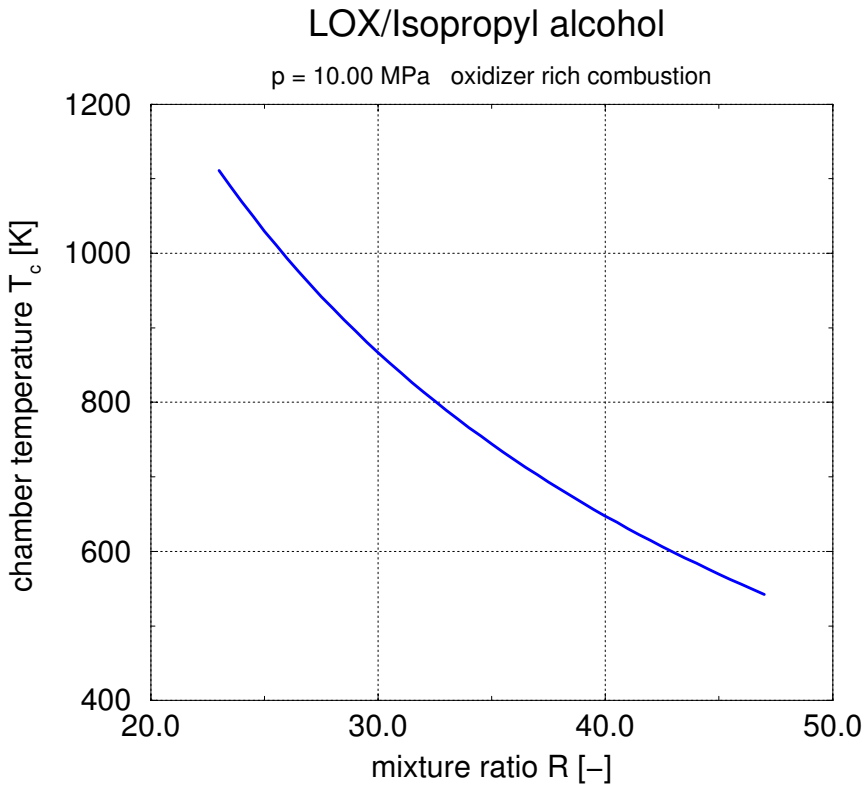

Figure 92: Oxidizer rich preburner temperature for LOX/Isopropyl alcohol

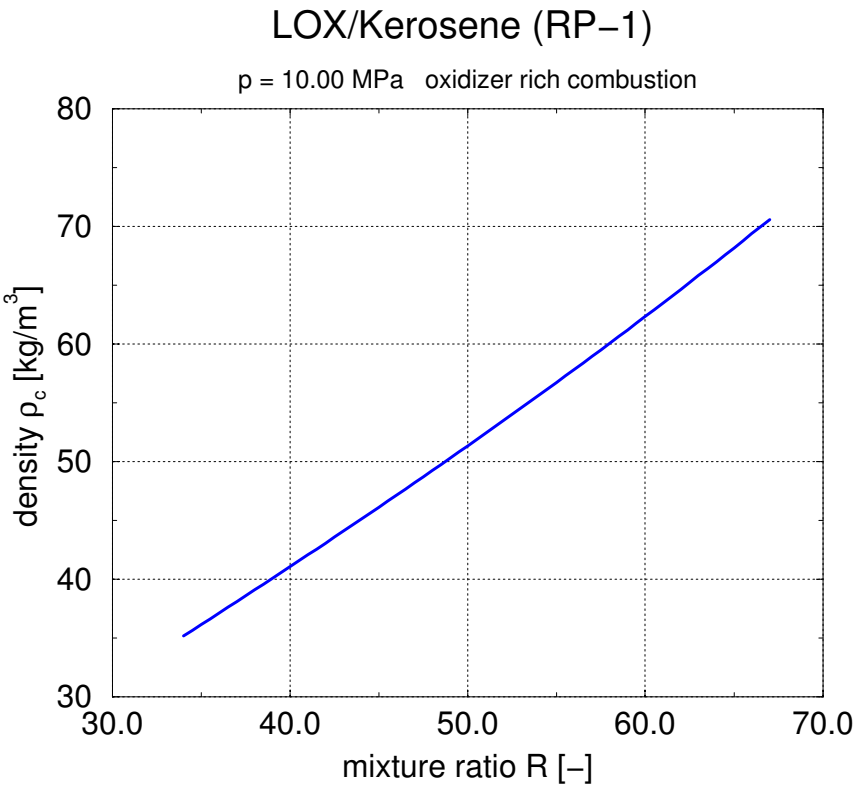

Figure 93: Oxidizer rich preburner hot gas density for LOX/RP-1

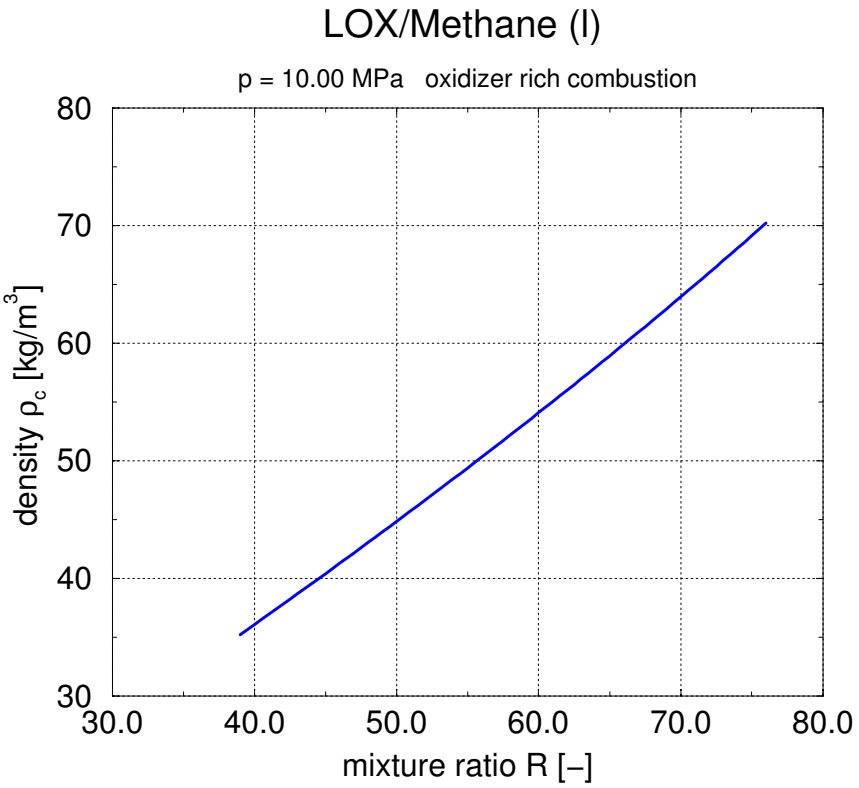

Figure 94: Oxidizer rich preburner hot gas density for LOX/Methane

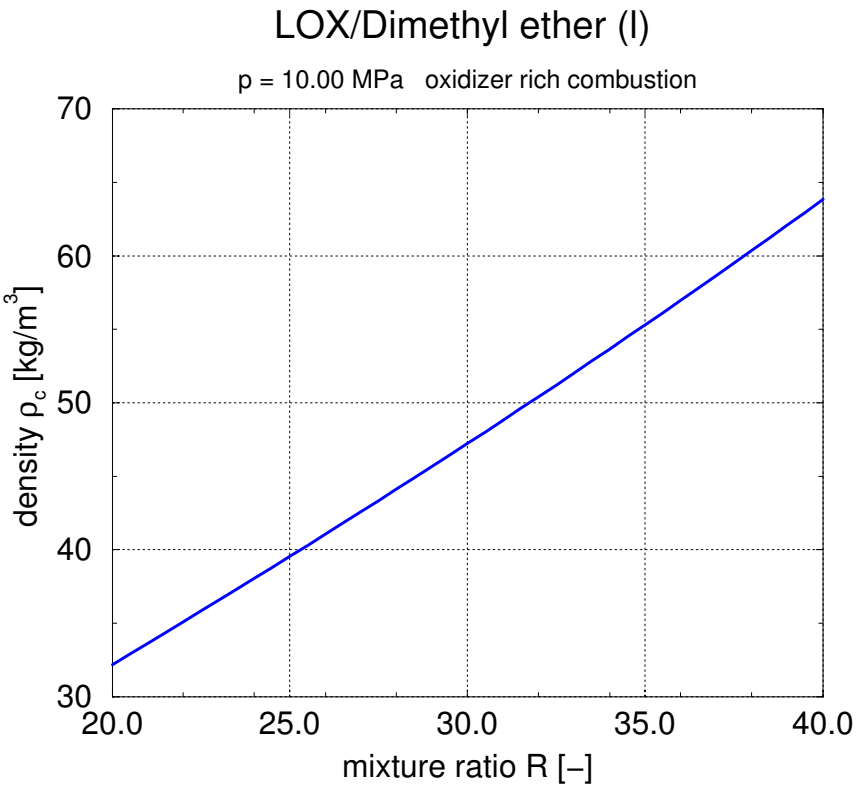

Figure 95: Oxidizer rich preburner hot gas density for LOX/Dimethyl ether

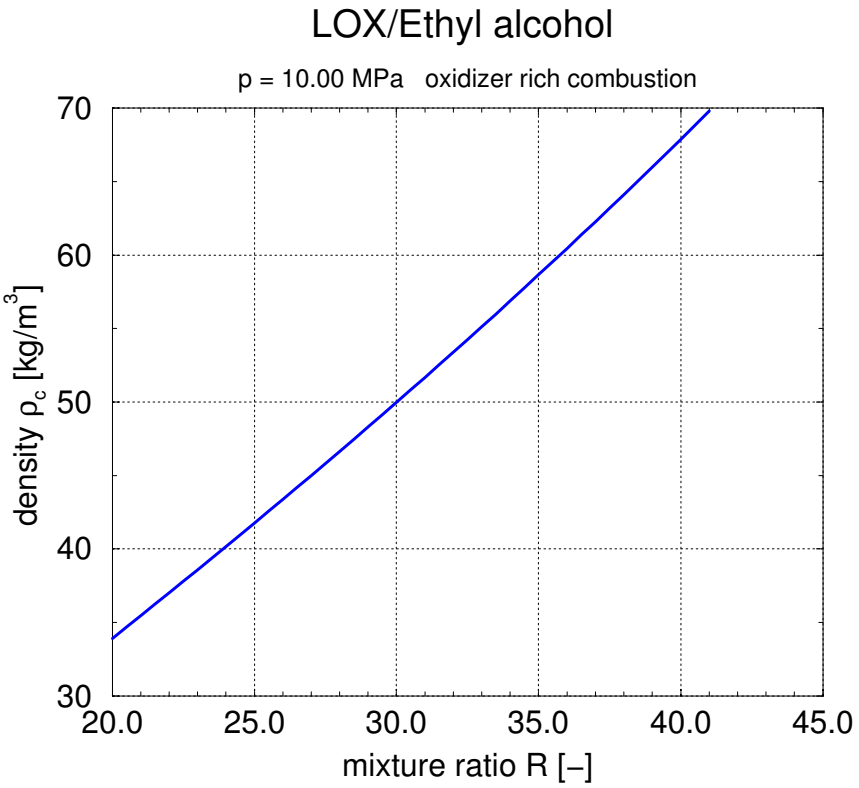

Figure 96: Oxidizer rich preburner hot gas density for LOX/Ethanol

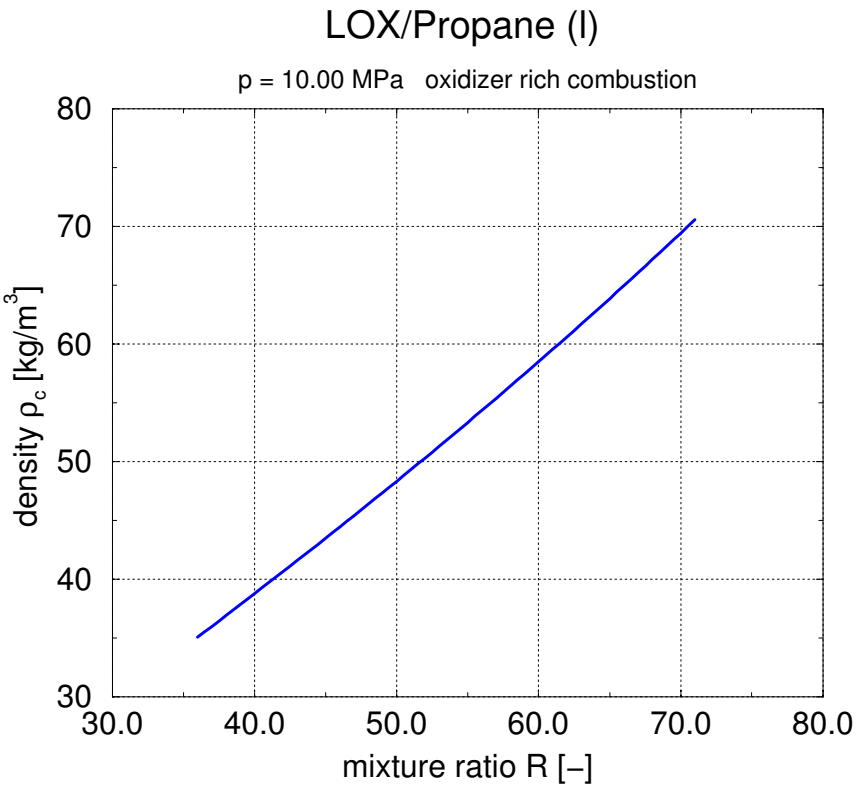

Figure 97: Oxidizer rich preburner hot gas density for LOX/Propane

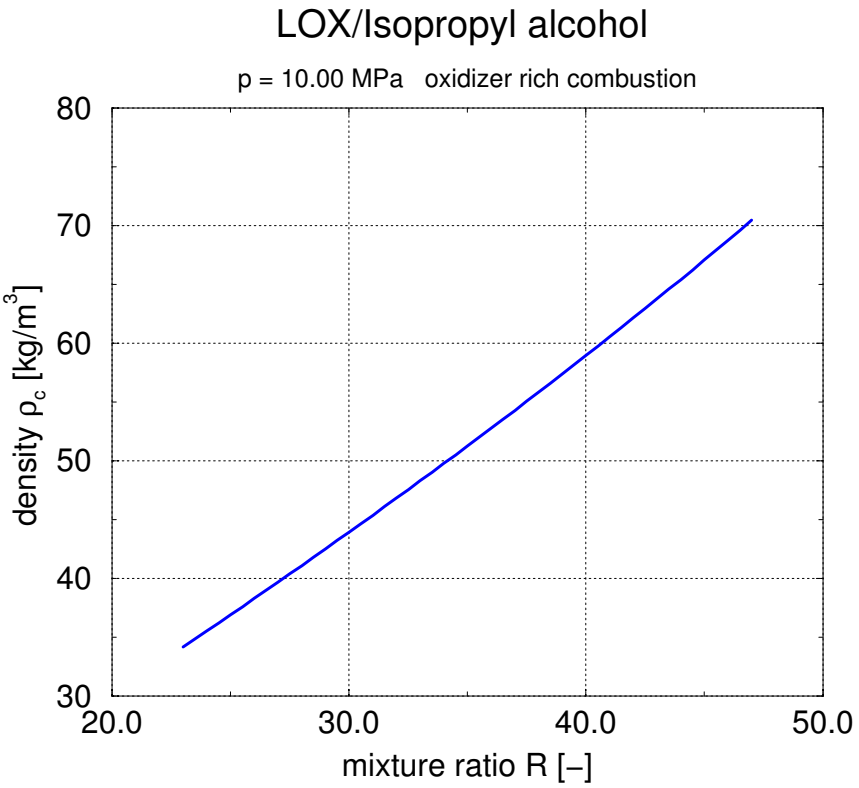

Figure 98: Oxidizer rich preburner hot gas density for LOX/Isopropyl alcohol

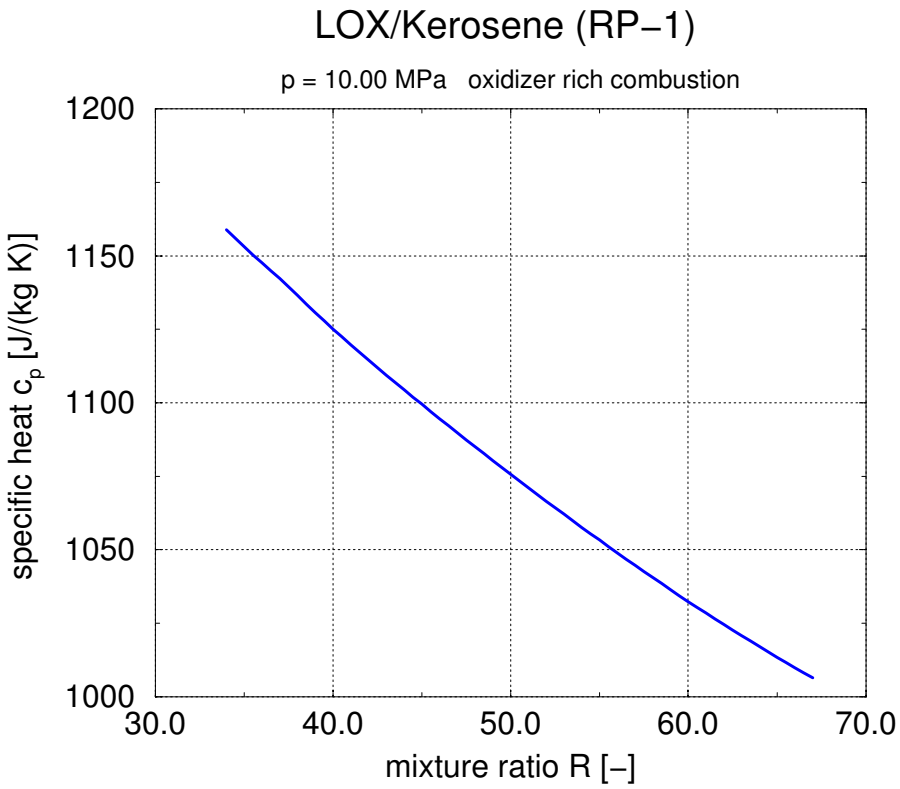

Figure 99: Oxidizer rich preburner specific heat for LOX/RP-1

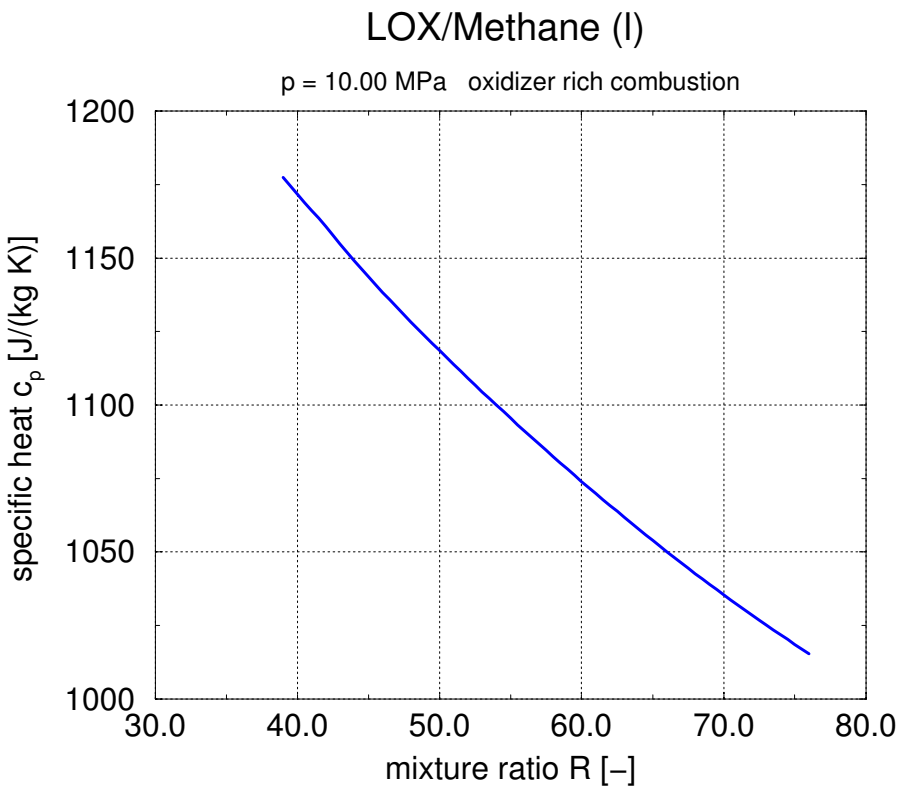

Figure 100: Oxidizer rich preburner specific heat for LOX/Methane

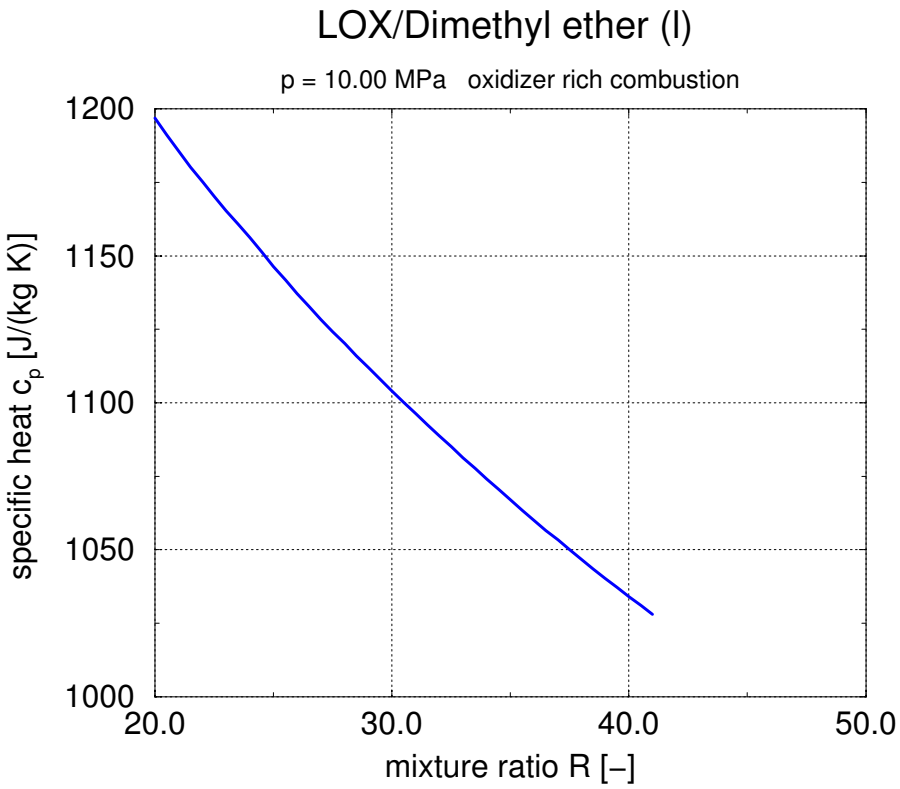

Figure 101: Oxidizer rich preburner specific heat for LOX/Dimethyl ether

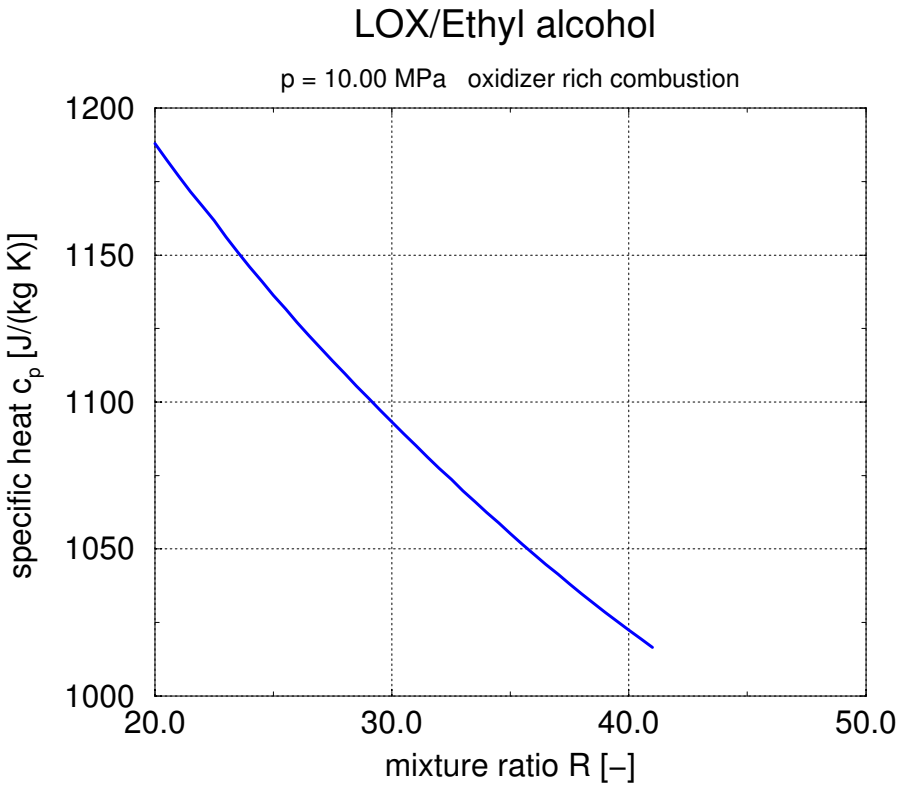

Figure 102: Oxidizer rich preburner specific heat for LOX/Ethanol

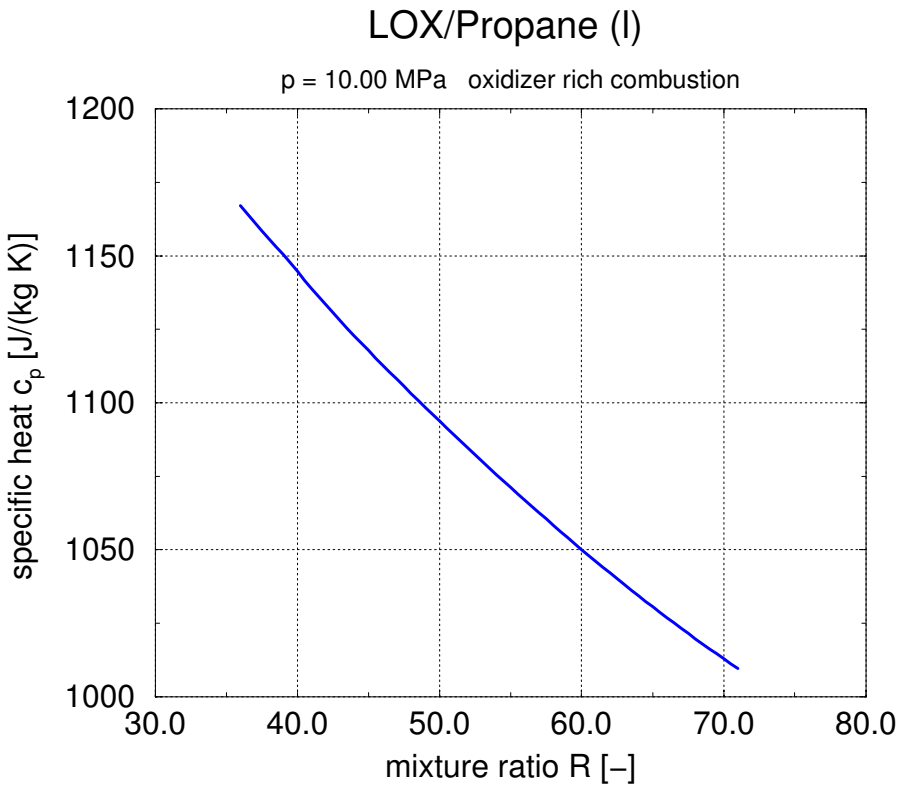

Figure 103: Oxidizer rich preburner specific heat for LOX/Propane

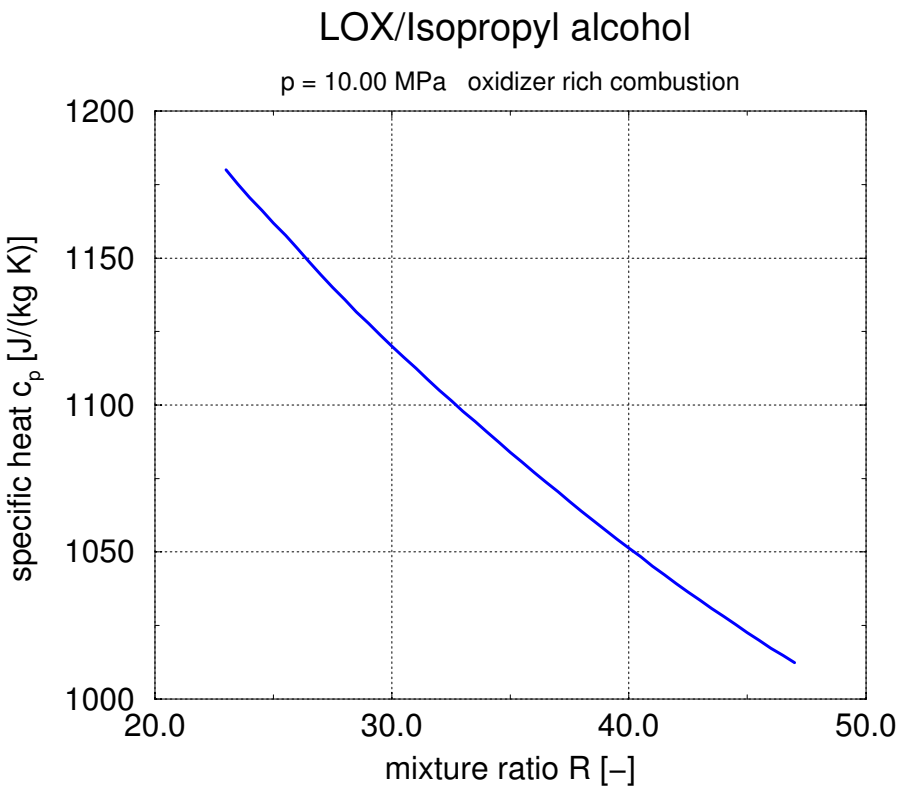

Figure 104: Oxidizer rich preburner specific heat for LOX/Isopropyl alcohol

3.8 Graphical Summary and Assessment

An interesting graphical representation of major propellant properties in dependence of their chemical composition is shown in Figure 105 through Figure 107. A strong influence of the number of C-atoms in a molecule can be stated if the propellants are subdivided in groups of different chemical bonding. Kerosene is assumed here as a paraffin with an average number of C-atoms slightly above 12. This assumption is consistent with data provided in [Edwards03].

The density of kerosene is the highest, while that of methane is the lowest for all species regarded in this report.

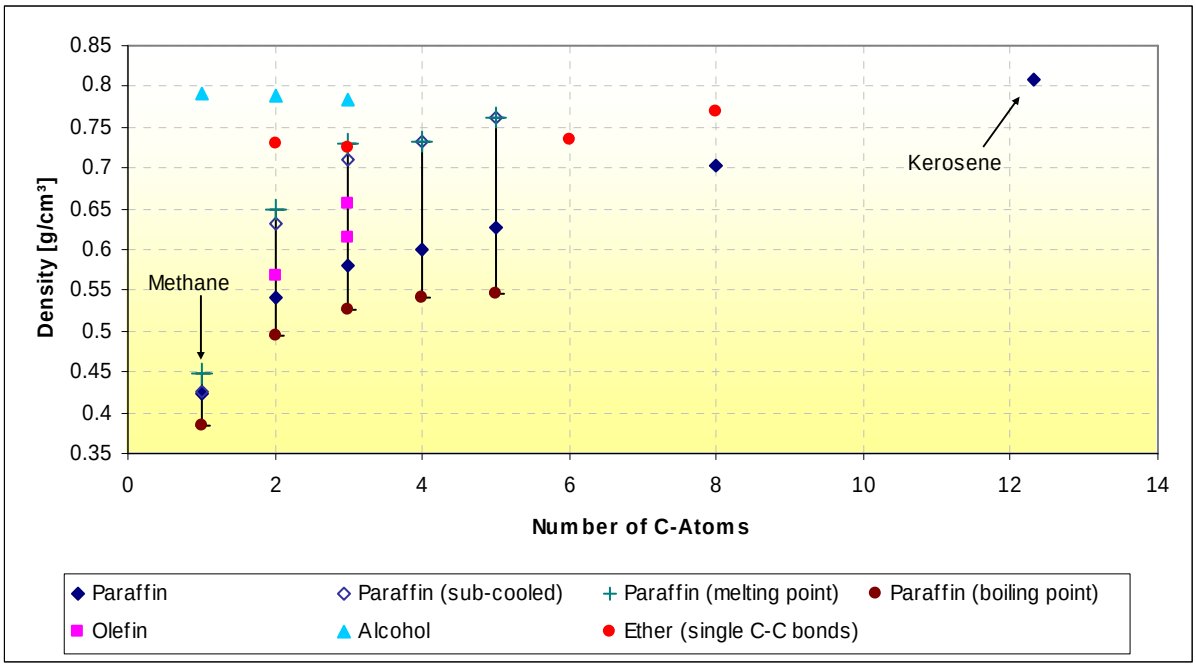

Figure 105: Density of propellants

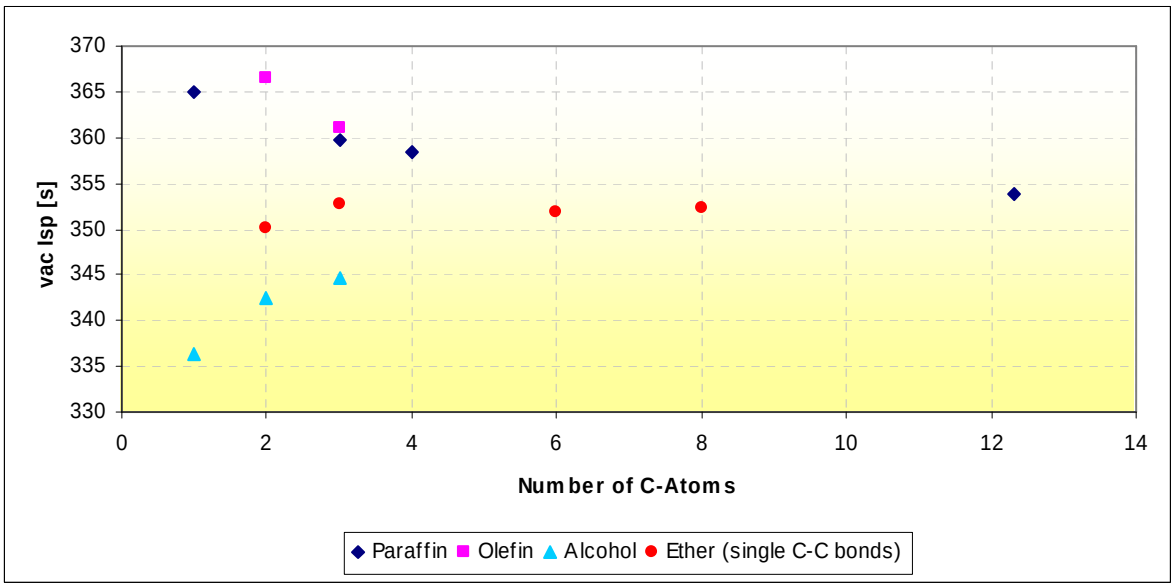

Figure 106: Vacuum specific impulse of propellants (oxidizer: LOX)

The optimum density specific impulse (product of specific impulse and mean density of oxidizer and fuel inside the tanks) delivers the best value for kerosene and the lowest for methane. Note also the interesting position of the subcooled paraffins ethane, propane and butane.

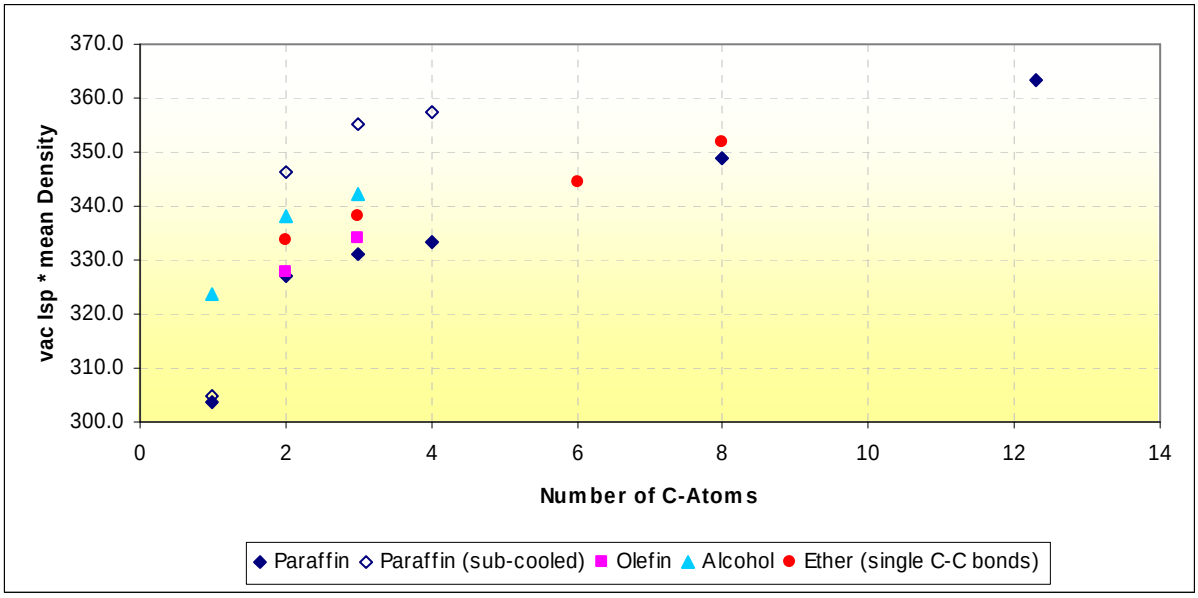

Figure 107: Product of vacuum specific impulse and mean propellant density (oxidizer: LOX)

4 Cooling capability and thermal stability

4.1 Representative green propellants

In accordance with the project description [Fratacci03], the following green propellants were selected as representative for the cooling capability and thermal stability study:

Methane	CH4
Alcohol (Ethanol, Methanol)	(C2H6O ,CH4O)
Propane	C3H8
Kerosene (RP-1, JP-7, JP-8, JP-10)	
Hydrogen Peroxide	H2O2
Ammonia	NH3
Hydroxyl Ammonium Nitrate (HAN)	[NH3OH]+ [NO3]-
Ammonium Dinitramide (ADN)	[NH4]+ [N(NO2)3]-

4.2 Important criteria for the assessment of coolants

4.2.1 Thermal stability and coking

The decomposition of hydrocarbons takes place when a certain fluid temperature is exceeded in the case of heat transfer. Due to a defined property of the fuel for the combustion process and as coolant in the regenerative cooling system, this has to be prevented. Certain bulk- and wall temperature limitations have to be considered.

Thermal cracking of hydrocarbons is dependant on wall temperatures, flow rates and pressure. Molecules with higher atomic mass can be decomposed at lower heat input. The following figure 108 shows as example the equilibrium diagram for CH4 decomposition:

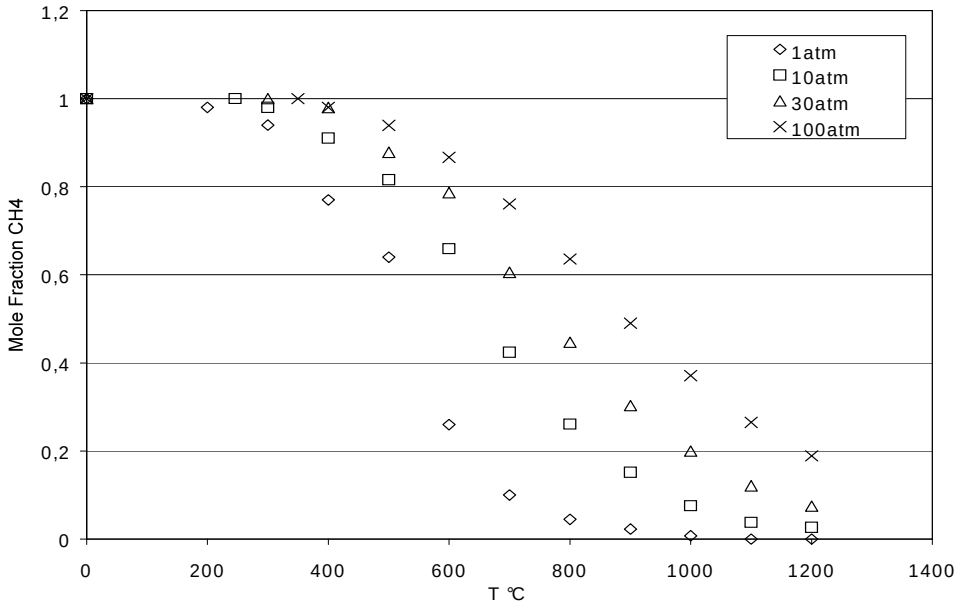

Figure 108: Thermal cracking as function of thermodynamic states [Byong02], [Steinberg95]

As representative examples the reaction equations which describe the thermal deposition (pyrolysis) of methane and propane are given:

methane: CH_4 -> $C + 2H_2$

propane: C_3H_8 -> $CH_4 + C_2H_4$

From figure 108, it can be observed that higher pressures decrease the tendency of thermal decomposition of methane. Also the temperature value for starting thermal decomposition is shifted towards higher values as the pressure of CH4 is increased.

Coking is the deposition of carbon compounds to the cooling channel wall. These layers are increasing with time. It influences the heat transfer and hydrodynamic behavior as follows:

Heat transfer is reduced due to an increase of the coolant side thermal resistance with an increasing layer thickness of carbon deposition.

Pressure loss is increased due to roughness elements on the cooling channel wall.

Single tube heat exchanger experiments have been accomplished to define certain wall temperature limits for the application of hydrocarbon fuels as coolant (see table 9). It can be observed that for each fuel, a wide range of maximum wall temperatures is available:

fuel	Tw,max [K]	Depos. Rate [g/m²h]	Author
Methane	500-650	<0.8	[Giovanetti83]
Methane	970		[Cook80]
Methane	770		[Rosenberg88]
Propane	650-670		[Byong02]
Propane	730		[Michel83], [Roback81], [Cook80]
Propane	400-580	3-5.8	[Giovanetti83]
RP-1	650		[Byong02]
RP-1	560-750	2-3.2	[Giovanetti83]
RP-1	590		[Michel83], [Roback81], [Cook80]
RP-1	570		[Rosenberg88]
Ethanol	-	Coking not observed	[Michel83]

Table 10: Wall temperature thresholds for coking

Coking can be observed in electrically heated tube experiments with an increase of wall temperatures at constant heating and flow parameters with time. Nitrogen pressurized tests had lower coking as air-pressurized tests; therefore oxygen seems to play an important role. Rocket-kerosene (RP-1) is better as Aerokerosene (JP-x) due to lower contamination. Coking of fuels is dependent on the wall material and coatings such as gold plating, platinum plating, nickel plating and silver plating. Pre cryogenic cooling can prevent decomposition.

4.2.2 Undesired chemical reactions with liner material

Corrosion of the liner wall material occurs if the fuel contains a certain part of sulfur. Copper corrosion produces rough wall layers with reduced thermal conductivity and causes an additional pressure loss in the cooling channels.

Contamination of sulfur and oxygen in the fuels are responsible for sulfurize and oxidize copper, which results in a deterioration of the copper wall. Carbon deposition from heated hydrocarbon fuels on a hot copper wall can cause copper corrosion. Example impurities are methyl-hydrosulfide, hydrogen-sulfide.

Fuel	Tw,max [K]	Sulfur Content
Methane	770	< 1ppm
Propane		No sulfur content allowed
RP-1	570	20 ppm
Ethanol	-	-

Table 11: Wall temperature limitations against corrosion of wall material [Rosenberg88]

4.2.3 Performance (pressure drop versus heat transfer)

The physical properties of the coolant are influencing the heat transfer. Good coolants are high density fluids with a high heat capacity c_p and low dynamic viscosity η. A comparison of the heat capacity of different coolants is given in figure 109.

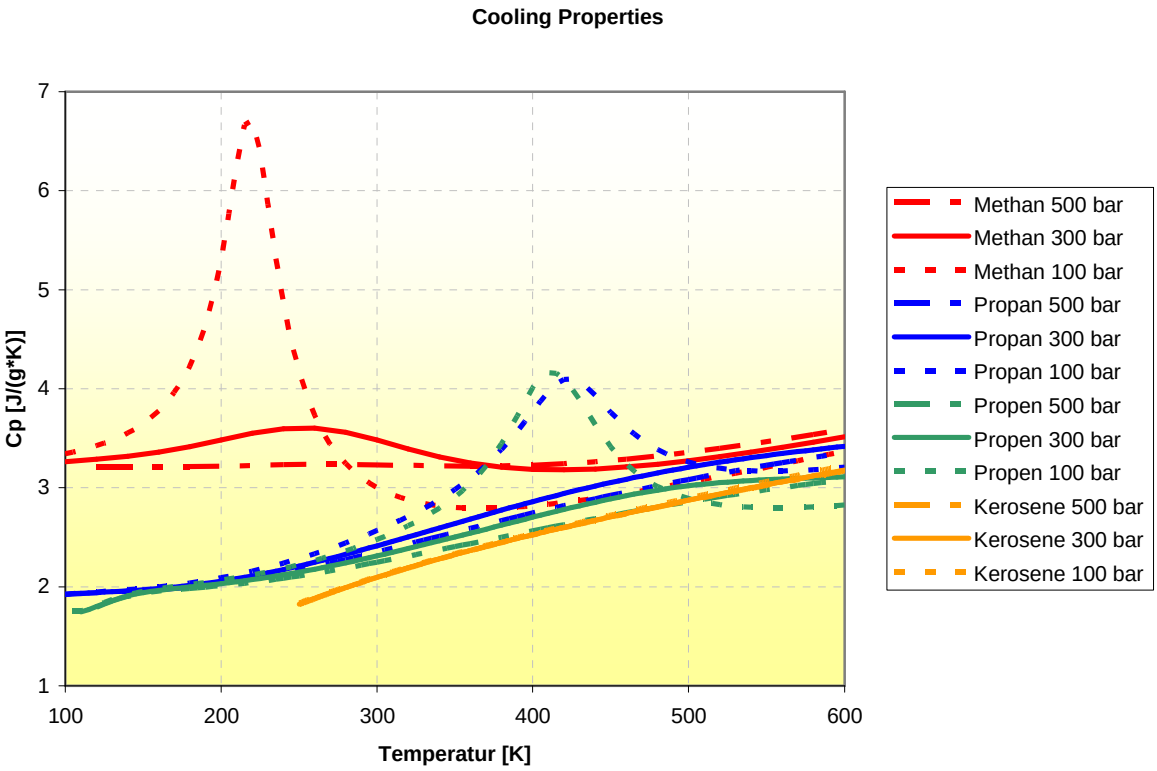

Figure 109: Heat capacity of selected propellants

High density fluids with a high heat capacity *cp* and low dynamic viscosity η result in high Reynolds-numbers *Re* and low volume flow. High Reynolds-numbers produce high coolant side heat transfer coefficients α and low tube friction numbers ς. Low volumetric flow rates keep the total pressure loss $\Delta ptot$ low.

To evaluate the thermodynamic region, in which the different types of fuels are used as a coolant, the following data is collected for typical hydrocarbon rocket engines:

fuel	Tstorage [K]	T [K]	P [bar]	Engine
methane	111	130 - 203	470 – 270	SE-12
propane	90	150 - 300	500 – 350	Example
Kerosene	290	300 – 480	510 – 270	RD-180
Kerosene	290	300	410 -	RD-169

Table 12: Thermodynamic regime of coolants in rocket engines

Heat transfer and pressure loss studies make the knowledge of the physical properties of the coolants necessary:

Fuel	Tcrit [K]	Pcrit [bar]
Methane	191	46.4
Propane	370	42.6
Aero-kerosene	598	23.9
Rocket-kerosene	677	25.0
RP-1	668	22.0
Ethanol	516.25	63.94

Table 13: Critical temperature and pressures of fuels

Figure 110 shows the behavior of different fuels as coolant for a tube flow section. The thermodynamic states of the fuels in the cooling system are obtained from representative data of combustion chambers. For a cylindrical tube flow section the necessary mass flow is evaluated to maintain the coolant wall temperature at Tw= 550K at different heat flux levels. The hydrodynamic loss is represented by the pressure gradient:

$$\frac{\partial P}{\partial z} = \frac{1}{2D}\rho v^2 \varsigma$$

along the tube.

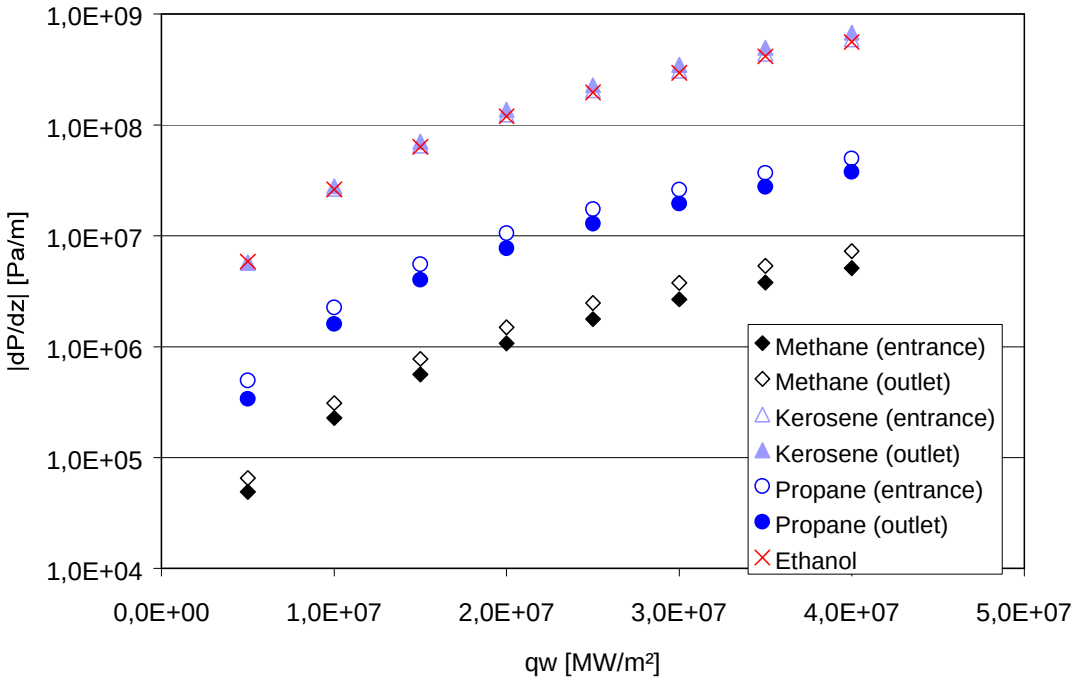

Figure 110: Characterisation of hydrodynamic losses for different fuels

From this simple analysis it can be observed that Ethanol and Kerosene have the highest coolant mass fluxes and produce therefore also the highest pressure losses. Methan is the favorite with respect to the hydrodynamic and heat transfer performance.

Additional studies have to be made, in order to verify, if the fuel is suitable for a regenerative cooling of wall structures.

4.2.4 Thermal stratification

Thermal stratification occurs in regeneratively cooled wall structures due to high amounts of thermal energy, which is asymmetrically transported to the coolant. The capability to transfer heat normal to the main flow direction in the turbulent core flow of the coolant has to be investigated.

4.2.5 Pseudo film boiling

All the fuels considered in this section have supercritical thermodynamic conditions, so the coolant will not enter the two-phase region. No phase interfaces occur in the flow, but pseudo boiling phenomena are reported and expected to occur.

4.3 Ranking of fuels with respect to cooling performance and thermal stability

From the available data in the literature the following evaluation can be given.

Fuel	Thermal Coking and decomposition	Cooling performance
Methane	**++**	**++**
Propane	**--**	**+**
Kerosene (RP-1)	**-**	**--**
Ethanol	**++**	**--**

Table 14: Ranking of selected fuels as coolant

4.4 Available experiments and systematic studies

Data from single tube heat exchanger experiments are collected in table 15. Table 16 contains information from system analytic investigations of the usage of different fuels in hydrocarbon engines.

For other green propellants (Ammonia, Hydrogen Peroxide, HAN, ADN) no single tube experiment data concerning characterization of heat transfer and thermal stability is available.

Fuel	Test Objective	T_{bulk}	P	Additional information	Reference
Methane	Electrical heated tube experiments	950℃ – 1150℃	1 atm	Aluminum tube, ∅ ½ inch, Flow rate 250 – 1500 ml/min	[Byong02]
Methane	Electrical heated tube experiments	0℃ – 1200℃	1 – 100 atm		[Steinberg95]
Methane	Electrical heated tube experiments	-145℃ – 130℃	4,5 - 200 bar	Steel + cooper + 1Cr18Ni9Ti tubes, ∅3mm, v=2 – 106 m/s	[Keming98]
Methane	Heated tube experiment	-250℉ – 250℉	450 – 1800 psi	V=50 – 150ft/s	[Michel83]
Methane	Heated tube experiments	160-230K	39 – 138 bar	V=30-90m/s, Tw=230-810K	[Giovanetti83]
Methane	Heated tube experiments			Stainless steel tubes	[Cook84]
Propane	Electrical heated tube experiments	10.2 – 197.9℃	20 – 274 bar	1Cr18Ni9Ti tubes, ∅3mm	[Keming98]
Propane	Heated tube experiment	-250℉ – 250℉	450 – 1800 psi	V=50 – 150ft/s	[Michel83]
Propane	Heated tube experiment		136-340 atm	V=6-30m/s, Twall=422-811m/s	[Roback81]
Propane	Heated tube experiment	160-230K	39 – 138 bar	V=30-90m/s, Tw=230-810K	[Giovanetti83]
Ethanol	Heated tube	-250℉ – 250℉	450 – 1800	V=50 – 150ft/s	[Michel83]

	experiment		psi		
RP-1	Electrical heated tube experiments	16 – 320 ℃	20 – 250	1Cr18Ni9Ti tubes, ∅1.7mm, v=10-16m/s	[Keming98]
RP-1	Electrical heated tube experiments	500℉	1000psi	Twall: 750℉ – 1000℉	[Stiegemeier02]
RP-1	Heated tube experiment		136-340 atm	V=6-30m/s, Twall=422-811m/s	[Roback81]
RP-1	Heated tube experiment	160-230K	39 – 138 bar	V=30-90m/s, Tw=230-810K	[Giovanetti83]
JP5	Electrical heated tube experiments	500℉	1000psi	Twall: 750℉ – 1000℉	[Stiegemeier02]
JP-7	Electrical heated tube experiments	500℉	1000psi	Twall: 750℉ – 1000℉	[Stiegemeier02]
JP-7	Heated tube experiment		136-340 atm	V=6-30m/s, Twall=422-811m/s	[Roback81]
JP-8	Electrical heated tube experiments	500℉	1000psi	Twall: 750℉ – 1000℉	[Stiegemeier02]
JP-10	Electrical heated tube experiments	500℉	1000psi	Twall: 750℉ – 1000℉	[Stiegemeier02]

Table 15: Single tube experiments

Fuel	Objective	Reference
JP-4, H2, N2H4, NH3	Study of different propellant combinations	[Curren59]
H2, Hydrocarbons	Investigation of regeneratively cooled chambers	[Schoenman85]
H2, Hydrocarbons, Oxygen	Booster engines, main stage engines	[Wagner75]
RP-1, Methane	Reusable liquid booster stages	[Burkhardt02]
RP-1, Methane, Propane, H2	Booster propulsion	[Johnson88]
H2, Kerosene, Methane	Low thrust engine study	[Mellish81]
Propane, Methane, RP-1, H2		[O´Brien81]
Propane, Methane, RP-1, H2	Low thrust engine study	[Shoji81]

Table 16: Analytical investigations, systematic studies, Higher order qualification parameters

Curren et al. [Curren59] has defined a selection criterion which takes into account temperature limitations concerning thermal stability (decomposition of the fuel) and to prevent coolant wall coking in case of carbon containing fuels. The maximum specific cooling potential Ψ_{max} is a quantity which is representative for the total heat, absorbed from the inlet temperature T_{in} to the maximum allowed coolant temperature T_{max} .

$$\Psi_{max} = \frac{\dot{m}_c}{A_2} \int_{Tin}^{T\,max} c_p dT = \frac{F \cdot ROF}{I \cdot A_2 \cdot \eta} \left(H_{max} - H_{in} \right)$$

The cooling utilization ratio φ is the ratio of the amount of heat rejected from a cooled engine Ψ_{ac} to the amount of heat the coolant is capable to absorb, due to limitations in maximum coolant temperatures T_{max}

$$\varphi = \frac{\Psi_{ac}}{\Psi_{max}} = \frac{H_{out} - H_{in}}{H_{max} - H_{in}}$$

A_2	combustion chamber throat area
c_p	coolant specific heat
F	thrust
H	coolant enthalpy
$I = \frac{F}{\dot{m}}$	specific impulse
$\dot{m}$	hot gas mass flow
$\dot{m}_c$	coolant mass flow
ROF	mixture ratio
T	temperature

These qualification criteria can be used with 1d-calculation methods to investigate systematically the regenerative cooling of combustion chambers.

5 References

[AirLiquide04a] http://www.airliquide.com/ [cited 03 Feb 2004]

[AirLiquide04b] AirLiquide Deutschland, personal communication, February 2004

[bp02] Safety Data Sheet Ethanol, Version 1, BP p.l.c., July 2002

[Burkhardt02] Burkhardt, H., Sippel, M., Herbertz, A., Klevanski, J., Comparative Study of Kerosene and Methane Propellant Engines for Reusable Liquid Booster Stages, 4th International Conference on Launcher Technology „Space Launcher Liquid Propulsion“, Liege (Belgium), 2002.

[Burkhardt04] Burkhardt, H., Sippel, M., Herbertz, A. and Klevanski, J.: Kerosene vs Methane: A Propellant Tradeoff for Reusable Liquid Booster Stages, accepted for publication J. of Spacecraft and Rockets

[Byong02] Byong, G.L., Jong, S.L., Dae, K.C., Sang, D.L., Coproduction of Hydrogen and Carbon Black by Thermal Cracking of Natural Gas Proceedings of the 9th APCChE Congress 2002, Christchurch, Edited by: P.A.Gostomski and K.R. Morison, eds., University of Canterbury,

[Cook80] Cook, R.T., Advanced Cooling Techniques for High Pressure Hydrocarbon-Fueled Rocket Engine, AIAA Paper 80-1266, June 1980.

[Cook84] Cook, R. T., Methane heat transfer investigation, NASA-CR-171051, 1984.

[Curren59] Curren, A., Price, H.G., Douglas, H., Analysis of Effects of Rocket-Engine Design Parameters on Regenerative-Cooling Capabilities of several Propellants, NASA Technical Note D-66, Lewis Research Center, 1959.

[Edwards03] Edwards, T.: Liquid Fuels and Propellants for Aerospace Propulsion: 1903-2003, J. of Propulsion and Power, Vol. 19, No. 6, Nov-Dec 2003

[Fratacci03] Fratacci, G. and Forestier, H.: Evaluation of Green Propellants for Space Applications, ITT/1-4282/03/NL/CH, Snecma Doc No. FLC 3-046, Issue 1, 24.3.2003

[Giovanetti83] Giovanetti, A. J., Spadaccini, L. J., Szetela, E. J., Deposit formation and heat transfer in hydrocarbon rocket fuels, NASA-CR-168277, 1983.

[IARC04a] International Agency for Research on Cancer (IARC), http://monographs.iarc.fr/monoeval/crthall.html [cited 10 Feb 2004]

[IARC04b] International Agency for Research on Cancer (IARC), **SEARCH** IARC Agents and Summary Evaluations, http://monographs.iarc.fr/htdig/search.html [cited 9 March 2004]

[ILO04] International Labour Organization, http://www.ilo.org/public/english/protection/safework/cis/products/icsc/dtasht/riskphrs/ [cited 10 Feb 2004]

[Johnson88] Johnson, P., Satterthwaite, S., Carson, C., Schnackel, J., Booster propulsion/vehicle impact study NASA-CR-179313, 1988.

[Keming98] Keming, L., Baoe, Y., Zhongli, Z., Investigation of Heat Transfer and Coking Characteristics of Hydrocarbon Fuels, Journal of Propulsion and Power, Vol. 14, No. 5, 1998.

[Koelle61] Koelle, H.: Handbook of astronautical engineering, McGraw-Hill, 1961

[Masters82] Masters, P.A., Aukermann, C. A., „Deposit Formation in Hydrocarbon Rocket Fuels with an Evaluation of a Propane Heat Transfer Correlation“, NASA TM-82911, June 1982.

[McBride96] McBride, B., Gordon, S.: Computer Program for Calculation of Complex Chemical Equilibrium Compositions and Applications, Volume II: Users Manual and Program Description, NASA-RP-1311, Jun 1996

[Mehta95] Mehta, G., Stone, Ingram, C., Bai, S.D., Sanders, T., Comparative Testing of Russian Kerosene and RP-1, AIAA Paper 95-2962, 1995.

[Mellish81] Mellish, J.A., Low-thrust chemical rocket engine, NASA-CR-165276, 1981.

[Michel83] Michel, R.W., Combustion Performance and Heat Transfer Characterization of LOX/Hydrocarbon type Propellants, NASA-CR-171712 and NASA-CR-171713, 1983.

[MIL67] Military Specification MIL-P-25576C with amendment 2, February 1967

[NIST04] NIST Standard Reference Database 69 - March 2003 Release: *NIST Chemistry WebBook* [online database], URL: http://webbook.nist.gov/chemistry/ [cited 03 Feb 2004]

[O´Brien81] O'Brien, C.J., Ewen, R.L., Advanced Hydrocarbon Rocket Engine Study, NASA Report 33452F, 1981.

[Oxford01] Safety Data Sheet Acetaldehyde, Revision No. EU/002, Oxford Chemicals, February 2001

[Rachner98] Rachner, M.: Die Stoffeigenschaften von Kerosin Jet A-1, Mitteilung 98-01, Deutsches Zentrum für Luft- und Raumfahrt, März 1998

[Roback81] Roback, R., Szetela, E. J., Spadaccini, L. J., Deposit formation in hydrocarbon rocket fuels, NASA-CR-165405 , 1981.

[Rosenberg88] Rosenberg, S.D., Gage, M.L., Compatibility of Hydrocarbon Fuels with Booster Engine Combustion Chamber Liners, AIAA Paper 88-3215, July 1988.

[Rosenberg89] Rosenberg, S.D., Gage, M.L., Corrosion Prevention in Hydrocarbon-Fueled Booster Engine Combustion Chamber Liners, AIAA Paper 89-2738, July 1989.

[Schoenman85] Schoenman, L., High Pressure Propulsion Advanced Concepts for Cooling, 36th Congress of the International Astronautical Federation, Stockholm, 1985.

[Shell04] Shell Deutschland, personal communication, February 2004

[Shoji81] Shoji, J. M., Low-thrust chemical rocket engine study, NASA-CR-165275, 1981.

[SigmaAldrich04] http://www.sigmaaldrich.com/suite7/Area_of_Interest/Europe_Home/Germany.html [cited 03 Feb 2004]

[Steinberg95] Steinberg, M., Energy Conversion & Management, Vol. 36, page 249-267, 1995.

[Stiegemeier02] Stiegemeier, B., Lawrence, KS, Meyer, M., 38th AIAA/ASME/SAE/ASEE Joint Propulsion Conference & Exhibit, AIAA Paper 2002-3873, Indianapolis.

[Valentian04] Valentian, D.: Note interne, FLT 00005/2004, Jan 2004

[Wacker02] Safety Data Sheet (91/155/EEC) Di-N-Butyl Ether, Version 1.2 (REG_EUROPE), Wacker Chemie GmbH, September 2002

[Wagner75] Wagner, W.R., Shoji, J.M., Advanced Regenerative Cooling Techniques for Future Space Transportation Systems, AIAA/SAE 11th Propulsion Conference, Anaheim, California, 1975.

6 Annex

6.1 IARC Carcinogenicity Classification

IARC Classification	
Group	**Meaning**
1	Carcinogenic to humans
2a	Probably carcinogenic to humans
2b	Possibly carcinogenic to humans
3	Unclassifiable as to carcinogenicity to humans

Table 17: IARC Classification of carcinogenicity [IARC04a]

6.2 Risk Phrases

R 1 Explosive when dry.
R 2 Risk of explosion by shock, friction, fire or other sources of ignition.
R 3 Extreme risk of explosion by shock, friction, fire or other sources of ignition.
R 4 Forms very sensitive explosive metallic compounds.
R 5 Heating may cause an explosion.
R 6 Explosive with or without contact with air.
R 7 May cause fire.
R 8 Contact with combustible material may cause fire.
R 9 Explosive when mixed with combustible material.
R 10 Flammable.
R 11 Highly flammable.
R 12 Extremely flammable.
R 13 Extremely flammable liquefied gas.
The phrase has been deleted by ATP 28 (6 August 2001), but may still appear in cards not modified since then.
R 14 Reacts violently with water.
R 15 Contact with water liberates extremely flammable gases.
R 16 Explosive when mixed with oxidizing substances.
R 17 Spontaneously flammable in air.
R 18 In use, may form flammable/explosive vapor air-mixture.
R 19 May form explosive peroxides.
R 20 Harmful by inhalation.
R 21 Harmful in contact with skin.
R 22 Harmful if swallowed.
R 23 Toxic by inhalation.
R 24 Toxic in contact with skin.
R 25 Toxic if swallowed.
R 26 Very toxic by inhalation.
R 27 Very toxic in contact with skin.
R 28 Very toxic if swallowed.
R 29 Contact with water liberates toxic gas.
R 30 Can become highly flammable in use.
R 31 Contact with acids liberates toxic gas.
R 32 Contact with acids liberates very toxic gas.
R 33 Danger of cumulative effects.
R 34 Causes burns.
R 35 Causes severe burns.
R 36 Irritating to eyes.
R 37 Irritating to respiratory system.
R 38 Irritating to skin.
R 39 Danger of very serious irreversible effects.
R 40 Limited evidence of a carcinogenic effect.
*The phrase has been **changed** by ATP 28 (6 August 2001). The corresponding phrase used in earlier cards reads:*
Possible risk of irreversible effects.
R 41 Risk of serious damage to eyes.
R 42 May cause sensitization by inhalation.
R 43 May cause sensitization by skin contact.
R 44 Risk of explosion if heated under confinement.
R 45 May cause cancer.
R 46 May cause heritable genetic damage.
R 47 May cause birth defects.
The phrase has been deleted by ATP 28 (6 August 2001), but may still appear in cards not modified since then.
R 48 Danger of serious damage to health by prolonged exposure.
R 49 May cause cancer by inhalation.
R 50 Very toxic to aquatic organisms.

R 51	Toxic to aquatic organisms.
R 52	Harmful to aquatic organisms.
R 53	May cause long-term adverse effects in the aquatic environment.
R 54	Toxic to flora.
R 55	Toxic to fauna.
R 56	Toxic to soil organisms.
R 57	Toxic to bees.
R 58	May cause long-term adverse effects in the environment.
R 59	Dangerous for the ozone layer.
R 60	May impair fertility.
R 61	May cause harm to the unborn child.
R 62	Possible risk of impaired fertility.
R 63	Possible risk of harm to the unborn child.
R 64	May cause harm to breast-fed babies.
R 65	Harmful: may cause lung damage if swallowed.
R 66	Repeated exposure may cause skin dryness or cracking.
R 67	Vapors may cause drowsiness and dizziness.
R 68	Possible risks of irreversible effects.

Table 18: Risk phrases [ILO04]

6.3 List of selected abstracts

METHANE

Methane heat transfer investigation

Citation: NASA-CR-171051, Doc I.D.: 19840020949NASA Center for Aerospace Information (CASI), NASA-CR-171051, 1984

Future high chamber pressure LOX/hydrocarbon booster engines require copper base alloy main combustion chamber coolant channels similar to the SSME to provide adequate cooling and reusable engine life. Therefore, it is of vital importance to evaluate the heat transfer characteristics and coking thresholds for LNG (94% methane) cooling, with a copper base alloy material adjacent to he fuel coolant. High pressure methane cooling and coking characteristics recently evaluated at Rocketdyne using stainless steel heated tubes at methane bulk temperatures and coolant wall temperatures typical of advanced engine operation except at lower heat fluxes as limited by the tube material. As expected, there was no coking observed. However, coking evaluations need be conducted with a copper base surface exposed to the methane coolant at higher heat fluxes approaching those of future high chamber pressure engines.

Methane heat transfer investigation

Cook, R. T. (Rockwell International Corp., Canoga Park, CA, United States), NASA Center for Aerospace Information (CASI), NASA-CR-171199, 1984

Future high chamber pressure LOX/hydrocarbon booster engines require copper-base alloy main combustion chamber coolant channels similar to the SSME to provide adequate cooling and reusable engine life. Therefore, it is of vital importance to evaluate the heat transfer characteristics and coking thresholds for LNG (94% methane) cooling, with a copper-base alloy material adjacent to the fuel coolant. High-pressure methane cooling and coking characteristics were recently evaluated using stainless-steel heated tubes at methane bulk temperatures and coolant wall temperatures typical of advanced engine operation except at lower heat fluxes as limited by the tube material. As expected, there was no coking observed. However, coking evaluations need be conducted with a copper-base surface exposed to the methane coolant at higher heat fluxes approaching those of future high chamber pressure engines.

Combustion performance and heat transfer characterization of LOX/hydrocarbon type propellants, volume 1

Michel, R. W. (Aerojet Liquid Rocket Co., Sacramento, CA, United States), NASA Center for Aerospace Information (CASI), NASA-CR-171713, 1983

A program to evaluate liquid oxygen and various hydrocarbon fuels as low cost alternative propellants suitable for future space transportation system applications is discussed. The emphasis of the program is directed toward low earth orbit maneuvering engine and reaction control engine systems. The feasibility of regeneratively cooling an orbit maneuvering thruster was analytically determined over a range of operating conditions from 100 to 1000 psi chamber pressure and 1000 to 10,000-1bF thrust, and specific design points were analyzed in detail for propane, methane , RP-1, ammonia, and ethanol; similar design point studies were performed for a film cooled reaction control thruster. Heat transfer characteristics of propane were experimentally evaluated in heated tube

tests. Forced convection heat transfer coefficients were determined over the range of fluid conditions encompassed by 450 to 1800 psi, -250 to +250 F, and 50 to 150 ft/sec, with wall temperatures from ambient to 1200 F. Seventy-seven hot firing tests were conducted with LOX/propane and LOC/ethanol, for a total duration of nearly 1400 seconds, using both heat sink and water-cooled calorimetric chambers.

Combustion performance and heat transfer characterization of LOX/hydrocarbon type propellants

Michel, R. W. (Aerojet Liquid Rocket Co., Sacramento, CA, United States), NASA Center for Aerospace Information (CASI), NASA-CR-171712, 1983

An evaluation of liquid oxygen (LOX) and various hydrocarbon fuels as low cost alternative propellants suitable for future space transportation system applications was done. The emphasis was directed toward low earth orbit maneuvering engine and reaction control engine systems. The feasibility of regeneratively cooling an orbit maneuvering thruster was analytically determined over a range of operating conditions from 100 to 1000 psi chamber pressure and 1000 to 10,000-1bF thrust, and specific design points were analyzed in detail for propane, methane, RP-1, ammonia, and ethanol; similar design point studies were performed for a film-cooled reaction control thruster. Heat transfer characteristics of propane were experimentally evaluated in heated tube tests. Forced convection heat transfer coefficients were determined. Seventy seven hot firing tests were conducted with LOX/propane and LOX/ethanol, for a total duration of nearly 1400 seconds, using both heat sink and water-cooled calorimetric chambers. Combustion performance and stability and gas-side heat transfer characteristics were evaluated.

High speed commercial transport fuels considerations and research needs

Lee, C. M. (NASA Lewis Research Center, Cleveland, OH, United States); Niedzwiecki, R. W. (NASA Lewis Research Center, Cleveland, OH, United States), NASA Center for AeroSpace Information (CASI), NASA-TM-102535 , 1989

NASA is currently evaluating the potential of incorporating High Speed Civil Transport (HSCT) aircraft in the commercial fleet in the beginning of the 21st century. NASA sponsored HSCT enabling studies currently underway with airframers and engine manufacturers, are addressing a broad range of technical, environmental, economic, and related issues. Supersonic cruise speeds for these aircraft were originally focused in the Mach 2 to 5 range. At these flight speeds, both jet fuels and liquid methane were considered potential fuel candidates. For the year 2000 to 2010, cruise Mach numbers of 2 to 3+ are projected for aircraft fuel with thermally stable liquid jet fuels. For 2015 and beyond, liquid methane fueled aircraft cruising at Mach numbers of 4+ may be viable candidates. Operation at supersonic speeds will be much more severe than those encountered at subsonic flight. One of the most critical problems is the potential deterioration of the fuel due to the high temperature environment. HSCT fuels will not only be required to provide the energy necessary for flight, but will also be subject to aerodynamic heating and, will be required to serve as the primary heat sink for cooling the engine and airframe. To define fuel problems for high speed flight, a fuels workshop was conducted at NASA Lewis Research Center. The purpose of the workshop was to gather experts on aviation fuels, airframe fuel systems, airport infrastructure, and combustion systems to discuss high speed fuel alternatives, fuel supply scenarios, increased thermal stability approaches and measurements, safety considerations, and to provide directional guidance for future R and D efforts. Subsequent follow-up studies defined airport infrastructure impacts of high speed fuel candidates. The results of these activities are summarized. In addition, an initial case study using modified in-house refinery simulation model Gordian code (1) is briefly discussed. This code can be used to simulate different types of refineries, emphasizing jet fuel production and relative cost factors.

Booster propulsion/vehicle impact study, 2

Johnson, P. (Martin Marietta Aerospace, Denver, CO, United States); Satterthwaite, S. (Martin Marietta Aerospace, Denver, CO, United States); Carson, C. (Martin Marietta Aerospace, Denver, CO, United States); Schnackel, J. (Martin Marietta Aerospace, Denver, CO, United States), NASA Center for AeroSpace Information (CASI), NASA-CR-179313 , 1988

This is the final report in a study examining the impact of launch vehicles for various boost propulsion design options. These options included: differing boost phase engines using different combinations of fuels and coolants to include RP-1, methane, propane (subcooled and normal boiling point), and hydrogen; variable and high mixture ratio hydrogen engines; translating nozzles on boost phase engines; and cross feeding propellants from the booster to second stage. Vehicles examined included a fully reusable two stage cargo vehicle and a single stage to orbit vehicle. The use of subcooled propane as a fuel generated vehicles with the lowest total vehicle dry mass. Engines with hydrogen cooling generated only slight mass reductions from the reference, all-hydrogen vehicle. Cross feeding propellants generated the most significant mass reductions from the reference two stage

vehicle. The use of high mixture ratio or variable mixture ratio hydrogen engines in the boost phase of flight resulted in vehicles with total dry mass 20 percent greater than the reference hydrogen vehicle. Translating nozzles for boost phase engines generated a heavier vehicle. Also examined were the design impacts on the vehicle and ground support subsystems when subcooled propane is used as a fuel. The most significant cost difference between facilities to handle normal boiling point versus subcooled propane is 5 million dollars. Vehicle cost differences were negligible. A significant technical challenge exists for properly conditioning the vehicle propellant on the ground and in flight when subcooled propane is used as fuel.

LOX/hydrocarbon combustion and cooling survey

Cook, R. T. (Rockwell International Corp., Canoga Park, CA, United States); Kirby, F. M. (Rockwell International Corp., Canoga Park, CA, United States), NASA Center for AeroSpace Information (CASI), 1986

Liquid oxygen (LOX) and hydrocarbon fuels (methane, propane, and RP-1) are very attractive for booster rocket engine applications because of their high bulk density and respectful performance. Vehicle payload capability is dependent on the attainable engine chamber pressure and the combustion efficiency of the selected propellant combination. Combustor design approaches are presented to attain maximum cooling, stability, combustion efficiency, and reusable life. Experimental combustion efficiency and hot-gas heat-transfer rates are discussed as related to combustor contour, thrust level scaling, and injector characteristics including mixture ratio biasing and film cooling. These experimental data are compared to theory, and empirical relationships are derived. Conventional cooling relationships and coking limits are presented for potential hydrocarbon fuels as derived from high heat flux and high pressure electrically heated tube experiments. Experimental results of combustor coolant liner materials compatibility with hydrocarbon fuels are discussed. The application of the results of these studies to future LOX/hydrocarbon engines is delineated.

RP-1 and methane combustion and cooling experiments

Bailey, C. R. (NASA Marshall Space Flight Center, Huntsville, AL, United States), NASA Center for AeroSpace Information (CASI), 1986

A program was conducted to investigate ignition, combustion, and heat transfer characteristics of liquid oxygen and either RP-1 or methane fuel applicable to advanced booster engines. Experimental data for both staged combustion and gas generator cycles were obtained for methane. Testing using RP-1 was conducted in support of the gas generator cycle. A pressure-fed combustion system rated at 40,000 pounds thrust was used for all testing. Preburner and gas generator combustion data for both propellant combinations were obtained at pressures ranging from 1500 to 3100 psi and temperatures from 1600 to 2000 degrees. Main injector evaluations were accomplished primarily with test firings using water-cooled calorimeter main combustion chamber. With this chamber, heat flux profiles and combustion performance were obtained at pressures to approximately 2200 psia. Several tests were conducted using a methane-cooled combustion chamber.

Methane heat transfer investigation

Cook, R. T. (Rockwell International Corp., Canoga Park, CA, United States), NASA Center for AeroSpace Information (CASI), NASA-CR-171051, 1984

Future high chamber pressure LOX/hydrocarbon booster engines require copper base alloy main combustion chamber coolant channels similar to the SSME to provide adequate cooling and reusable engine life. Therefore, it is of vital importance to evaluate the heat transfer characteristics and coking thresholds for LNG (94% methane) cooling, with a copper base alloy material adjacent to he fuel coolant. High pressure methane cooling and coking characteristics recently evaluated at Rocketdyne using stainless steel heated tubes at methane bulk temperatures and coolant wall temperatures typical of advanced engine operation except at lower heat fluxes as limited by the tube material. As expected, there was no coking observed. However, coking evaluations need be conducted with a copper base surface exposed to the methane coolant at higher heat fluxes approaching those of future high chamber pressure engines.

Methane heat transfer investigation

Cook, R. T. (Rockwell International Corp., Canoga Park, CA, United States), NASA Center for AeroSpace Information (CASI), NASA-CR-171199, 1984

Future high chamber pressure LOX/hydrocarbon booster engines require copper-base alloy main combustion chamber coolant channels similar to the SSME to provide adequate cooling and reusable engine life. Therefore, it is of vital importance to evaluate the heat transfer characteristics and coking thresholds for LNG (94%

methane) cooling, with a copper-base alloy material adjacent to the fuel coolant. High-pressure methane cooling and coking characteristics were recently evaluated using stainless-steel heated tubes at methane bulk temperatures and coolant wall temperatures typical of advanced engine operation except at lower heat fluxes as limited by the tube material. As expected, there was no coking observed. However, coking evaluations need be conducted with a copper-base surface exposed to the methane coolant at higher heat fluxes approaching those of future high chamber pressure engines.

Low-thrust Isp sensitivity study

Schoenman, L. (Aerojet Liquid Rocket Co., Sacramento, CA, United States), NASA Center for AeroSpace Information (CASI), NASA-CR-165621, 1982

A comparison of the cooling requirements and attainable specific impulse performance of engines in the 445 to 4448N thrust class utilizing LOX/RP-1, LOX/Hydrogen and LOX/Methane propellants is presented. The unique design requirements for the regenerative cooling of low-thrust engines operating at high pressures (up to 6894 kPa) were explored analytically by comparing single cooling with the fuel and the oxidizer, and dual cooling with both the fuel and the oxidizer. The effects of coolant channel geometry, chamber length, and contraction ratio on the ability to provide proper cooling were evaluated, as was the resulting specific impulse. The results show that larger contraction ratios and smaller channels are highly desirable for certain propellant combinations.

Low-thrust chemical rocket engine study

Mellish, J. A. (Aerojet Liquid Rocket Co., Sacramento, CA, United States), NASA Center for AeroSpace Information (CASI), NASA-CR-165276, 1981

Engine data and information are presented to perform system studies on cargo orbit-transfer vehicles which would deliver large space structures to geosynchronous equatorial orbit. Low-thrust engine performance, weight, and envelope parametric data were established, preliminary design information was generated, and technologies for liquid rocket engines were identified. Two major engine design drivers were considered in the study: cooling and engine cycle options. Both film-cooled and regeneratively cooled engines were evaluated. The propellant combinations studied were hydrogen/oxygen, methane/oxygen, and kerosene/oxygen.

Low-thrust chemical rocket engine study

Shoji, J. M. (Rockwell International Corp., Canoga Park, CA, United States), NASA Center for AeroSpace Information (CASI), NASA-CR-165275, 1981

An analytical study evaluating thrust chamber cooling engine cycles and preliminary engine design for low thrust chemical rocket engines for orbit transfer vehicles is described. Oxygen/hydrogen, oxygen/methane, and oxygen/RP-1 engines with thrust levels from 444.8 N to 13345 N, and chamber pressures from 13.8 N/sq cm to 689.5 N/sq cm were evaluated. The physical and thermodynamic properties of the propellant theoretical performance data, and transport properties are documented. The thrust chamber cooling limits for regenerative/radiation and film/radiation cooling are defined and parametric heat transfer data presented. A conceptual evaluation of a number of engine cycles was performed and a 2224.1 N oxygen/hydrogen engine cycle configuration and a 2224.1 N oxygen/methane configuration chosen for preliminary engine design. Updated parametric engine data, engine design drawings, and an assessment of technology required are presented.

Advanced oxygen-hydrocarbon Earth-to-orbit propulsion

O'Brien, C. J. (Aerojet Liquid Rocket Co., Sacramento, CA, United States), NASA Center for AeroSpace Information (CASI), 1981

Liquid oxygen/hydrocarbon (LO2/HC) rocket engine cycles for a surface to orbit transportation system were evaluated. A consistent engine system data base is established for defining advantages and disadvantages, system performance and operating limits, engine parametric data, and technology requirements for candidate engine systems. Preliminary comparisons of the engine cycles utilizing delivered specific impulse values are presented. Methane and propane staged combustion cycles are the highest LO2/HC performers. The hydrogen cooled LO2/methane dual throat engine was found to be the highest performing. Technology needs identified in the study include: high temperature turbines; oxidizer-rich preburners; LO2, methane, and propane cooling; methane and propane fuel-rich preburners; the HC fuel turbo pump; and application of advanced composite materials to the engine system. Parametric sensitivity analysis data are displayed which show the effect of variations in engine thrust, mixture ratio, chamber pressure, area ratio, cycle life, and turbine inlet temperature on specific impulse and engine weight.

LEO-to-GEO low thrust chemical propulsion

Shoji, J. M. (Rockwell International Corp., Canoga Park, CA, United States), NASA Center for AeroSpace Information (CASI), 1980

One approach being considered for transporting large space structures from low Earth orbit (LEO) to geosynchronous equatorial orbit (GEO) is the use of low thrust chemical propulsion systems. A variety of chemical rocket engine cycles evaluated for this application for oxygen/hydrogen and oxygen/hydrocarbon propellants (oxygen/methane and oxygen/RF-1) are discussed. These cycles include conventional propellant turbine drives, turbo alternator/electric motor pump drive, and fuel cell/electric motor pump drive as well as pressure fed engines. Thrust chamber cooling analysis results are presented for regenerative/radiation and film/radiation cooling.

Advanced high pressure engine study for mixed-mode vehicle applications

Luscher, W. P. (Aerojet Liquid Rocket Co., Sacramento, CA, United States); Mellish, J. A. (Aerojet Liquid Rocket Co., Sacramento, CA, United States), NASA Center for AeroSpace Information (CASI), NASA-CR-135141 , 1977

High pressure liquid rocket engine design, performance, weight, envelope, and operational characteristics were evaluated for a variety of candidate engines for use in mixed-mode, single-stage-to-orbit applications. Propellant property and performance data were obtained for candidate Mode 1 fuels which included: RP-1, RJ-5, hydrazine, monomethyl-hydrazine, and methane. The common oxidizer was liquid oxygen. Oxygen, the candidate Mode 1 fuels, and hydrogen were evaluated as thrust chamber coolants. Oxygen, methane, and hydrogen were found to be the most viable cooling candidates. Water, lithium, and sodium-potassium were also evaluated as auxiliary coolant systems. Water proved to be the best of these, but the system was heavier than those systems which cooled with the engine propellants. Engine weight and envelope parametric data were established for candidate Mode 1, Mode 2, and dual-fuel engines. Delivered engine performance data were also calculated for all candidate Mode 1 and dual-fuel engines.

Space storable regenerative cooling investigation

NASA Center for AeroSpace Information (CASI), NASA-CR-72704, 1971

Performance tests and specifications for space storable regenerative cooling system with liquid oxygen and methane propellants

Thermal feasibility of using methane or hydrogen fuel for direct cooling of a first-stage turbine-stator

Colladay, R. S. (NASA Lewis Research Center, Cleveland, OH, United States), NASA Center for AeroSpace Information (CASI), NASA-TN-D-6042, 1970

Methane or hydrogen fuel direct cooling of first stage stator of SST aircraft turbine numerical heat transfer analysis

Rocket Testing of Four Flox-Light Hydrocarbon Propellant Combinations

Masters, A. I. (Pratt and Whitney Aircraft, Applied Research Dept. West Palm Beach, FL United States); Colbert, J. E. (Pratt and Whitney Aircraft, Applied Research Dept. West Palm Beach, FL United States), NASA Center for AeroSpace Information (CASI), AIAA Paper 66-624 , 1966

At the first Joint Propulsion Specialists Conference it was shown that the basis of interest in the flox-light hydrocarbon propellants was their unique ability to fulfill a variety of rocket engine and space vehicle requirements. The flox-hydrocarbon combinations provide: (1) high performance, (2) high density, (3) hypergolic ignition, (4) space storability, and (5) the capability of cooling the thrust chamber with the fuel. It was also shown that methane, propane, butene-1, and a eutectic blend of n-pentane and isopentane were four of the most promising fuels for use with flox. An experimental program is evaluate the performance, ignition, and cooling characteristics of the most promising flox-light hydrocarbon combinations in low pressure (nominal 100 psia) engines. Because the prime advantage of light hydrocarbons over other high performance space storable fuels is their cooling characteristics, the first experimental work was primarily an evaluation of thrust chamber cooling. Both transpiration and regenerative cooling were investigated. To facilitate the cooling study, modified RL10 injectors designed for gaseous fuel and liquid oxidizer were used rather than attempting to design and test a new injector. The feasibility of both regenerative and transpiration cooling was established, and additional rocket

testing is being done. The objectives of this testing are to evaluate the performance and ignition characteristics with liquid-liquid injection, and to investigate altitude performance using regenerative and transpiration cooling.

PROPANE

LOX/hydrocarbon combustion and cooling survey

Cook, R. T. (Rockwell International Corp., Canoga Park, CA, United States); Kirby, F. M. (Rockwell International Corp., Canoga Park, CA, United States), NASA Center for AeroSpace Information (CASI), 1986.

Liquid oxygen (LOX) and hydrocarbon fuels (methane, propane, and RP-1) are very attractive for booster rocket engine applications because of their high bulk density and respectful performance. Vehicle payload capability is dependent on the attainable engine chamber pressure and the combustion efficiency of the selected propellant combination. Combustor design approaches are presented to attain maximum cooling, stability, combustion efficiency, and reusable life. Experimental combustion efficiency and hot-gas heat-transfer rates are discussed as related to combustor contour, thrust level scaling, and injector characteristics including mixture ratio biasing and film cooling. These experimental data are compared to theory, and empirical relationships are derived. Conventional cooling relationships and coking limits are presented for potential hydrocarbon fuels as derived from high heat flux and high pressure electrically heated tube experiments. Experimental results of combustor coolant liner materials compatibility with hydrocarbon fuels are discussed. The application of the results of these studies to future LOX/hydrocarbon engines is delineated.

Deposit formation and heat transfer in hydrocarbon rocket fuels

Giovanetti, A. J. (United Technologies Corp., East Hartford, CT, United States); Spadaccini, L. J. (United Technologies Corp., East Hartford, CT, United States); Szetela, E. J. (United Technologies Corp., East Hartford, CT, United States), NASA Center for AeroSpace Information (CASI), NASA-CR-168277 , 1983

An experimental research program was undertaken to investigate the thermal stability and heat transfer characteristics of several hydrocarbon fuels under conditions that simulate high-pressure, rocket engine cooling systems. The rates of carbon deposition in heated copper and nickel-plated copper tubes were determined for RP-1, propane, and natural gas using a continuous flow test apparatus which permitted independent variation and evaluation of the effect on deposit formation of wall temperature, fuel pressure, and fuel velocity. In addition, the effects of fuel additives and contaminants, cryogenic fuel temperatures, and extended duration testing with intermittent operation were examined. Parametric tests to map the thermal stability characteristics of RP-1, commercial-grade propane, and natural gas were conducted at pressures of 6.9 to 13.8 MPa, bulk fuel velocities of 30 to 90 m/s, and tube wall temperatures in the range of 230 to 810 K. Also, tests were run in which propane and natural gas fuels were chilled to 230 and 160 K, respectively. Corrosion of the copper tube surface was detected for all fuels tested. Plating the inside of the copper tubes with nickel reduced deposit formation and eliminated tube corrosion in most cases. The lowest rates of carbon deposition were obtained for natural gas, and the highest rates were obtained for propane. For all fuels tested, the forced-convection heat transfer film coefficients were satisfactorily correlated using a Nusselt-Reynolds-Prandtl number equation.

Deposit formation in hydrocarbon rocket fuels

Roback, R.; Szetela, E. J.; Spadaccini, L. J., United Technologies Research Center, East Hartford, CT, United States, NASA Center for AeroSpace Information (CASI), NASA-CR-165405 , 1981

An experimental program was conducted to study deposit formation in hydrocarbon fuels under flow conditions that exist in high-pressure, rocket engine cooling systems. A high pressure fuel coking test apparatus was designed and developed and was used to evaluate thermal decomposition (coking) limits and carbon deposition rates in heated copper tubes for two hydrocarbon rocket fuels, RP-1 and commercial-grade propane. Tests were also conducted using JP-7 and chemically-pure propane as being representative of more refined cuts of the baseline fuels. A parametric evaluation of fuel thermal stability was performed at pressures of 136 atm to 340 atm, bulk fuel velocities in the range 6 to 30 m/sec, and tube wall temperatures in the range 422 to 811 K. Results indicated that substantial deposit formation occurs with RP-1 fuel at wall temperatures between 600 and 800 K, with peak deposit formation occurring near 700 K. No improvements were obtained when deoxygenated JP-7 fuel was substituted for RP-1. The carbon deposition rates for the propane fuels were generally higher than those obtained for either of the kerosene fuels at any given wall temperature. There appeared to be little difference between commercial-grade and chemically-pure propane with regard to type and quantity of deposit. Results of tests conducted with RP-1 indicated that the rate of deposit formation increased slightly with pressure over the range 136 atm to 340 atm. Finally, plating the inside wall of the tubes with nickel was found to significantly reduce carbon deposition rates for RP-1 fuel.

Advanced oxygen-hydrocarbon Earth-to-orbit propulsion

O'Brien, C. J. (Aerojet Liquid Rocket Co., Sacramento, CA, United States)NASA Center for AeroSpace Information (CASI), 1981

Liquid oxygen/hydrocarbon (LO2/HC) rocket engine cycles for a surface to orbit transportation system were evaluated. A consistent engine system data base is established for defining advantages and disadvantages, system performance and operating limits, engine parametric data, and technology requirements for candidate engine systems. Preliminary comparisons of the engine cycles utilizing delivered specific impulse values are presented. Methane and propane staged combustion cycles are the highest LO2/HC performers. The hydrogen cooled LO2/methane dual throat engine was found to be the highest performing. Technology needs identified in the study include: high temperature turbines; oxidizer-rich preburners; LO2, methane, and propane cooling; methane and propane fuel-rich preburners; the HC fuel turbo pump; and application of advanced composite materials to the engine system. Parametric sensitivity analysis data are displayed which show the effect of variations in engine thrust, mixture ratio, chamber pressure, area ratio, cycle life, and turbine inlet temperature on specific impulse and engine weight.

Deposit formation in hydrocarbon rocket fuels: Executive summary

Roback, R.; Szetela, E. J.; Spadaccini, L. J., United Technologies Research Center, East Hartford, CT, United States, NASA Center for AeroSpace Information (CASI), NASA-CR-165492 , 1981

An experimental program was conducted to study deposit formation in hydrocarbon fuels under flow conditions that exist in high-pressure, rocket engine cooling systems. A high pressure fuel coking test apparatus was designed and developed and was used to evaluate thermal decomposition (coking) limits and carbon deposition rates in heated copper tubes for two hydrocarbon rocket fuels, RP-1 and commercial-grade propane. Tests were also conducted using JP-7 and chemically-pure propane as being representative of more refined cuts of the baseline fuels. A parametric evaluation of fuel thermal stability was performed at pressures of 136 atm to 340 atm, bulk fuel velocities in the range 6 to 30 m/sec, and tube wall temperatures in the range 422 to 811K. In addition, the effect of the inside wall material on deposit formation was evaluated in selected tests which were conducted using nickel-plated tubes. The results of the tests indicated that substantial deposit formation occurs with RP-1 fuel at wall temperatures between 600 and 800K, with peak deposit formation occurring near 700K. No improvements were obtained when de-oxygenated JP-7 fuel was substituted for RP-1. The carbon deposition rates for the propane fuels were generally higher than those obtained for either of the kerosene fuels at any given wall temperature. There appeared to be little difference between commercial-grade and chemically-pure propane with regard to type and quantity of deposit. The results of tests conducted with RP-1 indicated that the rate of deposit formation increased slightly with pressure over the range 136 atm to 340 atm. Finally, plating the inside wall of the tubes with nickel was found to significantly reduce carbon deposition rates for RP-1 fuel.

Experimental evaluation of catalytic combustion with heat removal at near stoichiometric conditions

Bulzan, D. L. (NASA Lewis Research Center, Cleveland, OH, United States), NASA Center for AeroSpace Information (CASI), NASA-TM-81748, 1980

Two concentric tube configurations were tested. Tests were conducted at an inlet pressure of 150,000 Pa, inlet fuel air mixture temperatures from 780 to 960 K, combustion air flow rates from 0.78 to 1.5 g/s, equivalence ratios up to 0.90, and a range of cooling air flow rates. Propane and propylene fuels were used. Both configurations used air flowing through the center tube for cooling and combustion in the annulus on the catalytic surface. One configuration had the catalyst applied to the outside surface of the inner tube. Conversion of the fuel was very low for this configuration. The other configuration had the catalyst applied to the inside surface of the outer tube. Conversion of the fuel was considerably better in this configuration.

ETHANOL

Microfabricated Liquid Rocket Motors

Epstein, Alan H.; Joppin, C.; Kerrebrock, J. L.; Schneider, Steven J., NASA Center for AeroSpace Information (CASI), March 2003

Under NASA Glenn Research Center sponsorship, MIT has developed the concept of micromachined, bipropellant, liquid rocket engines. This is potentially a breakthrough technology changing the cost-performance tradeoffs for small propulsion systems, enabling new applications, and redefining the meaning of the term low-cost-access-to-space. With this NASA support, a liquid-cooled, gaseous propellant version of the thrust chamber

and nozzle was designed, built, and tested as a first step. DARPA is currently funding MIT to demonstrate turbopumps and controls. The work performed herein was the second year of a proposed three-year effort to develop the technology and demonstrate very high power density, regeneratively cooled, liquid bipropellant rocket engine thrust chamber and nozzles. When combined with the DARPA turbopumps and controls, this work would enable the design and demonstration of a complete rocket propulsion system. The original MIT-NASA concept used liquid oxygen-ethanol propellants. The military applications important to DARPA imply that storable liquid propellants are needed. Thus, MIT examined various storable propellant combinations including N2O4 and hydrazine, and H2O2 and various hydrocarbons. The latter are preferred since they do not have the toxicity of N2O4 and hydrazine. In reflection of the newfound interest in H2O2, it is once again in production and available commercially. A critical issue for the microrocket engine concept is cooling of the walls in a regenerative design. This is even more important at microscale than for large engines due to cube-square scaling considerations. Furthermore, the coolant behavior of rocket propellants has not been characterized at microscale. Therefore, MIT designed and constructed an apparatus expressly for this purpose. The report details measurements of two candidate microrocket fuels, JP-7 and JP-10.

Technology and Advanced Development for a Non-Toxic Orbital Maneuvering System and Reaction Control System for Orbiter Upgrade

Hayes, W. A. (GenCorp Aerojet, Sacramento, CA United States); Ferrante, Fred A. (GenCorp Aerojet, Sacramento, CA United States); Engelmann, G. L., (GenCorp Aerojet, Sacramento, CA United States); Gibson, V. A., (GenCorp Aerojet, Sacramento, CA United States); Phillipsen, P. C. (GenCorp Aerojet, Sacramento, CA United States), NASA Center for AeroSpace Information (CASI), 1999

NASA intends to pursue technology applications to upgrade the Space Shuttle Orbiter OMS and RCS systems with non-toxic propellants. The primary objectives of an upgraded OMS/RCS are improved safety and reliability, reduced operations and maintenance costs while meeting basic OMS/RCS operational and performance requirements. The OMS/RCS has a high degree of direct interaction with the crew and requires subsystem and components that are compatible with integration into the orbiter vehicle with regard to external mold-line, power and thermal control The non-toxic propulsion technology is also applicable to future Human Exploration and Development of Space (HEDS) missions. The HEDS missions have similar requirements for attitude control and lander descent/ascent propulsion and which will emphasize the use of In-Situ Resource for propellants. When used as a regenerative coolant as in the Shuttle Orbiter OMS combustion chamber, non-toxic fuels such as ethanol are limited in their cooling capacity by the bulk temperature rise permitted to prevent film boiling or possible coking. Typical regeneratively cooled chambers are constructed from highly conductive copper, which maximizes heat transfer, or from low conductivity materials like stainless steel that can also exacerbate cooling problems. For an ethanol cooled application the heat transfer into the fluid must be controlled to reduce the fuel coolant bulk temperature rise. An approach to provide this control is the subject of this report. This report is being issued to document work done by Aerojet on NASA contract NAS 8-98042. Specifically, this project investigates of the use of ethanol, a designated non-toxic fuel, as a coolant for the Space Shuttle Orbital Maneuvering System Engine combustion chamber. The project also addresses a cost reducing fabrication technique for construction of such a combustion chamber. The study contained three major sub-tasks: an analytical investigation and trade study which included layout of a flight type chamber concept, the fabrication and evaluation of formed platelet liner panels and the preparation and testing of mechanical properties specimens representative of a novel hot gas wall concept.

Summary of LO2/Ethanol OMS/RCS Technology and Advanced Development 99-2744

Curtis, Leslie A. (NASA Marshall Space Flight Center, Huntsville, AL United States); Hurlbert, Eric A. (NASA Johnson Space Center, Houston, TX United States), NASA Center for AeroSpace Information (CASI), 1999

NASA is pursuing non-toxic propellant technologies applicable to RLV and Space Shuttle orbital maneuvering system (OMS) and reaction control system (RCS). The primary objectives of making advancements in an OMS/RCS system are improved safety, reliability, and reduced operations and maintenance cost, while meeting basic operational and performance requirements. An OMS/RCS has a high degree of direct interaction with the vehicle and crew and requires subsystem and components that are compatible with integration into the vehicle with regard to external mold-line, power, and thermal control. In July 1997, a Phase I effort for the technology and advanced development of an upgrade of the space shuttle was conducted to define the system architecture, propellant tank, feed system, RCS thrusters, and OMS engine. Phase I of the project ran from July 1997 to October 1998. Phase II is currently being planned for the development and test of full-scale prototype of the system in 1999 and 2000. The choice of pressure-fed liquid oxygen (LO2) and ethanol is the result of numerous trade studies conducted from 1980 to 1996. Liquid oxygen and ethanol are clean burning, high-density propellants that provide a high degree of commonality with other spacecraft subsystems including life support, power, and thermal control, and with future human exploration and development of space missions. The key to

this pressure-fed system is the use of subcooled liquid oxygen at 350 psia. In this approach, there is 80 degrees R of subcooling, which means that boil-off will not occur until the temperature has risen to 80 R. The sub-cooling results naturally from loading propellants at 163 R, which is the saturation temperature at 14.7 psia, and then pressurizing to 350 psia on the launch pad. Thermal insulation and conditioning techniques are then used to limit the LO2 temperature to 185 R maximum, and maintain the sub-cooling. The other key is the wide temperature range of ethanol, -173 F to +300 F, which can provide heat to gasify liquid oxygen or provide a good coolant.

Non-Toxic Orbiter Maneuvering System (OMS) and Reaction Control System

Hurlbert, Eric A. (NASA Johnson Space Center, Houston, TX United States), NASA Center for AeroSpace Information (CASI), 1999

NASA is pursuing the technology and advanced development of a non-toxic (NT) orbital maneuvering system (OMS) and reaction control system (RCS) for shuttle upgrades, RLV, and reusable first stages. The primary objectives of the shuttle upgrades program are improved safety, improved reliability, reduced operations time and cost, improved performance or capabilities, and commonality with future space exploration needs. Non-Toxic OMS/RCS offers advantages in each of these categories. A non-toxic OMS/RCS eliminates the ground hazards and the flight safety hazards of the toxic and corrosive propellants. The cost savings for ground operations are over $24M per year for 7 flights, and the savings increase with increasing flight rate up to $44M per year. The OMS/RCS serial processing time is reduced from 65 days to 13 days. The payload capability can be increased up to 5100 lbs. The non-toxic OMS/RCS also provides improved space station reboost capability up to 20 nautical miles over the current toxic system of 14 nautical miles. A NT OMS/RCS represents a clear advancement in the SOA over MMH/NTO. Liquid oxygen and ethanol are clean burning, high-density propellants that provide a high degree of commonality with other spacecraft subsystems including life support, power, and thermal control, and with future human exploration and development of space missions. The simple and reliable pressure-fed design uses sub-cooled liquid oxygen at 250 to 350 psia, which allows a propellant to remain cryogenic for longer periods of time. The key technologies are thermal insulation and conditioning techniques are used to maintain the sub-cooling. Phase I successfully defined the system architecture, designed an integrated OMS/RCS propellant tank, analyzed the feed system, built and tested the 870 lbf RCS thrusters, and tested the 6000 lbf OMS engine. Phase 11 is currently being planned for the development and test of full-scale prototype of the system in 1999 and 2000

Small rocket research and technology

Schneider, Steven (NASA Lewis Research Center, Cleveland, OH, United States); Biaglow, James (NASA Lewis Research Center, Cleveland, OH, United States), NASA Center for AeroSpace Information (CASI), 1993

Small chemical rockets are used on nearly all space missions. The small rocket program provides propulsion technology for civil and government space systems. Small rocket concepts are developed for systems which encompass reaction control for launch and orbit transfer systems, as well as on-board propulsion for large space systems and earth orbit and planetary spacecraft. Major roles for on-board propulsion include apogee kick, delta-V, de-orbit, drag makeup, final insertions, north-south stationkeeping, orbit change/trim, perigee kick, and reboost. The program encompasses efforts on earth-storable, space storable and cryogenic propellants. The earth-storable propellants include nitrogen tetroxide (NTO) as an oxidizer with monomethylhydrazine (MMH) or anhydrous hydrazine (AH) as fuels. The space storable propellants include liquid oxygen (LOX) as an oxidizer with hydrazine or hydrocarbons such as liquid methane, ethane, and ethanol as fuels. Cryogenic propellants are LOX or gaseous oxygen (GOX) as oxidizers and liquid or gaseous hydrogen as fuels. Improved performance and lifetime for small chemical rockets are sought through the development of new predictive tools to understand the combustion and flow physics, the introduction of high temperature materials to eliminate fuel film cooling and its associated combustion inefficiency, and improved component designs to optimize performance. Improved predictive technology is sought through the comparison of both local and global predictions with experimental data. Results indicate that modeling of the injector and combustion process in small rockets needs improvement. High temperature materials require the development of fabrication processes, a durability data base in both laboratory and rocket environments, and basic engineering property data such as strength, creep, fatigue, and work hardening properties at both room and elevated temperature. Promising materials under development include iridium-coated rhenium and a ceramic composite of mixed hafnium carbide and tantalum carbide reinforced with graphite fibers.

Investigation of the cooling properties of ethanol at pressures up to 800x9.8x104n/m2

Aladev, I. T.; Malkina, L. I.; Merkel, E. YU; Povarnin, P. I., Israeli Program for Scientific Translations Ltd., Jerusalem, Israel.

NASA Center for AeroSpace Information (CASI), 1967

Cooling properties, thermal decomposition, and pseudoboiling in ethanol flowing through stainless steel pipe

Hydrogen Peroxide

Upper Stage Flight Experiment 10K Engine Design and Test Results

Ross, R. (Orbital Sciences Corp., Chandler, AZ United States); Morgan, D. (Orbital Sciences Corp., Chandler, AZ United States); Crockett, D. (Orbital Sciences Corp., Chandler, AZ United States); Martinez, L. (Orbital Sciences Corp., Chandler, AZ United States); Anderson, W. (NASA Marshall Space Flight Center, Huntsville, AL United States); McNeal, C. (NASA Marshall Space Flight Center, Huntsville, AL United States), NASA Center for AeroSpace Information (CASI), AIAA Paper 2000-3558

A 10,000 lbf thrust chamber was developed for the Upper Stage Flight Experiment (USFE). This thrust chamber uses hydrogen peroxide /JP-8 oxidizer/fuel combination. The thrust chamber comprises an oxidizer dome and manifold, catalyst bed assembly, fuel injector, and chamber/nozzle assembly. Testing of the engine was done at NASA‘s Stennis Space Center (SSC) to verify its performance and life for future upper stage or Reusable Launch Vehicle applications. Various combinations of silver screen catalyst beds, fuel injectors, and combustion chambers were tested. Results of the tests showed high C* efficiencies (97% - 100%) and vacuum specific impulses of 275 - 298 seconds. With fuel film cooling, heating rates were low enough that the silica/quartz phenolic throat experienced minimal erosion. Mission derived requirements were met, along with a perfect safety record.

Development of a Pressure-Fed Rocket Engine Using Hydrogen Peroxide and JP-8

Wu, P.-K. (Kaiser Marquardt, Van Nuys, CA United States); Fuller, R. P. (Kaiser Marquardt, Van Nuys, CA United States); Morlan, P. W., (Kaiser Marquardt, Van Nuys, CA United States); Ruttle, D. W., (Kaiser Marquardt, Van Nuys, CA United States); Nejad, A. S., (Kaiser Marquardt, Van Nuys, CA United States); Anderson, W. E. ,(Orbital Sciences Corp., Chandler, AZ United States), NASA Center for AeroSpace Information (CASI), AIAA Paper 99-2877 , 1999

A pressure-fed rocket engine using hydrogen peroxide and JP-8 was designed and demonstrated for upper stage space transportation applications. The engine utilizes silver plated screen catalyst to decompose 85% hydrogen peroxide (by weight). The decomposed high-temperature gas causes the JP-8 to auto-ignite and undergo chemical reaction. An ablative chamber using silica phenolic was used as the combustion chamber. The present effort includes catalyst development, injector evaluation, and chamber char and erosion characterization. Wagonwheel-type distribution and support plates were used in the catalyst bed design to reduce pressure drop, to increase active area, and to avoid flow channeling. Various fuel injection and mixing approaches were investigated and the combustion efficiency was in the range from 89 to 98%, depending on injector design and operating conditions. Fuel film cooling, up to 40% of the total fuel flow, was found to be ineffective with the current engine configuration. A ring injector was selected because of the satisfactory performance and its low cost. The char and erosion rates were determined through hot-fire tests. The char depth was found to be a function of axial distance, which was related to the progress of chemical reaction. Correlation of the char and erosion rates was developed as a design database for future applications,

HAN

Combustion of HAN-Based Monopropellant Droplets in Reduced Gravity,

Shaw, B. D. (California Univ., MAE Dept. Davis, CA United States), NASA Center for AeroSpace Information (CASI), 2001.

Hydroxylammonium nitrate (HAN) is a major constituent in a class of liquid monopropellants that have many attractive characteristics and which display phenomena that differ significantly from other liquid monopropellants. They are composed primarily of HAN, H2O and a fuel species, often triethanolammonium nitrate (TEAN). HAN - based propellants have attracted attention as liquid gun propellants, and are attractive for NASA spacecraft propulsion applications. A representative propellant is XM46. This mixture is 60.8% HAN, 19.2% TEAN and 20% H2O by weight. Other HAN-based propellant mixtures are also of interest. For example, methanol and glycine have been investigated as potential fuel species for HAN -based monopropellants for thruster applications. In the present research, experimental and theoretical studies are performed on combustion of HAN-based monopropellant droplets. The fuel species considered are TEAN, methane and glycine. Droplets initially in the mm size range are studied at pressures up to 30 atm. These pressures are applicable to spacecraft thruster applications. The droplets are placed in environments with various amounts of Ar, N2, O2, NO2 and N2O.

Reduced gravity is employed to enable observations of burning rates and flame structures to be made without the complicating effects of buoyant and forced convection. Normal gravity experiments are also performed in this research program. The experiment goals are to provide accurate fundamental data on deflagration rates, gas phase temperature profiles, transient gas-phase flame behaviors, the onset of bubbling in droplets at lower pressures, and the low-pressure deflagration limit. Theoretical studies are performed to provide rational models of deflagration mechanisms of HAN -based liquid propellants. Besides advancing fundamental knowledge, this research should aid in applications (e.g., spacecraft thrusters and liquid propellant guns) of this unique class of monopropellants.

Selection of Alternate Fuels for HAN-Based Monopropellants

Meinhardt, D. S. (Primex Aerospace, Inc., Seattle, WA United States); Wucherer, E. J. (Primex Aerospace, Inc., Seattle, WA United States); Jankovsky, R. S. (NASA Lewis Research Center, Cleveland, OH United States); Schmidt, E. W. (Schmidt (E. W.), Bellevue, WA United States), NASA Center for AeroSpace Information (CASI),1998

Efforts to develop a monopropellant with reduced toxicity and improved safety and handling characteristics (compared to hydrazine) have led to increased interest in propellants based on hydroxylammonium nitrate (HAN, [N(+)H3OH]NO3(-)). Various attempts at using HAN -based liquid gun propellant XM-46 in monopropellant rocket applications have been disappointing. Primex Aerospace Company (PAC) has determined that an alternate fuel component in the HAN-based propellant formulation is necessary for rocket propulsion applications. This paper presents an outline of the fuel and propellant selection methodology and provides evaluation results for several formulations.

HAN-Based Monopropellant Propulsion System with Applications

Jankovsky, Robert S. (NASA Lewis Research Center, Cleveland, OH United States); Oleson, Steven R. (NYMA, Inc., Brook Park, OH United States), NASA Center for AeroSpace Information (CASI), NASA-TM-107407 , 1997

NASA is developing a new monopropellant propulsion system for small, cost-driven spacecraft with AV requirements in the range of 10-150 m/sec. This system is based on a hydroxylammonium nitrate (HAN)/water/fuel monopropellant blend which is extremely dense, environmentally benign, and promises good performance and simplicity. State-of-art (SOA) small spacecraft typically employ either hydrazine or high pressure stored gas. Herein, a ‚typical' small satellite bus is used to illustrate how a HAN -based monopropellant propulsion system fulfills small satellite propulsion requirements by providing mass and/or volume savings of SOA hydrazine monopropellants with the cost benefits of a stored nitrogen gas.